THE PROCEEDINGS OF THE PHYSICAL SOCIETY

Section A

VOL. 65, PART 10 1 October 1952 No. 394 A

COMPLEX STRUCTURE AND NUCLEAR STRUCTURE

The following four contributions were read at the Society's meeting at Southampton on 19th December 1951.

A Theoretical Attempt to Predict the Excited States of Nuclei in the Neighbourhood of ^{208}Pb

BY M. H. L. PRYCE

Clarendon Laboratory, Oxford

.A
5
2

MS. received 21*st March* 1952 ; *read before the Society at Southampton on* 19*th December* 1951

ABSTRACT. ^{208}Pb has a double closed shell of 82 protons and 126 neutrons. The classification of the lowest excited states of ^{207}Pb, ^{207}Tl, ^{209}Pb, ^{209}Bi, which differ by one nucleon, should thus follow the single-particle model closely. The attempt is made to classify the lowest excited states of ^{208}Pb, ^{208}Tl, ^{208}Hg, ^{210}Pb, ^{210}Bi and ^{210}Po, which differ by two particles, in terms of the one-particle model, taking the interaction of the two particles as a perturbation. Considerable uncertainties in the order of the energy levels remain, but some definite conclusions are possible. The existence of an isomeric state of ^{210}Bi (RaE) with very high spin ($I=8$?) is predicted. This fits in with known facts about the alpha-particle emitting isomeric state.

The method can also be applied to ^{208}Tl, ^{208}Bi and the excited states of ^{208}Pb which arise by lifting one nucleon into the next shell, leaving a hole. It meets with considerable success for ^{208}Tl. Discrepancies with known facts in the case of ^{208}Pb suggest a more complex picture, according to which the first excited state would have $I=0$ and even parity. Such a state has never been observed, but its existence is not completely excluded by observation.

§ 1. INTRODUCTION

THE shell model proposed by Haxel, Jensen and Suess (1949), and by Mayer (1949, 1950 a) has been so successful in accounting for the shell properties and ground state spins of nuclei that it is tempting to subject it to further tests. That it throws useful light on the spin of excited states is well known from the study of isomeric transitions, but any attempt at a detailed prediction of excited states in this domain is in general frustrated, in view of the approximate nature of the individual particle description, by the large number of levels arising from the various nuclear configurations involved, the uncertainty concerning nuclear interactions, and the intricacy of the calculations. This complexity is much reduced, at least for the lower lying excited levels, in a nucleus which is close to a double closed shell of protons and neutrons. For a nucleus composed of a double closed shell *plus* one proton, or one neutron, the lowest levels are, within the limitations of the model, those of a single particle moving in the equivalent potential of the core, and constitute no further theoretical problem. The same is true, with slight modifications, for nuclei consisting of a double closed shell less one proton or neutron. Nuclei differing by two nucleons from a closed shell offer a testing ground for more detailed applications of the model, while not yet leading to such a degree of complexity that comparison with experiment is impossible. Each extra nucleon may be ascribed a definite energy state, and in zero approximation all states arising from this configuration will have the same energy. When the interaction between the two nucleons is taken into account the degeneracy will be removed, the different resulting energy levels being classified by the resultant angular momentum (nuclear spin).

In order to carry out this programme certain assumptions concerning the nuclear forces are necessary. The results will be more sensitive to these if the range of the nuclear forces is comparable with the nuclear size (as in the lighter nuclei) than if the nucleus is large compared with the range. In the latter case it may be expected that the most important parameters are (i) the 'strength' of the central singlet interaction, and (ii) the 'strength' of the central triplet interaction, regardless of the exchange nature of the force, while the shape and exchange character of the central force, and any tensor or spin–orbit forces, may be expected to play only a minor part. The present calculations take into account only these two parameters.

For this reason the paper is confined to nuclei in the neighbourhood of ^{208}Pb (82 protons and 126 neutrons), as this is the only double closed shell nucleus which is (i) sufficiently large in relation to the range of nuclear forces, and (ii) in or near the region of nuclear stability. The nuclei of interest are therefore

(i) ^{209}Pb and ^{209}Bi, containing one extra nucleon;
(ii) ^{210}Pb (RaD), ^{210}Bi (RaE) and ^{210}Po (RaF), with two extra nucleons;
(iii) ^{207}Pb (AcD) and ^{207}Tl (AcC″), deficient by one nucleon;
(iv) ^{206}Pb (RaG), ^{206}Tl and ^{206}Hg, deficient by two nucleons;
(v) ^{208}Tl (ThC″), ^{208}Bi, with one nucleon and one hole, and the excited states of ^{208}Pb itself.

Of these, ^{206}Pb, ^{207}Pb, ^{208}Pb and ^{209}Bi are stable, ^{210}Po emits alpha-particles, ^{208}Bi probably decays by electron capture, and the remainder are beta-active. The nuclear diameter in this region is about 17×10^{-13} cm (circumference 5×10^{-12} cm), which is to be compared with about 2×10^{-13} cm for the range of the force.

The biggest stable, or nearly stable, double closed shell before ^{208}Pb is ^{16}O, whose diameter is only 7×10^{-13} cm, which is not really big enough to justify the approximations. The energy levels which fill at nucleon numbers 20 and 28 do not fall into sufficiently separated groups for ^{40}Ca, ^{48}Ca or ^{56}Ni to count as double closed shells for our purpose.

§ 2. ^{209}Pb AND ^{209}Bi

Little is known experimentally about the excited levels of these nuclei. The spin of the ground state of ^{209}Bi is 9/2 and the magnetic moment indicates that the odd (83rd) proton is in an $h_{9/2}$ state. The shell model gives $h_{9/2}$, $f_{7/2}$, $f_{5/2}$, $p_{3/2}$, $p_{1/2}$ and $i_{13/2}$ as low lying states. Analogy with earlier closed shells would suggest the order $h_{9/2}$, $f_{7/2}$, $p_{3/2}$ . . . , with $i_{13/2}$ probably interpolated before $p_{3/2}$, or even before $f_{7/2}$. The order of the levels in ^{207}Pb, a nucleus with one hole in the corresponding neutron shell, discussed in §4, suggests that possibly the order is $h_{9/2}$, $i_{13/2}$, $f_{7/2}$. . . . In lighter nuclei where this neutron shell is starting to fill, however, the ground state of nuclei with 83 neutrons is $f_{7/2}$. There is indirect evidence from the following work, and from the levels of ^{211}Bi (AcC), which should be similar, that these levels are close together. Information on the excited states could in principle be obtained from the inelastic scattering of neutrons in bismuth, from the reaction ^{208}Pb(dn)^{209}Bi, and from gamma-radiation following electron capture in ^{209}Po. The energy needed to dissociate ^{209}Bi into ^{208}Pb and a proton can be calculated from a closed cycle (Kinsey *et al.* 1951). It is 3·79 Mev.

The ground state spin of ^{209}Pb is not known. Information about the excited states is available from the reaction ^{208}Pb(dp)^{209}Pb (Harvey 1951 a). There are proton groups corresponding to excited states at 0·75 Mev, 1·56 Mev, 2·03 Mev, and 2·54 Mev. The dissociation energy into ^{208}Pb and a neutron is 3·87 Mev. The resolution of this experiment is only 0·5 Mev, and some of these levels may be unresolved multiplets. According to the shell model the lowest group of states is $i_{11/2}$, $g_{9/2}$, $g_{7/2}$, $d_{5/2}$, $d_{3/2}$, $s_{1/2}$ and $j_{15/2}$. The spin–orbit coupling, which is presumably large for the high angular momenta, may bring $j_{15/2}$ well down towards the bottom of the group, and may push $i_{11/2}$ above $g_{9/2}$. The ft-value of the beta decay of ^{209}Pb is compatible with either $g_{9/2}$ or $i_{11/2}$ for the ground state, but not with $j_{15/2}$. The low intensity of the proton group corresponding to the first excited state at 0·75 Mev (14 Mev deuterons, 15 Mev protons) might be taken as an indication of high angular momentum transfer, and suggests that this is the $j_{15/2}$ level.

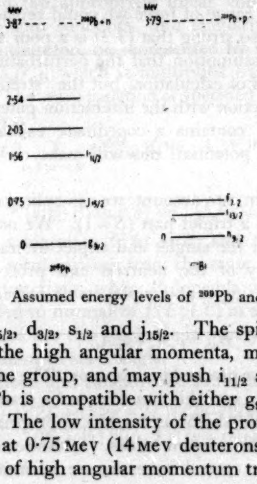

Fig. 1. Assumed energy levels of ^{209}Pb and ^{209}Bi.

These considerations suggest that the ground state is $g_{9/2}$ (or $i_{11/2}$), the 0·75 Mev state is $j_{15/2}$, the 1·56 Mev state is $i_{11/2}$ (or $g_{9/2}$) and the 2·03 Mev state is $d_{5/2}$ or $g_{7/2}$, but the evidence is very inconclusive. It is summarized in tentative form in fig. 1. Further information could be obtained from the study of the so far undetected gamma-radiation following the decay of ^{209}Tl.

§ 3. ^{210}Bi (RaE)

We shall treat ^{210}Bi as a system consisting of a neutron and a proton moving in the equivalent field of the closed shell. Concerning this field we shall assume that it is spherically symmetrical and gives rise to the one-particle states discussed above. This means, of course, that it contains strong spin–orbit interaction to give the necessary doublet splittings. We shall treat the perturbation arising from the proton–neutron interaction as small compared with the spin–orbit splitting (in other words, we adopt *jj*-coupling). This is probably a tolerabel approximation, but a quantitative estimate indicates that it may break down when the proton and neutron wave functions overlap strongly.

We shall further assume that the perturbation in the energy is proportional to the probability $\bar{\rho}$ (per unit volume) that the neutron and proton are in each other's immediate neighbourhood. If we were dealing with spinless particles whose wave function is $\Psi(\mathbf{r}_n, \mathbf{r}_p)$ this would be

$$\bar{\rho} = \int |\Psi(\mathbf{r}, \mathbf{r})|^2 \, d^3\mathbf{r}. \qquad \ldots\ldots(3.1)$$

The effect of spin is considered below.

The justification for this assumption is not very firmly based. If the proton–neutron potential $V(|\mathbf{r}_n - \mathbf{r}_p|)$ were weak, we could, ignoring spin as above, and now also any exchange character of V, write the first-order perturbation as

$$E_{np} = \iint |\Psi(\mathbf{r}_n, \mathbf{r}_p)|^2 V(|\mathbf{r}_n - \mathbf{r}_p|) \, d^3\mathbf{r}_n \, d^3\mathbf{r}_p, \qquad \ldots\ldots(3.2)$$

and for sufficiently short range of force we could replace $V(r) A\delta^3(\mathbf{r})$, giving $A\bar{\rho}$. Actually the potential is so strong that (3.2) is a poor approximation. We shall nevertheless retain our assumption that the perturbation energy is $A\bar{\rho}$, for lack of a more precise method of calculation, but the 'strength' will not be assumed to have so direct a connection with the interaction potential as above.

It is clear that if V contains a coordinate exchange operator (as in the Heisenberg or Majorana potential) this will make no difference to (3.2) in the limit of zero range.

If now we take the spin into account, we can split the joint wave function into a singlet part ($S=0$) and a triplet part ($S=1$). We now have to introduce two 'strengths' A_s and A_t for the singlet and triplet interactions. If we denote by $\bar{\rho}_s$ and $\bar{\rho}_t$ the probability of the neutron and proton being in each other's immediate vicinity in the singlet and triplet states respectively, then we can write the mutual energy as

$$E_{np} = \bar{\rho}_s A_s + \bar{\rho}_t A_t. \qquad \ldots\ldots(3.3)$$

To evaluate $\bar{\rho}_s$ and $\bar{\rho}_t$ we proceed in two steps. The unperturbed wave function is in terms of *jj*-coupling, and this has first to be translated into *LS*-coupling. Then for each resultant L which occurs, the appropriate $\bar{\rho}$ must be calculated, and these summed over the relevant values. Cross-terms involving different L's do not occur, since for the central forces we are assuming L and S are constants of the motion.

The neutron will be assumed to be in a state of angular momentum j, compounded of an orbital momentum l and spin $\frac{1}{2}$ ($j = l \pm \frac{1}{2}$); and similarly for the proton we assume j' and l'. The resultant angular momentum of the system is I. We denote the state of the system by $|I; j, j'\rangle_{jj}$ to emphasize its *jj*-coupling nature. It can be expressed as a superposition of states of definite total orbital momentum L and definite total spin S which we denote by $|I; L, S\rangle_{LS}$ to emphasize their *LS*-coupling character. Since S only takes on the values 0 and 1, the sum consists of only four terms:

$$|I; j, j'\rangle_{jj} = \sqrt{\alpha}|I; I, 0\rangle_{LS} + \sqrt{\beta}|I; I, 1\rangle_{LS} + \sqrt{\gamma}|I; I+1, 1\rangle_{LS} + \sqrt{\delta}|I; I-1, 1\rangle_{LS}. \qquad \ldots\ldots(3.4)$$

The calculation of the probability amplitudes $\sqrt{\alpha}$ etc. is fairly straightforward. For the case $j=l+\frac{1}{2}$, $j'=l'+\frac{1}{2}$, their squares, α etc. which are what we shall need, are

$$\left.\begin{aligned}\alpha&=\frac{(I+l+l'+2)(l+l'+1-I)}{2(2l+1)(2l'+1)},\\ \beta&=\frac{(l-l')^2(I+l+l'+2)(l+l'+1-I)}{2(2l+1)(2l'+1)I(I+1)},\\ \gamma&=\frac{(I+1+l-l')(I+1+l'-l)(l+l'-I)(l+l'+1-I)}{2(2l+1)(2l'+1)(I+1)(2I+1)},\\ \delta&=\frac{(I+l-l')(I+l'-l)(I+l+l'+1)(I+l+l'+2)}{2(2l+1)(2l'+1)I(2I+1)}.\end{aligned}\right\}\quad\ldots\ldots(3.5)$$

The expression for the other combinations of $j=l\pm\frac{1}{2}$, $j'=l'\pm\frac{1}{2}$ can be obtained from (3.5) by the simple transformation of replacing l by $-(l+1)$ if $j=l-\frac{1}{2}$, and l' by $-(l'+1)$ if $j'=l'-\frac{1}{2}$.

The wave function of a single neutron can be written as the product of a radial function $\psi_{\mathrm{n}}(r_{\mathrm{n}})$ and the appropriate linear combination of products of spherical harmonics and spin functions, and similarly for the proton. Each of the terms in (3.4) will therefore be represented by a wave function with the radial dependence $\psi_{\mathrm{n}}(r_{\mathrm{n}})\psi_{\mathrm{p}}(r_{\mathrm{p}})$, which is multiplied by the appropriate angular and spin wave function. The wave function of specified L (and $m_L=M$), ignoring the spin part, is of the form

$$\psi_{\mathrm{n}}(r_{\mathrm{n}})\psi_{\mathrm{p}}(r_{\mathrm{p}})\sum_{m+m'=M}C^{LM}_{lml'm'}Y_l^{m}(\theta_{\mathrm{n}},\phi_{\mathrm{n}})Y_{l'}^{m'}(\theta_{\mathrm{p}},\phi_{\mathrm{p}}).$$

Its contribution to $\bar{\rho}$ is

$$\iint\Big|\sum C^{LM}_{lml'm'}Y_l^{m}(\theta,\phi)Y_{l'}^{m'}(\theta,\phi)\Big|^2\sin\theta\,d\theta\,d\phi\int|\psi_{\mathrm{n}}^2(r)\psi_{\mathrm{p}}^2(r)|r^2\,dr.\quad\ldots\ldots(3.6)$$

Let us call the angular integral in (3.6) $4\pi P$, and the radial integral $Q/4\pi$. Q is the same for all the terms arising from the same configuration, depending only on the radial wave functions, while P depends only on L, l and l'. The factor 4π has been included to normalize $P(L;l,l')$ in such a way that it is unity if the angular correlation of the two nucleons is purely random. P is therefore a measure of their correlation in solid angle.

It is given by (cf. Carlson and Rushbrooke 1950, eqn. 17)

$$P(L;l,l')=\frac{(2l+1)(2l'+1)(2g-2L)!\,(2g-2l)!\,(2g-2l')!\,(g!)^2}{(2g+1)!\,\{(g-L)!\,(g-l)!\,(g-l')!\}^2}$$

if $2g=L+l+l'$ is even and

$$P(L;l,l')=0\quad\ldots\ldots(3.7)$$

if $L+l+l'$ is odd.

The interaction energy is therefore given by

$$E_{\mathrm{np}}=\alpha P(I;l,l')A_{\mathrm{s}}Q+[\beta P(I;l,l')+\gamma P(I+1;l,l')+\delta P(I-1;l,l')]A_{\mathrm{t}}Q,\quad\ldots\ldots(3.8)$$

in which the quantities P, α, β, γ and δ are directly calculable. For convenience we write

$$\left.\begin{aligned}&\epsilon_{\mathrm{s}}=A_{\mathrm{s}}Q,\quad \epsilon_{\mathrm{t}}=A_{\mathrm{t}}Q,\\ \text{and}\quad &a_{\mathrm{s}}=\alpha P(I;l,l'),\\ &a_{\mathrm{t}}=\beta P(I;l,l')+\gamma P(I+1;l,l')+\delta P(I-1;l,l'),\end{aligned}\right\}\quad\ldots\ldots(3.9)$$

so that the expression for E_{np} becomes

$$E_{\mathrm{np}} = a_s\epsilon_s + a_t\epsilon_t. \qquad \ldots\ldots(3.10)$$

The quantities ϵ_s and ϵ_t have the dimensions of energy. They are determined by the degree of overlap of the radial wave functions of the neutron and proton, and by the strength of the proton–neutron potential. The numerical quantities a_s and a_t depend, for a given configuration (i.e. j, j', l, l' given), only on the resultant angular momentum I.

At this stage it is instructive to make a rough estimate of the order of magnitude of the ϵ's. If we consider those single-particle states in which the l-value appears for the first time in the enumeration of the states in order of energy, the radial wave functions have no nodes, and their maxima are fairly sharp and overlap considerably (e.g. the configuration ($\mathrm{j}_{15/2}$, $\mathrm{h}_{9/2}$)). Such configurations will have the largest value of Q. Assuming that the nuclear radius R is about $8{\cdot}4\times10^{-13}$ cm, and that the effective 'spread' S of the radial wave function is about 2×10^{-13} cm, one estimates

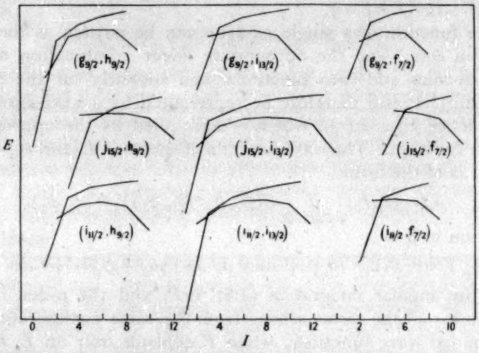

Fig. 2. Dependence of the interaction energy E_{np} in ^{210}Bi on nuclear spin I for the nine configurations considered. Energy scale is arbitrary. ($3a_t+2a_s$ drawn to same scale for each configuration, corresponding to the assumption $\epsilon_t/\epsilon_s = 1{\cdot}5$).

$$(4\pi Q)^{-1} \simeq s(R-\tfrac{1}{2}s)^2 \simeq 110\times10^{-39}\,\mathrm{cm}^3.$$

Further, if we suppose that V is adequately represented by a square well 35 MeV deep and of range 2×10^{-13} cm, and for A we take $4\pi\int r^2V\,dr$, then $A/4\pi \simeq -93\times10^{-39}$ MeV cm^3. So $\epsilon = AQ \simeq -0{\cdot}85$ MeV. We shall take this figure as a guide to the order of magnitude only. For configurations in which there is little radial overlap it may be much smaller.

Table 1 shows the numerical parameters a_t and a_s for the nine configurations formed from $\mathrm{g}_{9/2}$, $\mathrm{j}_{15/2}$, $\mathrm{i}_{11/2}$ for the neutron, and $\mathrm{h}_{9/2}$, $\mathrm{i}_{13/2}$, $\mathrm{f}_{7/2}$ for the proton. In order to show the relative behaviour inside each configuration in graphical form, the definite value 1·5 has been chosen for the ratio $\epsilon_t/\epsilon_s = A_t/A_s$. This value corresponds roughly to the relative strengths of Yukawa potentials of equal range which will account for the low-energy proton–neutron and proton–proton scattering data. Having fixed this ratio, E_{np} now depends only on one undetermined scale factor. Figure 2 shows E_{np} plotted against I for the nine configurations, the energy scale being arbitrary. The general qualitative features which emerge are very insensitive to the ratio ϵ_t/ϵ_s.

Table 1. Coefficients of ϵ_s and ϵ_t for RaE

Configuration	I	0	1	2	3	4	5	6	7	8	9	10	11	12	13	14
($g_{9/2}$, $h_{9/2}$) (odd)	a_s	0	0·051	0	0·120	0	0·210	0	0·358	0	0·859					
	a_t	5·000	2·525	1·212	0·999	0·629	0·699	0·373	0·640	0·202	0·955					
($g_{9/2}$, $i_{13/2}$) (even)	a_s			2·203	0	0·870	0	0·518	0	0·327	0	0·183	0			
	a_t			1·469	1·061	0·174	0·891	0·049	0·877	0·018	1·040	0·007	1·951			
($g_{9/2}$, $f_{7/2}$) (odd)	a_s		2·222	0	0·779	0	0·420	0	0·218	0						
	a_t		1·111	1·255	0·065	0·908	0·014	0·956	0·004	1·713						
($j_{15/2}$, $h_{9/2}$) (even)	a_s				0	0·090	0	1·064	0	0·258	0	0·414	0	0·960		
	a_t				3·427	0·758	1·048	0·658	0·571	0·604	0·346	0·636	0·190	1·040		
($j_{15/2}$, $i_{13/2}$) (odd)	a_s		3·733	0	1·368	0	0·818	0	0·556	0	0·391	0	0·269	0	0·158	0
	a_t		1·867	1·951	0·114	1·203	0·027	0·963	0·010	0·897	0·004	0·944	0·002	1·158	0·001	2·201
($j_{15/2}$, $f_{7/2}$) (even)	a_s					1·523	0	0·622	0	0·360	0	0·195	0			
	a_t					1·218	0·668	0·237	0·772	0·080	0·966	0·028	1·858			
($i_{11/2}$, $h_{9/2}$) (odd)	a_s		2·727	0	0·979	0	0·559	0	0·346	0	0·191	0				
	a_t		1·364	1·480	0·082	0·986	0·019	0·894	0·006	1·023	0·002	1·891				
($i_{11/2}$, $i_{13/2}$) (even)	a_s		0	0·006	0	0·115	0	0·182	0	0·273	0	0·431	0	0·985		
	a_t		4·846	1·655	1·273	0·973	0·714	0·732	0·463	0·640	0·303	0·662	0·174	1·067		
($i_{11/2}$, $f_{7/2}$) (odd)	a_s			0	0·010	0	0·196	0	0·346	0	0·842					
	a_t			3·030	0·833	0·734	0·653	0·429	0·671	0·219	0·936					

The energy of the complete system is the sum of the energy of the closed shell, the energy of the neutron, the energy of the proton, and the interaction energy:

$$E = E_0 + E_n + E_p + E_{np}. \qquad \ldots\ldots(3.11)$$

Owing to the uncertainty discussed in §2 concerning E_n and E_p only limited conclusions can be drawn, but certain points emerge clearly.

It will be seen from fig. 2 that in each configuration (i) the lowest energy is attained for the lowest possible value of I, (ii) even and odd values of I behave differently, (iii) proceeding from the lowest I-value in steps of 2, the energy increases monotonically, (iv) descending from the highest I-value in steps of 2, the energy first increases to a maximum and (with one exception) decreases again.

From this it can be inferred that the ground state of RaE corresponds to the lowest I-value of some configuration.

Another conclusion of great interest is that there must be an isomeric state of very high spin (at least 8). This follows from the fact that in each configuration the state of maximum I is lower in energy than all states whose I differs by less than 7 units, and it is a fair inference that the maximum I-state which has the lowest energy among the various configurations is below all other states which do not differ in I by less than 6 or 7 units. Such a state will obviously have an astronomical lifetime against gamma-ray emission, and against beta-emission to any plausible energetically allowed state of ^{210}Po. Its most probable mode of decay will be by alpha-particle emission to ^{206}Tl. An alpha-emitting isomer of RaE is in fact known (Neumann, Howland and Perlman 1950), whose energy above the ground state is estimated to be 0·18 ± 0·11 MeV. Of the nine configurations which have been studied all have a maximum I-value of at least $I = 8$. Consideration of the single-particle energies (E_n, E_p) and the overlap of the radial wave functions make the following combinations possible competitors for the isomeric state: $(g_{9/2}, h_{9/2})_{I=9}$, $(g_{9/2}, i_{13/2})_{I=11}$, $(g_{9/2}, f_{7/2})_{I=8}$, $(j_{15/2}, h_{9/2})_{I=12}$, $(j_{15/2}, i_{13/2})_{I=14}$.

A certain amount is known experimentally concerning the energy levels of RaE. It is formed in the natural radioactive sequence by the beta-decay of RaD, leading to an excited state. The transition energy is very low, probably about 18 kev (Bannerman and Curran 1952). No measurable decay to the ground state takes place. The lifetime of RaD (taken with the assumption $I = 0$, even, for RaD) is compatible with $I = 0$ or 1 for the resultant state of RaE. There are at least six soft gamma-rays following the beta-decay, of which the most energetic has an energy of 46·7 kev (Tsien 1946, Feather 1949). This indicates at least three intermediate states. In addition there is the isomeric state already mentioned. Also the work of Harvey (1951 a) with the reaction ^{209}Bi(dp)^{210}Bi indicates levels at 1·65, 2·2 and 2·8 MeV. The present analysis would suggest that these 'levels' are the unresolved configurations (or rather the densest part) formed from the proton in its ground ($h_{9/2}$) state and the neutron in the states corresponding to the 1·56, 2·03 and 2·54 MeV levels in ^{209}Pb. (The absence of a group corresponding to the 0·75 level can be ascribed to a combination of the high spin and the large splitting of the configuration). The work of Kinsey, Bartholomew and Walker (1951) on the neutron-capture gamma-rays of bismuth also throws light on the question, and is discussed more fully below.

The spin and parity of the ground state of RaE have been deduced from the shape of the beta-spectrum (RaE → RaF) to be $I = 2$ (even). This assignment, though plausible, is subject to some doubt as it rests on assumptions concerning the form of the fundamental beta-decay interaction. If it is correct, the ground state is $(g_{9/2}, i_{13/2})_{I=2}$.

The state in which RaE is formed in the beta-decay of RaD is one of the following: $(g_{9/2}, h_{9/2})_{I=0}$, $(j_{15/2}, i_{13/2})_{I=1}$, $(g_{9/2}, f_{7/2})_{I=1}$, $(i_{11/2}, h_{9/2})_{I=1}$, $(i_{11/2}, i_{13/2})_{I=1}$.

The assignment of the intermediate states is narrowed down by this analysis, but much ambiguity remains.

In the configurations we have studied there are several states with the same parity and same value of I. If any of these fall close together in energy on a first-order calculation, then second-order effects may be important (configurational interaction), with the result that the levels are pushed apart and their character mixed. This further increases the ambiguity of the interpretation.

The gamma-ray spectrum resulting from the capture of thermal neutrons by ^{209}Bi (leading to RaE) consists of a broad line of energy 4·17 MeV (maximum) (Kinsey, Bartholomew and Walker 1951). A comparison of this energy with the binding energy of a neutron in RaE obtained from a closed cycle shows a discrepancy of 0·37 MeV (Kinsey, Bartholomew and Walker 1951), the binding energy deduced being 4·54 MeV. A comparison of this value with the value 3·87 MeV in ^{209}Pb gives some indication of the magnitude of the proton–neutron interaction ($4·54-3·87=0·67$ MeV, not all of which is necessarily due to E_{np} since the field of the core is altered slightly). On the basis of the present calculations one would not expect the capture radiation to lead to the ground state, but rather to a group of excited states, for the spin of the capture state $(s_{1/2}, h_{9/2})$ is either 4 or 5 (odd), so that gamma-emission is most likely to states of spin $I=2$ (odd), 3, 4, 5, 6, (7). The observed width of the line (0·07 MeV more than the instrumental width) and the energy discrepancy of 0·37 MeV can be fitted into the scheme which we have obtained above, as may be seen from fig. 3, which gives a highly speculative picture of the levels. The subsequent de-excitation of these levels is presumably by a cascade of soft gamma-rays (which would not have been detected with a pair spectrometer), and may lead either to the ground state or to the isomeric state (in conformity with its known mode of production).

To show that the various data can be reconciled with the ideas outlined above, fig. 3 shows the level scheme which results from a definite choice of numerical values for the parameters. For convenience levels with different I's have been separated. These are far from being uniquely determined by the data, and the figure should not be taken as more than extremely speculative. In particular, no significance should be given to the precise order of the levels. It will be seen that the known facts fit satisfactorily into the scheme. In the ^{209}Bi(dp)^{210}Bi reaction the groups of levels reached are those marked a and d ; in the capture radiation of bismuth it will be mainly a selection of a levels in the spin range $I=3$–6. The parameters have been chosen so as to bring five levels into the lowest 50 kev in a way which might be fitted to the known gamma-rays.* This coincidence of so many levels in a narrow energy range appears to be the result of chance, and this is a rather unsatisfactory feature of the proposed scheme. It will be noticed that three of these five levels have spin 1, the other two having

---

* The level scheme proposed by Bannerman and Curran involves six levels. More experimental work is still needed to decide the level scheme, but if a sixth level is required, $(i_{11/2}, h_{9/2})_{I=1}$ might supply it.

$I=0$ and 2. The existence of possible isomeric levels with an energy around 0·2 MeV, however, follows naturally from the parameters chosen to give the correct discrepancy in the capture radiation energy, and speaks in favour of the scheme. The values of ϵ_t chosen lie in the range 0·1 – 0·5 MeV, in satisfactory agreement with the calculated order of magnitude.

The situation is further complicated by the possibility of low levels arising by raising a nucleon from the core and pairing it off with one of the odd nucleons in a state of high *j*, as discussed at the end of §7.

Our result, that in any configuration the state of minimum spin has the lowest energy, contradicts a rule enunciated by Nordheim (1950). This states that in odd–odd nuclei the lowest level is that of minimum or maximum *I* according to which makes the spins of the neutron and proton most nearly parallel. Empirically it is fairly reliable for light and medium nuclei, though it does not hold without exception. Our formulae for the interaction energy show that for reasonably low *j*-values the state of maximum spin is indeed the lowest level in the cases where Nordheim's rule demands it, provided a suitably high value of ϵ_t/ϵ_s is taken, but that for high *j*-values the value of ϵ_t/ϵ_s required to make the rule hold is impossibly high. It is quite possible that the effect of the range of the force, which is more important in lighter nuclei, favours the high spins. In any case, in view of the known exceptions, the present results should be taken rather as elucidating its range of validity than as a contradiction to it.*

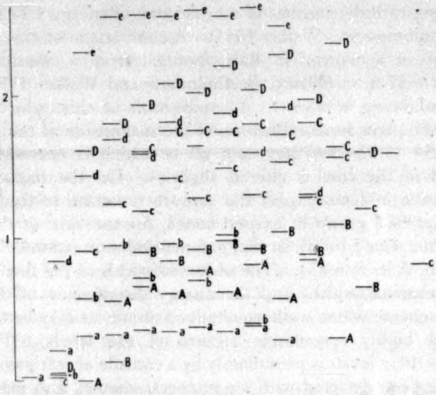

Fig. 3. Very tentative diagram of energy levels of ^{210}Bi arising from the nine configurations considered. The figure is to be interpreted only as suggesting in a general way the predicted complexity of the level scheme. Details are not meant to be correct. Key: $A=(g_{9/2}, i_{13/2})$, $B=(j_{15/2}, h_{9/2})$, $C=(j_{15/2}, f_{7/2})$, $D=(i_{11/2}, i_{13/2})$, $a=(g_{9/2}, h_{9/2})$, $b=(g_{9/2}, f_{7/2})$, $c=(j_{15/2}, i_{13/2})$, $d=(i_{11/2}, h_{9/2})$, $e=(i_{11/2}, f_{7/2})$. Capital letters indicate even states, lower case odd states.

---

* Actually, even for lighter nuclei the present results, although not directly applicable to nuclei far from closed shells, seem to be in better agreement with experiment than Nordheim's. In ^{26}Al, for example, the present calculations applied to $(d_{5/2})^2$ give $I=0$ lowest, in agreement with the superallowed character of the beta-decay, as contrasted to Nordheim's $I=5$. In ^{58}Co and ^{60}Co $(f_{7/2}, p_{3/2})$, the present calculations indicate that $I=2$, $I=5$ are very close (crossing over for $\epsilon_t/\epsilon_s=1{\cdot}59$), in agreement with known isomeric states of probable spins 2 and 5, whose order is opposite in the two isotopes.

§ 4. ^{210}Pb (RaD) AND ^{210}Po (RaF)

These nuclei will be regarded as two neutrons, or two protons, moving in the field of the core. The identity of the two particles introduces a small modification to the calculations of § 3. The wave functions must be made antisymmetrical, and this means that the two nucleons can only be close together in the singlet state, so that only the singlet interaction is effective. The mutual energy is

$$2\alpha P(I; l, l')\epsilon_s \qquad \ldots\ldots(4.1)$$

(except when $j=j'$, $l=l'$, when the factor 2 is absent). A general feature of (4.1) is that the interaction energy is zero for alternate values of I.

If we consider RaD, and use the assignment of neutron levels discussed in § 2, it follows that the ground state probably arises from $(g_{9/2})^2{}_{I=0}$. The remaining states, $I=2$, 4, 6, 8, of this configuration (odd values are forbidden by the Pauli principle) are higher and follow in that order. The gap between 0 and 2 is considerably greater than between the remainder (the numerical values suggested by the fitting of the RaE levels would indicate that $I=0$ lies about 0·5 MeV below $I=2$). There will be other levels corresponding to $(g_{9/2}, j_{15/2})$ of which those with $I=4$, 6, 8, 10, 12 will have an energy about 0·75 MeV above the 'head' of $(g_{9/2})^2$, while those with $I=3$, 5, 7, 9, 11 will be lowered by neutron–neutron interaction ($I=3$ lowest). Similarly there will be levels arising from $(j_{15/2})^2$, whose head will be about 1·5 MeV above the head of $(g_{9/2})^2$. Owing to the high j-value and the concentrated nature of the radial wave function, $(j_{15/2})^2{}_{I=0}$ may be strongly depressed and may possibly even compete with $(g_{9/2})^2{}_{I=0}$ for the ground state.

RaD is formed in a highly excited state in the beta decay of RaC″(^{210}Tl). Gamma-rays of energy 3·1, 4·0 and 4·9 MeV are known. If we apply the present ideas to RaC″, regarding it as a proton hole (in an $s_{1/2}$ state) and three neutrons, and assume the three neutrons in their ground state to act as one neutron in a $g_{9/2}$ state, then we conclude that the ground state is $I=5$ (even). Since the beta-decay appears to be allowed, RaD must be formed in a state of spin at least 4. The gamma-rays therefore presumably do not go direct to the ground state. In the alpha-decay of RaC′, RaD is formed in the ground state, and since its formation from RaC″ is a rare mode of decay, nothing seems to be known experimentally concerning its lower excited levels. It is therefore not profitable at present to work out anything in great detail.

Similar results apply to ^{210}Po, with two protons. Since, however, there is some reason to believe that the $h_{9/2}$, $i_{13/2}$ and $f_{7/2}$ states are closer together than the corresponding neutron states, there will be more overlap of the configurations. In particular, it is not clear which will be the lower of the two states $(h_{9/2})^2{}_{I=0}$, $(i_{13/2})^2{}_{I=0}$, and they may in fact be quite close together (though configurational interaction will tend to push them apart). The claim has been made by Zavelsky, Umarov and Matushevsky (1949) that the beta decay of RaE is complex, leading most of the time to an excited state of ^{210}Po 85 kev above ground. Although their interpretation of their experiments does not seem very convincing, such an excited state could be fitted into the theoretical scheme. It would not emit gamma-rays. Otherwise the only known gamma-ray emitted by ^{210}Po is that following electron capture in ^{210}At, of energy about 1 MeV.

.A
5
2

§ 5. ^{207}Pb AND ^{207}Tl (AcC″)

These nuclei can be treated as holes in the closed shell. The energy required to remove a particle, leaving a hole in a definite state, will roughly speaking be the one-particle energy of that state, plus the 'pairing' energy, which in the short-range approximation is the same as the interaction energy $(j+\frac{1}{2})\epsilon_s$ of two similar particles in the same orbital with resultant $I=0$ (Mayer 1950 b). The low-lying energy levels of these nuclei will therefore follow approximately inversely the order of the one-particle states. The available low levels for ^{207}Pb on the shell model are $p_{1/2}$, $p_{3/2}$, $f_{5/2}$, $f_{7/2}$, $h_{9/2}$ and $i_{13/2}$, and for ^{207}Tl $s_{1/2}$, $d_{3/2}$, $d_{5/2}$, $g_{7/2}$ and $h_{11/2}$. For ^{207}Pb there is enough experimental material to fix all these levels except $h_{9/2}$. The level diagram is shown in fig. 4 (the reasons for this assignment of levels are given in the Appendix). The $h_{9/2}$ level is probably somewhere about 2·3 Mev. The levels shown above 2 Mev (which are formed by electron capture in ^{207}Bi) are more complex in structure, involving excitation of other nucleons in the closed shell.

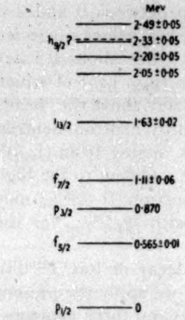
Mev
2·49 ± 0·05
$h_{9/2}$?
2·33 ± 0·05
2·20 ± 0·05
2·05 ± 0·05
$i_{13/2}$
1·63 ± 0·02
$f_{7/2}$
1·11 ± 0·06
$p_{3/2}$
0·870
$f_{5/2}$
0·565 ± 0·01
$p_{1/2}$
0

Fig. 4. Energy levels of ^{207}Pb.

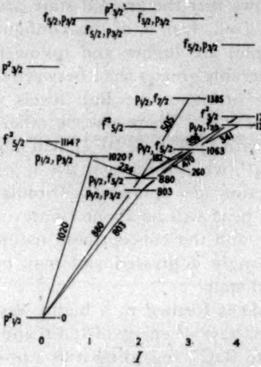
$p^2_{3/2}$
$f_{5/2}, p_{3/2}$
$f_{5/2}, p_{3/2}$
$f_{5/2}, p_{3/2}$
$f_{5/2}, p_{3/2}$
$p^2_{3/2}$
$p_{1/2}, f_{7/2}$
1385
$f^2_{5/2}$
$f^2_{7/2}$
1275
$p_{1/2}, f_{7/2}$
1221?
$f^2_{5/2}$
1114?
505
541
$p_{1/2}, f_{5/2}$
1063
$p_{1/2}, p_{3/2}$
1020?
182
234
260
$p_{1/2}, f_{5/2}$
880
$p_{1/2}, p_{3/2}$
803
1020
880
803
$p^2_{1/2}$
0
0
1
2
3
4
I

Fig. 5. Tentative level diagram of ^{208}Pb. Energies are in kev.

^{207}Tl is known to have an excited state 0·35 Mev above ground (long-range alphas of AcC), but experimental evidence beyond that is meagre. The ground state and first excited state are presumably $s_{1/2}$ and $d_{3/2}$ respectively.

§ 6. ^{206}Pb, ^{206}Tl AND ^{206}Hg

The methods already developed for RaD, RaE and RaF apply to these nuclei. The fact that we are dealing with two holes instead of two particles makes only minor differences. The energy of a single hole must be taken to be minus the energy of the particle in the corresponding state. The interaction energy, on the other hand, has the same sign for two holes as for two particles, and is given by the same formula. It is also readily verified that, more generally, in *jj*-coupling, the interaction of a hole with a particle (as in ^{208}Tl or ^{208}Bi, or the excited states of ^{208}Pb) has the same sign, so that no distinction need be made between holes and particles in discussing the effects of mutual interaction.

We shall discuss only ^{206}Pb in detail. Its levels are based on those of ^{207}Pb (one hole), the lowest five of which are well established. Fifteen gamma-rays of ^{206}Pb are known (Alburger and Friedlander 1951). There is therefore some hope of correlating theory and experiment.

Let us first consider the energies of the heads of the several configurations. Were it not for the pairing energy, these would in zero approximation (neglecting configurational interaction and the effects of the difference in the effective field of the core) be given by adding the two corresponding single-hole energies. This is shown in the second column of table 2. The third column shows the coefficients a_s of ϵ_s, in the expression (4.1) which gives the effect of mutual interaction.

Table 2. Levels of ^{206}Pb

Configuration	Energy of head (uncorrected) (Mev)	$\longleftarrow$			a_s				$\longrightarrow$
		$I=$ 0	1	2	3	4	5	6	7
$(p_{1/2})^2$	0·0	1							
$(p_{1/2}, f_{5/2})$	0·565			$\frac{6}{5}$	0				
$(p_{1/2}, p_{3/2})$	0·87		0	$\frac{4}{5}$					
$(f_{5/2})^2$	1·13	3		$\frac{24}{35}$		$\frac{2}{7}$			
$(p_{1/2}, f_{7/2})$	1·11				0	$\frac{8}{9}$			
$(f_{5/2}, p_{3/2})$	1·43		0	$\frac{12}{35}$	0	$\frac{8}{7}$			
$(p_{1/2}, i_{13/2})$	1·62							0	$\frac{14}{15}$
$(f_{5/2}, f_{7/2})$	1·67		0	$\frac{8}{35}$	0	$\frac{40}{77}$	0	$\frac{200}{143}$	
$(p_{3/2})^2$	1·74	2		$\frac{2}{5}$					

The correction for the pairing effect in the levels of ^{207}Pb is the sum of the pairing energies of the two states in the configuration (a positive correction), together with a negative correction to allow for the change of zero (conventionally the ground state of ^{206}Pb). Theoretically the pairing energy in an orbit j is $(j+\frac{1}{2})\epsilon_s$, being evaluated for the configuration j^2, so that in principle the pairing correction and the configurational splitting are not independent.

The following results emerge. The ground state is $(p_{1/2})^2{}_{I=0}$. The first excited state is either $(p_{1/2}, f_{5/2})_{I=2}$ or $(p_{1/2}, p_{3/2})_{I=2}$ or possibly $(f_{5/2})^2{}_{I=0}$. All the states up to at least 1·5 Mev are even states (the first odd states are $(p_{1/2}, i_{13/2})$ with $I=6$ and 7).

There is experimental evidence that the first excited state is at 803 kev. It results from the emission of short-range alpha-particles from ^{210}Po, which is followed by a single gamma-ray (Alburger and Friedlander 1951, Grace *et al.* 1951). The spin is inferred to be $I=2$ (even) from the alpha–gamma angular correlation (de Benedetti, private communication to H. Halban). This evidence does not exclude states of parity opposite to that of I being lower, since these could not be reached in the alpha-decay of Po; nor does it exclude $I=0$ being lower, as such a state would not emit gamma-rays (though it is unlikely that the resultant orbital electron emission would have been missed). Nevertheless it seems reasonable to assume that the first excited state is indeed at 803 kev with $I=2$ (even). Although the gamma-rays have been resolved to 1·2%, and their energy measured to ½%, this accuracy is not sufficient to fit them unambiguously into a term diagram. The present considerations help to some extent, but very considerable ambiguity remains. An attempt at a level scheme bearing the various factors in mind is shown in fig. 5. No part of this is to be regarded as more than very tentative. This is particularly true of the assignment of the first excited state of ($p_{1/2}$, $p_{3/2}$), which makes some of the selection rules easier than ($p_{1/2}$, $f_{5/2}$) but the indications are very slight. On the other hand, the picture that this gives of many levels within the first 2 Mev is probably reliable.

§ 7. ^{208}Tl, ^{208}Bi AND THE EXCITED STATES OF ^{208}Pb

^{208}Tl (ThC″) can be regarded as made up of a proton hole and a neutron. The relevant one-particle levels are therefore those of ^{207}Tl for the hole, and of ^{209}Pb for the neutron. We therefore expect the lowest levels to arise from ($s_{1/2}$, $g_{9/2}$) and ($d_{3/2}$, $g_{9/2}$)—which should form a doublet and a quartet respectively. The levels of ThC″ have been exhaustively studied (Surugue 1937) and the experimental evidence is in good agreement with this assignment (though other assignments of the neutron state would fit just as well). Table 3 lists the experimental levels (line 1), the theoretical spin (line 2) and calculated values of a_t and a_s (lines 3 and 4). All the states have even parity. The intensities of the long-range alpha groups of ThC fit in well with the predicted spins. It will be noticed that the quartet is reasonably fitted by the values $\epsilon_t=-225$ kev, $\epsilon_s\simeq-130$ kev. The doublet splitting indicates $\epsilon_t-\epsilon_s=-72$ kev (the ϵ's are of course different in the two cases). The spacing between the two groups is about 150 kev more than would be calculated using the 350 kev spacing in ^{207}Tl.

Table 3. Levels of ^{208}Tl

Experimental energy (kev)	0	40	328	472	492	616
Predicted spin	5	4	3	6	4	5
a_t	1·000	0·444	1·667	0·734	0·495	0·394
a_s	0·000	0·556	0·000	0·629	0·202	0·000

^{208}Bi is similarly made up of a neutron hole (levels $p_{1/2}$, $f_{5/2}$, $p_{3/2}$ etc., as in ^{207}Pb) and a proton (levels $h_{9/2}$, $i_{13/2}$, $f_{7/2}$ etc., as in ^{209}Bi). Since the first three proton levels are probably fairly close together, and the first two levels of ^{207}Pb are only 0·54 Mev apart, there are probably at least 24 levels of ^{208}Bi below 1 Mev. The ground state is probably $I=5$ (even).

Only negative evidence exists concerning ^{208}Bi. It is supposed to be unstable against electron capture to ^{208}Pb, with a very long life. The high predicted spin value supports this.

One would imagine that the lowest excited levels of the closed shell nucleus ^{208}Pb itself would arise from the excitation of either a proton or a neutron, and that they could be treated in terms of a particle and a hole. The high energy (2·62 Mev) of the first observed level would at first sight appear to be understandable on this view, but a more detailed comparison with known facts reveals difficulties. For one thing, the difference in the binding energies of a neutron in ^{208}Pb (7·38 Mev) and in ^{209}Pb (3·87 Mev), and of a proton in ^{208}Pb (8·05 Mev) and in ^{209}Bi (3·79 Mev), suggests that about 3·5 Mev and 4·2 Mev is required to lift a neutron and a proton respectively to a level in the next shell. It is therefore difficult to understand in this way a level as *low* as 2·62 Mev. In addition, the lowest levels would be expected all to have either rather high spins, or odd parity, or both. If a neutron is excited, for example, one would expect the levels to arise from $(p_{1/2}, g_{9/2}) : I = 4, 5$ (odd) or $(f_{5/2}, g_{9/2}) : I = 2-7$ (odd). If a proton, then $(s_{1/2}, h_{9/2}) : I = 4, 5$ (odd), $(s_{1/2}, i_{13/2}) : I = 6, 7$ (even), $(s_{1/2}, f_{7/2}) : I = 3, 4$ (odd), or $(d_{3/2}, h_{9/2}) : I = 3-7$ (odd), etc. There is evidence, however, that the 2·62 Mev level has $I = 1$ or 2 (even). It is clear that none of the above combinations can explain this.

A possible way out of the difficulty is to suppose that the lowest excited levels correspond to the excitation of *two* nucleons, which both go into a state of high angular momentum and pair off with zero resultant. The pairing energy gained in this way can be very high (e.g. for the $j_{15/2}$ neutron state it might well amount to 5 Mev), so that it may be energetically more economical to excite two nucleons than one. The different excited levels would then correspond to the configuration of the holes out of which the two nucleons came. The resulting level diagram would bear some resemblance to the level schemes of ^{206}Pb, ^{206}Tl and ^{206}Hg, all raised up in energy and superposed. On any such view, the theoretically expected level diagram is extremely complex.

This explanation is not without its difficulties, however, for one inevitable consequence is that the lowest excited state should have $I = 0$ (even). No experimental evidence exists for such a state, which would presumably emit electron–positron pairs and orbital electrons. Its energy would presumably be about 2 Mev and, if it were excited, its characteristic radiations would be easily detected. If it exists, it may be that failure to detect it arises from its not being formed to any appreciable extent following the beta decay of ThC″—which probably leads in the first instance to a state of fairly high spin, from which it would not be fed—and that when the 2·62 Mev is reached the overwhelming majority of gamma-rays lead to the ground state.

Although this conjecture may appear fanciful, one must remember that in another double closed shell nucleus, ^{16}O, the first excited state has $I = 0$ (even) and emits pairs—presumably for very similar reasons to those outlined above.

If this explanation is correct, one might expect a similar phenomenon in RaE. Raising one neutron from the core to pair off the odd neutron in a $j_{15/2}$ orbit, for instance, may give rise to a low energy state. The RaE problem must therefore be considered as still open. Similar levels can also occur in ^{209}Bi and ^{209}Pb.

§ 8. DISCUSSION

In this paper an elaborate deductive structure has been erected on extremely flimsy foundations. Not only has it been assumed that it is safe to calculate nuclear energies as though one were dealing with an essentially independent-particle model—and the recent successes of the strong spin–orbit model indicate that this approach is valid beyond what appears to be superficially reasonable—but use has been made of definite assignments of orbital states and energies of the individual particles, often based on very little direct evidence. The intention of this work is frankly exploratory, and for that reason the methods of calculation have been as simple as possible. This has been achieved by assuming that the forces are of very short range, ignoring non-central forces and assuming rigorous *jj*-coupling. The apparent success of much of the resulting theory in reconciling available experimental data must not be taken too seriously as support for the hypotheses. Other assignments might do just as well or better, and fatal discrepancies may yet be found. Further analysis, both theoretical and experimental, is now required.

On the theoretical side, much can still be learnt from the careful study of the available experimental material. The present work was started two years ago with the view of understanding the energy levels of RaE, as a modest beginning to a study of nuclear energies generally, but no real progress was made until the interpretation of the data on ^{207}Pb was found. This gave sufficient confidence in the general predictions of the shell model, and definite enough results, for an extrapolation to the next shell to be attempted. Not until further qualitative work of this kind has been carried out will it be profitable to refine the methods of calculation.

On the experimental side, more work to test the predictions of the theory would amost certainly yield results. In particular, more work on the gamma-ray spectrum of ^{206}Pb, either with greater precision or using coincidence techniques, is to be welcomed. Further study of the gamma-rays of RaE (i.e. following the decay of RaD), with the view of establishing the spins and parities of the levels, would be useful. A direct determination of the spin of the ground state of RaE would be an invaluable check on this work and on beta-decay theory. Much higher resolution in (dp) experiments would be capable of giving extremely valuable information. The levels revealed with the present resolution are in most cases whole groups of levels. The development of a similarly fine technique with (dn) reactions would also contribute to the understanding of nuclear structure. An attempt to find a possible pair-emitting state in ^{208}Pb (and possibly in ^{206}Pb and ^{210}Po), perhaps by direct excitation with fast neutrons or gamma-rays, would throw light on the difficult problem of the excited states of a closed shell. An analysis of the gamma-rays from ^{209}Tl, ^{209}Po and RaC″ would also be very useful.

The predicted levels of RaE and ^{206}Pb, in their large numbers, make it clear that, unless the present ideas are very far wrong, heavy nuclei possess, in general, many more levels than have been detected experimentally so far. The reason is, of course, that the primary excitation is very limited, and the subsequent cascade of gamma-rays can only explore a very limited region of the level diagram. In ^{208}Pb, for instance, there are probably about a hundred levels between 2 and 4 Mev of which only some six are known at present.

ACKNOWLEDGMENTS

I would like to thank Mr. Martin Redlich, who checked my algebra in eqn. (3.5), established the general formula (3.6) and did a part of the computation, and Dr. G. E. Lee Whiting, who carried out further computation and checks. I also wish to thank Drs. B. B. Kinsey, M. Goldhaber and B. W. Sargent for stimulating discussions.

APPENDIX

THE LEVELS OF ^{207}Pb

Recent experimental work furnishes an almost certain level scheme for ^{207}Pb. The crucial pieces of information are:

(i) The measured spin and magnetic moment of the ground state, indicating $p_{1/2}$.

(ii) The short-range alpha-groups of ^{211}Po(AcC′), indicating three excited levels at 0·54 ± 0·04, 0·88 ± −0·04 and 1·11 ± 0·06 Mev (Neumann and Perlman 1951).

(iii) The discovery by Campbell and Goodrich (1950) of an isomeric transition of energy about 1·05 Mev. Its lifetime, 0·9 sec, places it unambiguously in the M4 class (Goldhaber and Sunyar 1951), in line with the expected $i_{13/2}-f_{5/2}$ transition in this neutron shell.

(iv) The measurement of the gamma-rays following electron capture in ^{207}Bi (Neumann and Perlman 1951, Grace and Prescott 1951) of energies 0·565, 1·063, 1·46, 2·05, 2·20, 2·33, 2·49 Mev (and a soft one whose energy is either 0·137 or 0·064 Mev). The 1·063 Mev radiation can be identified with the isomeric transition. It is in cascade with the 0·565 Mev gamma-ray.

(v) The existence of a weak gamma-ray of energy 0·870 Mev in the spectrum of ^{207}Tl(AcC″) → ^{207}Pb(AcD) (Surugue 1946).

(vi) The short-range groups in the reactions ^{206}Pb(dp)^{207}Pb and ^{208}Pb(dt)^{207}Pb. Both show unresolved groups interpreted by Harvey (1951 a, b) as two levels at 0·61 and 0·95 Mev, but which are also consistent with three levels at 0·54, 0·87 and 1·11 Mev, and broad groups corresponding to levels in the region 2·0–2·8 Mev. The (dt) reaction indicates a level at 1·61 Mev and another at 2·33 Mev. The (dp) reactions reveals further levels at 3·60, 4·42, 4·66 and 5·28 Mev (incompletely resolved, and so possibly more numerous).

The limited energy available in the decay of AcC″ suggests that the 0·870 Mev gamma-ray is a transition to the ground state of ^{207}Pb, implying a level at 0·870 Mev. This is clearly the 0·88 ± 0·04 Mev level revealed by the alpha-group.

The 1·063 Mev isomeric transition must be interpreted as $i_{13/2}$, $f_{5/2}$, and so cannot be to ground. Its coincidence with the 0·565 Mev gamma-ray indicates that it is between levels at 1·628 and 0·565 Mev, the latter clearly being the level at 0·54 ± 0·04 Mev in the alpha-groups. The $i_{13/2}$ level is then at 1·63 Mev, in excellent agreement with the level observed in the (dt) reaction, and there are four experimentally established levels below it (revealed by the four alpha-groups of AcC′). Since it is long lived, the $h_{9/2}$ level cannot be below it, for the M2 transition to it would take place much too quickly. At first sight it would also appear that the $f_{7/2}$ level cannot be below it, since the E3 transition to that would be fairly rapid. But this would leave only the $p_{1/2}$, $p_{3/2}$ and $f_{5/2}$ levels to be fitted into the four experimentally established places, and the only way to find the fourth is by assigning the $f_{7/2}$ to the 1·11 Mev level. This now fixes the $p_{3/2}$ level at 0·870 Mev, and the $f_{5/2}$ level at 0·565 Mev. The energy difference between $i_{13/2}$ and $f_{7/2}$ is thus 0·52 ± 0·06 Mev, and a comparison with the empirical results of Goldhaber and Sunyar shows that the partial lifetime could be anywhere between 0·01 and 100 sec. The observed predominant decay of the $i_{13/2}$ state to $f_{5/2}$ with a lifetime of 0·9 sec is therefore compatible with the proposed scheme. It may be remarked that the alternative hypotheses, that the 0·565 Mev transition, and not the 1·063 MeV transition, is the lifetime determining one in the isomeric state cannot be made to fit the facts.

This assignment of the 1·063 MeV gamma-ray in the level scheme conflicts with the scheme proposed by Neumann and Perlman, who, however, were unaware of the isomeric nature of the transition, and assumed that it corresponded to the transition from the 1·11 MeV level to ground.

The four gamma-rays of energy above 2 MeV most probably correspond to ground state transitions, for, as pointed out by Neumann and Perlman, the estimated energy available in the decay of ^{207}Bi is insufficient to lead to levels above 2·5 MeV. The 1·46 MeV gamma-ray can be fitted in within the experimental error as a transition between the 2·05 and 0·565 MeV levels, or between the 2·33 and 0·870 MeV levels.

According to Prescott (unpublished) not more than 10% of the transitions from the isomeric state go via the $f_{7/2}$ level, which would give rise to a cascade of three gamma-rays all with about 0·5 MeV energy. This means that any possible confusion of these gamma-rays does not seriously affect the value deduced for the energy of the $f_{5/2}$ level, which we shall take to be 0·565 ± 0·01 MeV.

Prescott also finds that in coincidence with the K x-rays he observes a gamma-ray of energy approximately 0·55 MeV. The absence of coincidences with the 1·063 MeV line confirms that this is an isomeric transition, while the other coincidences indicate that either direct capture into the 0·565 MeV state is taking place, and/or that it is formed by prompt gamma-transitions. Prescott also finds indications of a gamma-ray of energy 1·78 ± 0·05 MeV in the total spectrum. This could be a transition from the 2·33 to the 0·565 MeV level.

The position of the $h_{9/2}$ level is left undetermined. It is unlikely to be formed strongly from the direct decay of ^{207}Bi, for considerable internal rearrangement is necessary, although the spin of the ^{207}Bi is probably also $h_{9/2}$. One would expect the ^{208}Pb(dt)^{207}Pb reaction to give rise to the levels corresponding to one neutron hole, and the level at 2·33 MeV is therefore possibly the $h_{9/2}$. This cannot be the same as the 2·33 MeV level found by Neumann and Perlman, since this radiates to the ground state.

The four levels above 2 MeV most probably arise from configurations in which at least one nucleon is excited to the next shell.

REFERENCES

Alburger, D. E., and Friedlander, G., 1951, *Phys. Rev.*, **81**, 523.
Bannerman, R. C., and Curran, S. C., 1952, *Phys. Rev.*, **85**, 134.
Campbell, E. C., and Goodrich, M., 1950, *Phys. Rev.*, **78**, 640.
Carlson, B. C., and Rushbrooke, G. S., 1950, *Proc. Camb. Phil. Soc.*, **46**, 626.
Feather, N., 1949, *Nucleonics*, **5**, 22.
Goldhaber, M., and Sunyar, A. W., 1951, *Phys. Rev.*, **83**, 906.
Grace, M. A., Allen, R. A., West, D., and Halban, H., 1951, *Proc. Phys. Soc.* A, **64**, 493.
Grace, M. A., and Prescott, J. R., 1951, *Phys. Rev.*, **84**, 1059.
Harvey, J. A., 1951 a, *Thesis*, M.I.T. ; 1951 b, *Phys. Rev.*, **81**, 353.
Haxel, O., Jensen, J. H. D., and Suess, H. E., 1949, *Phys. Rev.*, **75**, 1766.
Kinsey, B. B., Bartholomew, G., and Walker, W. H., 1951, *Phys. Rev.*, **82**, 380.
Mayer, M. G., 1949, *Phys. Rev.*, **75**, 1894 ; 1950 a, *Ibid.*, **78**, 16 ; 1950 b, *Ibid.*, **78**, 22.
Neumann, H. M., Howland, J. J., and Perlman, I., 1950, *Phys. Rev.*, **77**, 720.
Neumann, H. M., and Perlman, I., 1951, *Phys. Rev.*, **81**, 958.
Nordheim, L. W., 1950, *Phys. Rev.*, **78**, 294.
Surugue, J., 1937, *Ann. Phys., Paris*, **8**, 484 ; 1946, *J. Phys. Radium*, **7**, 145.
Tsien, San-Tsiang, 1946, *Phys. Rev.*, **69**, 38.
Zavelsky, A. S., Umarov G. Ya., and Matushevsky, S. Kh., 1949, *J. Exp. Theor. Phys., U.S.S.R.*, **19**, 1136.

The Angular Distribution of γ-Radiation from Aligned Nuclei

By N. R. STEENBERG
The Clarendon Laboratory, Oxford

MS. received 21st March 1952, *and read before the Physical Society at Southampton on 19th December* 1951

ABSTRACT. The angular distribution of γ-radiation from nuclei aligned at low temperature is given as a series of Legendre polynomials, $I(\theta)=1+\Sigma_K A_K(T)\,P_K(\cos\theta)$ the A_K being temperature dependent. The formulation is applicable to cascade processes of arbitrary multipole orders and nuclear spins. An approximation valid for low degrees of alignment is given, as is the angular distribution from completely aligned nuclei. Application is made to ^{60}Co.

---

§ 1. INTRODUCTION

If radioactive nuclei can be partially aligned at low temperatures, that is, caused to occupy states such that the spins are preponderantly in one direction, an anisotropy can be expected in the emitted γ-radiation. In the case of a single emission the theory of this effect has been given by Spiers (1949). In the following the angular distribution is given in the form of a series of Legendre polynomials, $I(\theta)=1+\Sigma_K A_K(T)P_K(\cos\theta)$ where θ is the angle between the direction of emission and the axis of alignment and T is the absolute temperature. The A_K are temperature dependent and are such that the angular distribution from an arbitrary cascade can readily be given provided the decay scheme is such that at each stage the γ-radiation is of one multipole order only, or if β-emission from the oriented nucleus precedes the γ-emission (or emissions) the total angular momentum of the β–neutrino system has one value only.

The first two terms of the series give the polar diagram, (*a*) for arbitrary nuclear spins where no multipole orders higher than quadrupole are involved, (*b*) for arbitrary multipole orders where no initial nuclear spins greater than 5/2 are involved.

An approximation valid for low degrees of alignment is given, applicable to arbitrary nuclear spins and multipole orders. The maximum possible value of anisotropy, for completely aligned nuclei can also be readily obtained.

Alignment of nuclear spins can be accomplished by allowing a strong magnetic field H ($\sim 10^6$ gauss) to act on the nuclear magnetic moment μ, at low temperatures ($\sim 0{\cdot}01^\circ$K). Under such conditions, if the lifetime of the unstable nucleus of spin J is sufficiently long, the population of states of varying z-component of spin M assumes a Boltzmann distribution. If $W(M)$ is the relative population of state M

$$W(M)=\exp\beta M\Big/\sum_{M=-J}^{J}\exp\beta M,$$

where $\beta=H\mu/\boldsymbol{k}TJ$. This method has been described as the 'brute force' method of aligning nuclei.

If $I_M(\theta)$ is the angular distribution of γ-radiation emitted by nuclei with z-component of spin M, the angular distribution from all such states is

$$I(\theta)=\sum_{M=-J}^{J}W(M)I_M(\theta). \qquad \ldots\ldots(1)$$

Bleaney (1951) has suggested a method whereby the magnetic field of the atomic electrons is used to align nuclei. In this case the interaction is such that, in general, M is not a 'good' quantum number. However in special cases (e.g. ^{60}Co, Bleaney 1951) the present work is a good approximation.

Pound (1949) has suggested a still further method of aligning nuclei in which the interaction of a crystalline electric field gradient with the nuclear quadrupole moment Q is utilized. In this case the population function is, in Pound's notation

$$W(M) = \exp \gamma M^2 \Big/ \sum_{M=-J}^{J} \exp \gamma M^2$$

where

$$\gamma = -\frac{3}{4} \frac{eQ}{J(2J-1)kT} \frac{\partial E_z}{\partial z}$$

assuming axial symmetry. The angular distribution is then given by eqn. (1) with this population function.

§ 2. SINGLE EMISSION

Consider a transition in which a nucleus of spin J decays to a nucleus of spin J_1 emitting a single γ-ray of multipole order L, which can be represented by $(J \xrightarrow{L} J_1)$ where $|J - J_1| \leqslant L \leqslant J + J_1$. Spiers (1949) has shown that the distribution from a single initial state M can be written

$$I_M(\theta) = \Sigma_m |C^{J\ J_1\ L}_{M,\ M-m,\ m}|^2 I^L_m(\theta) \qquad \ldots\ldots(2)$$

independently of the character (electric or magnetic) of the radiation. The $C^{J\ J_1\ L}_{M,\ M-m,\ m}$ are Wigner (Clebsch–Gordon) coefficients which add states of angular momentum J_1 and L to form a single state of angular momentum J with z-component M. They are given by Condon and Shortley (1935). In Condon's notation $C^{J\ J_1\ L}_{M,\ M-m,\ m} = (J_1, L, M-m, m | J_1, L, J, M)$. We can write

$$I^L_m(\theta) = \sum_{\sigma=-1}^{1} |A^{Lm}_\sigma(\theta)|^2,$$

where $A^{Lm}_\sigma(\theta\phi)$ represents for $\sigma = \pm 1, 0$ the components of the magnetic vector potential of multipole order L in the form of a spherical wave. Solutions of Maxwell's equations in this form were obtained by Heitler (1936) (see also Goertzel 1946).

The following expansion of $I^L_m(\theta)$ is derived in Appendix I.

$$I^L_m(\theta) = 1 + \sum_K (2K+1) \left\{1 - \frac{K(K+1)}{2L(L+1)}\right\} C^{L\ K\ L}_{0,\ 0,\ 0} C^{L\ K\ L}_{m,\ 0,\ m} P_K(\cos\theta) \qquad \ldots\ldots(3)$$

which can be written

$$I^L_m(\theta) = 1 + \Sigma_K a_K(L) \Pi_K(m, L) P_K(\cos\theta).$$

K takes only the even values 2, 4, ... $2L$. The Legendre polynomials $P_K(\cos\theta)$ are normalized in the sense that $P_K(1) = 1$. The expressions $\Pi_K(m, L)$ are essentially the coefficients $C^{L\ K\ L}_{m,\ 0,\ m}$ omitting a normalizing factor,

$$\Pi_K(m, L) = \sum_{\nu=0}^{K} \frac{(-1)^\nu (L+m)!\,(L-m)!\,K!}{[(K-\nu)!\,\nu!]^2 (L+m-\nu)!\,(L-m-K+\nu)!}$$

and
$$a_K(L) = (2K+1) \left\{1 - \frac{K(K+1)}{2L(L+1)}\right\} \left\{\frac{(2L+1)(2L-K)!\,K!^2}{(2L+K+1)!}\right. \Pi_K(0, L).$$

The first two $\Pi_K(m, L)$ are

$$\Pi_2(m, L) = [3m^2 - L(L+1)],$$

$$\Pi_4(m, L) = \tfrac{1}{12}[35m^4 - 5(6L^2+6L-5)m^2 + 3L(L+1)(L+2)(L-1)].$$

The first two $a_K(L)$ are

$$a_2(L) = -\left\{1 - \frac{3}{L(L+1)}\right\}\frac{5}{(2L+3)(2L-1)},$$

$$a_4(L) = \left\{1 - \frac{10}{L(L+1)}\right\}\frac{81}{(2L+5)(2L+3)(2L-1)(2L-3)}.$$

It is not difficult to show that

$$\Sigma_m |C^{J\,J_1\,L}_{M,\,M-m,\,m}|^2\, \Pi_K(m, L) = S_K(J, J_1, L)\Pi_K(M, J) \qquad \ldots\ldots(4)$$

where S_K is independent of M, for $C^{J\,J_1\,L}_{M,\,M-m,\,m} C^{L\,K\,L}_{m,\,0,\,m}$ represents a decomposition in which J is decomposed into J_1 and L, and L is further decomposed into K and L. An alternative is to decompose J into K and J' and J' into J_1 and L obtaining the same final states (this is a generalization of the simple alternatives of LS and jj coupling in atomic spectra), therefore

$$C^{J\,J_1\,L}_{M,\,M-m,\,m} C^{L\,K\,L}_{m,\,0,\,m} = \Sigma_{J'} W_{J'} C^{J\,K\,J'}_{M,\,0,\,M} C^{J'\,J_1\,L}_{M,\,M-m,\,m}.$$

Multiplying both sides by $C^{J\,J_1\,L}_{M,\,M-m,\,m}$ and summing over m we obtain

$$\Sigma_m |C^{J\,J_1\,L}_{M,\,M-m,\,m}|^2 C^{L\,K\,L}_{m,\,0,\,m} = \Sigma_{J'} W_{J'} C^{J\,K\,J'}_{M,\,0,\,M}\, \delta_{J,\,J'} = W_J C^{J\,K\,J}_{M,\,0,\,M},$$

whence eqn. (4) follows (W_J is determined by this equation).

The $S_K(J, J_1, L)$ in all cases of interest assume relatively simple forms. The following are derived in Appendix II:

$$S_K(J, J-L, L) = \frac{(2L)!\,(2J-K)!}{(2L-K)!\,(2J)!},$$

$$S_K(J, J-L+1, L) = S_K(J, J-L, L)\left[1 - \frac{K}{2}(K+1)\frac{(J-L+1)}{L(J+1)}\right],$$

$$S_K(J, J+L, L) = \frac{(-1)^K(2L)!\,(2J+1)!}{(2L-K)!\,(2J+K+1)!},$$

$$S_K(J, J+L-1, L) = S_K(J, J+L, L)\left[1 - \frac{K}{2}(K+1)\frac{(J+L)}{JL}\right].$$

Due to the relatively small probability of dipole transitions the following also may be needed:

$$S_2(J, J, 2) = -\frac{3(2J+5)(2J-3)}{J(J+1)(2J+3)(2J-1)},$$

$$S_4(J, J, 2) = \frac{36}{J(J+1)(2J+3)(2J-1)}.$$

Thus we have

$$I_M(\theta) = 1 + \Sigma_K a_K(L) S_K(J, J_1, L)\Pi_K(M, J) P_K(\cos\theta).$$

It should be noted that $\Pi_K(M, J) = 0$ if $K > 2J$. Thus the maximum value of K is restricted to $K \leqslant 2p$ where p is integral and satisfies $p \leqslant J$, $p \leqslant L$. Thus if $J = 0$ or $\frac{1}{2}$ no angular effect at all can be obtained, if $J = 1$ or $3/2$ only the term in $P_2(\cos\theta)$ is required regardless of L, if $J = 2$ or $5/2$ only the first two terms are required and so forth.

The complete polar diagram is given by

$$I(\theta)=\Sigma_M W(M)I_M(\theta)=1+\Sigma_K A_K(T)P_K(\cos\theta), \qquad \ldots\ldots(5)$$

where

$$\left.\begin{aligned}A_K(T)&=a_K(L)S_K(J,J_1,L)B_K(T),\\ B_K(T)&=\Sigma_M W(M)\Pi_K(M,J).\end{aligned}\right\} \qquad \ldots\ldots(6)$$

If $W(M)=\exp\beta M/\Sigma_M\exp\beta M$ the summation over M can be carried out explicitly since

$$\sum_{M=-J}^{J} e^{\beta M}=\frac{\sinh\beta(2J+1)/2}{\sinh\beta/2},$$

$$\sum_M e^{\beta M}M^2=\frac{d^2}{d\beta^2}\sum_M e^{\beta M}=\frac{d^2}{d\beta^2}\left[\frac{\sinh\beta(2J+1)/2}{\sinh\beta/2}\right]$$

and so forth, so that

$$\Sigma_M W(M)\Pi_2(M,J)=2J(J+1)-\tfrac{3}{2}[(2J+1)ab-b^2]=B_2(T),$$

$$\Sigma_M W(M)\Pi_4(M,J)=\tfrac{1}{12}\{8J(J+1)(J+2)(J-1)-\tfrac{5}{2}(2J+1)(8J^2+8J-9)ab$$
$$+\tfrac{45}{2}(4J^2+4J-1)b^2-\tfrac{105}{2}(2J+1)ab^3+\tfrac{105}{2}b^4\}=B_4(T),$$

where $a=\coth\beta(2J+1)/2$, $b=\coth\beta/2$. If more terms are required, or $W(M)$ is more complex, it would appear that for calculating purposes the angular distribution is better left in the form of eqn. (5).

§ 3. APPROXIMATIONS*

(i) *For Low Degrees of Alignment*

$\Pi_K(M,J)$ involves only even powers of M. This implies, since $I_M(\theta)=I_{-M}(\theta)$, that it is immaterial whether nuclei are aligned in both sense and direction, i.e. all spins pointing in the $+z$ direction, or aligned in direction only, spins divided between the $+z$ and $-z$ directions. Thus, for orientation by a magnetic field

$$I(\theta)=\sum_M\left\{\frac{e^{\beta M}}{\Sigma e^{\beta M}}\right\}I_M(\theta)=\sum_M\left\{\frac{\cosh\beta M}{\Sigma\cosh\beta M}\right\}I_M(\theta)=\sum_M W'(M)I_M(\theta).$$

For small values of β we can expand $\cosh\beta M$ and take only the term in β^2 obtaining

$$W'(M)=\frac{1}{(2J+1)}\left\{1+\frac{\beta^2}{6}[3M^2-J(J+1)]\right\}=\frac{1}{(2J+1)}\left\{1+\frac{\beta^2}{6}\Pi_2(M,J)\right\}.$$

Since $\Sigma_M\Pi_K(M,J)=0$, and $\Sigma_M\Pi_K(M,J)\Pi_2(M,J)=0$ unless $K=2$ while $\Sigma_M[\Pi_2(M,J)]^2=\tfrac{1}{5}J(J+1)(2J-1)(2J+1)(2J+3)$ it follows from eqn. (5) that we can write

$$I_{\beta\to 0}(\theta)=1+\tfrac{1}{6}\beta^2\alpha(L)h(J,J_1)\tfrac{1}{2}(3\cos^2\theta-1), \qquad \ldots\ldots(7)$$

where $h(J,J_1)=(2J+3)(J+1)$ if $J_1=J-L$, $h(J,J_1)=J(2J-1)$ if $J_1=J+L$, $\alpha(L)=[3-L(L+1)]/(L+1)(2L+3)$. The same expressions hold for Pound's method if we replace β^2 by 2γ.

An exact criterion for the validity of this approximation would be difficult to give but some investigation shows that it would be 'good' for $\beta^2\leqslant 1/J(J+1)$.

If ϵ is defined as the anisotropy $\epsilon=[I(\pi/2-I(0)]/I(\pi/2)$, this can also be approximated for small β

$$\epsilon_{\beta\to 0}=\frac{-\tfrac{1}{4}\beta^2\alpha(L)h(J,J_1)}{1-\tfrac{1}{12}\beta^2\alpha(L)h(J,J_1)}=-\tfrac{1}{4}\beta^2\alpha(L)h(J,J_1) \qquad \ldots\ldots(8)$$

for β^2 sufficiently small.

---

* Some of the results given here have appeared previously (Steenberg 1951).

(ii) *Completely Oriented Nuclei*

For very large values of β nearly all the nuclei will be in the state with $M=J$, i.e. saturation. This occurs practically for β greater than 4. Then $e^{\beta J}$ is much greater than $e^{\beta M}$ for $M\neq J$ and $I_{\beta\to\infty}(\theta)=I_J(\theta)$ and since

$$\Pi_K(J,J)=\frac{(2J)!}{K!\,(2J-K)!}\qquad (K\text{ even})$$

$$I_{\beta\to\infty}(\theta)=1+\sum_K a_K(L)S_K(J,J_1\,L)\frac{(2J)!}{K!\,(2J-K)!}P_K(\cos\theta).$$

The value of ϵ at saturation is

$$\epsilon_{\beta\to\infty}=\frac{\sum\limits_K a_K(L)S_K(J,J_1,L)\dfrac{(2J)!}{K!\,(2J-K)!}\left[\dfrac{(-1)^{K/2}K!}{2^K(K/2)!}-1\right]}{1+\sum\limits_K a_K(L)S_K(J,J_1,L)\dfrac{(2J)!}{K!\,(2J-K)!}\;\dfrac{(-1)^{K/2}K!}{2^K(K/2)!}}.\quad\ldots\ldots(9)$$

A particular simplification occurs if $J_1=J-L$ for then

$$I_J(\theta)=\Sigma_m|C^{J\;\;J-L\;\;L}_{J,\,J-m,\,m}|^2 I^L_m(\theta)=\Sigma_m\delta_{mL}I^L_m(\theta)$$

and $I_{\beta\to\infty}(\theta)=I_J(\theta)=I^L_L(\theta)$. The $I^L_L(\theta)$ are given by Arnold (1950). In Arnold's notation $I^L_L(\theta)=F^L_L(\theta)$. The following are taken from Arnold's results (and normalized):

$$I_2^2(\theta)=\tfrac{5}{4}(1-\cos^4\theta),$$
$$I_3^3(\theta)=\tfrac{105}{64}(1-\cos^2\theta-\cos^4\theta+\cos^6\theta),$$
$$I_4^4(\theta)=\tfrac{63}{32}(1-2\cos^2\theta+2\cos^6\theta-\cos^8\theta),$$
$$I_5^5(\theta)=\tfrac{1155}{512}(1-3\cos^2\theta+2\cos^4\theta+2\cos^6\theta-3\cos^8\theta+\cos^{10}\theta).$$

§ 4. MULTIPLE EMISSION

Consider a decay scheme represented by $(J\xrightarrow{j_1}J_1\xrightarrow{j_2}J_2\xrightarrow{j_3}J_3)$ where j_1, j_2 etc. are the total angular momenta of emitted particles 1, 2, etc. If, as will subsequently be assumed, particles 2 and 3 are photons we write L_2, L_3 in place of j_2 and j_3. It should be noted that the half lives of the intermediate nuclei of spins J_1 and J_2 must be sufficiently short that no re-alignment takes place. We consider here a three stage cascade but the formulation extends in an obvious way to a cascade of any number of particles.

Assuming particle 3 is a photon, the angular distribution of all photons, L_3 ($\equiv j_3$), coming from a single initial state M is

$$I^{(3)}_M(\theta)=\Sigma_{M_1M_2m_3}|C^{J\;\;J_1\;\;j_1}_{M,\,M_1,\,M-M_1}C^{J_1\;\;J_2\;\;j_2}_{M_1,\,M_2,\,M_1-M_2}C^{J_2\;\;J_3\;\;L_3}_{M_2,\,M_2-m_3,\,m_3}|^2 I^{L_3}_{m_3}(\theta).\quad\ldots\ldots(10)$$

This result can be obtained by a simple extension of the method used by Spiers (1949) to obtain eqn. (2).

$I^{L_3}_{m_3}(\theta)$ is expanded in the form of eqn. (3), as for single emission,

$$I^{L_3}_{m_3}(\theta)=1+\Sigma_K a_K(L_3)\Pi_K(m_3,L_3)P_K(\cos\theta)$$

and the summations indicated in eqn. (10) can all be performed using the properties of the Π_K expressed in eqn. (4). Thus eqn. (10) reduces simply to

$$I^{(3)}_M(\theta)=1+\Sigma_K a_K(L_3)S_K(J_2,J_3,L_3)S_K(J_1,j_2,J_2)S_K(J,j_1,J_1)\Pi_K(M,J)P_K(\cos\theta).\quad\ldots\ldots(11)$$

K is now restricted to $K\leqslant 2p_3$ where p_3 is integral and satisfies $p_3\leqslant L_3$, $p_3\leqslant J$, $p_3\leqslant J_1$, $p_3\leqslant J_2$.

If particle 2 is a photon as well the same procedure is applied ($L_2 \equiv j_2$), giving

$$I^{(2)}_M(\theta) = 1 + \sum_{K=2}^{2p_2} a_K(L_2) S_K(J_1, J_2, L_2) S_K(J, j_1, J_1) \Pi_K(M, J) P_K(\cos\theta), \quad \ldots\ldots(12)$$

where p_2 is integral and satisfies $p_2 \leqslant J, J_1, L_2$.

If particle 1 is a photon its angular distribution will be calculated as if it were a single emission. If it is a β-particle which is not observed eqns. (11) and (12) still hold and j_1 is the total angular momentum of the β–neutrino system. Assuming particle 1 is not observed, the observed angular distribution of photons 2 and 3 is $I(\theta) = \Sigma_M W(M)[\delta_2 I^{(2)}_M(\theta) + \delta_3 I^{(3)}_M(\theta)]$ where δ_2 and δ_3 are detection efficiencies. If $W(M) = \exp\beta M/\Sigma \exp\beta M$, and it is so desired, the summation over M can be performed giving

$$I(\theta) = 1 + \Sigma_K[\delta_2' A^{(2)}_K(T) + \delta_3' A^{(3)}_K(T)] P_K(\cos\theta),$$

where $\delta_2' = \delta_2/(\delta_2 + \delta_3)$, $\delta_3' = \delta_3/(\delta_2 + \delta_3)$.

This formula can be approximated for small values of β by a method analogous to that used for single emission, giving

$$I_{\beta\to 0}(\theta) = 1 + \tfrac{1}{6}\beta^2 q(J, J_1) P_2(\cos\theta)\{\delta_2'\alpha(L_2) h(J_1, J_2) + \delta_3'\alpha(L_3) h(J_2, J_3) g(J_1, J_2)\}. \quad \ldots\ldots(13)$$

$\alpha(L)$ and h are defined in § 3(i), and

$$g(J_1, J_2) = \frac{J_1(2J_1 - 1)}{J_2(2J_2 - 1)} \text{ if } J_2 = J_1 + L_2, \quad g(J_1, J_2) = \frac{(J_1 + 1)(2J_1 + 3)}{(J_2 + 1)(2J_2 + 3)} \text{ if } J_2 = J_1 - L_2,$$

$$q(J, J_1) = g(J, J_1) \text{ if } j_1 = |J - J_1|,$$

$$q(J, J_1) = \frac{(2J - 1)}{(2J_1 - 1)}\left[\frac{JJ_1 - 3(J + J_1)}{J_1(J_1 + 1)}\right] \quad \text{if} \quad j_1 = J_1 - J + 1,$$

$$q(J, J_1) = \frac{(2J + 3)}{(2J_1 + 3)}\left[\frac{J_1(J + 1) - 3(J - J_1 + 1)}{J_1(J_1 + 1)}\right] \quad \text{if} \quad j_1 = J - J_1 + 1.$$

For the saturation angular distribution the same considerations apply as in the case of single emission, namely $I_{\beta\to\infty}(\theta) = I_J(\theta)$. In particular if $j_1 = J - J_1$, $L_2 = J_1 - J_2$, $L_3 = J_2 - J_3$

$$I_J(\theta) = \delta_2 I^{L_2}_{L_2}(\theta) + \delta_3 I^{L_3}_{L_3}(\theta).$$

§ 5. APPLICATION TO ^{60}Co

This procedure can be illustrated by its application to ^{60}Co. This nucleus has been successfully aligned recently (Daniels, Grace and Robinson 1951) by Bleaney's method (Gorter *et al.* 1951 also report success with this nucleus). It is known that the γ-cascade in ^{60}Ni is $(4 \xrightarrow{2} 2 \xrightarrow{2} 0)$ both transitions electric quadrupole (Brady and Deutsch 1950). Recent work (Deutsch and Scharff-Goldhaber 1951) suggests that the ground state of ^{60}Co has spin 5. We therefore assume a transition $(5 \xrightarrow{1(\beta)} 4 \xrightarrow{2(\gamma)} 2 \xrightarrow{2(\gamma)} 0)$. Now from eqn. (3)

$$I^2_{m_3}(\theta) = I^2_{m_2}(\theta) = 1 - \tfrac{5}{42}(3m^2 - 6) P_2(\cos\theta) - \tfrac{1}{42}(35m^4 - 155m^2 + 72) P_4(\cos\theta).$$

Since in this case $L_2 = J_1 - J_2$ and $L_3 = J_2 - J_3$ the product of the factors S_K in $I^{(2)}_M(\theta)$ and $I^{(3)}_M(\theta)$ are identical and from eqns. (10) and (11) we get

$$I^{(2)}_M(\theta) = I^{(3)}_M(\theta) = I_M(\theta) = 1 - \frac{5}{7}\frac{\Pi_2(M, J)}{J(2J - 1)} P_2(\cos\theta) - \frac{12}{7}\frac{\Pi_4(M, J) P_4(\cos\theta)}{J(J - 1)(2J - 3)(2J - 1)}$$

and $I(\theta) = (\delta_2 + \delta_3)\Sigma_M W(M) I_M(\theta)$; the detection efficiencies appear as a common factor and can be disregarded. Finally, with $J = 5$

$$I(\theta) = \Sigma_M W(M) I_M(\theta) = 1 - \tfrac{1}{42}(40 - 11ab + b^2)P_2(\cos\theta)$$
$$- \tfrac{1}{168}(128 - 121ab + 51b^2 - 11ab^3 + b^4)P_4(\cos\theta)$$

$a = \coth 11\beta/2$, $b = \coth \tfrac{1}{2}\beta$.

A plot of the anisotropy, $\epsilon = [I(\pi/2 - I(0))]/I(\pi/2)$ derived from this function is given in the figure, curve (*a*). Also included are curves representing the decay schemes $(4 \xrightarrow{0(\beta)} 4 \xrightarrow{2(\gamma)} 2 \xrightarrow{2(\gamma)} 0)$ curve (*b*), $(4 \xrightarrow{1} 4 \xrightarrow{2} 2 \xrightarrow{2} 0)$ curve (*c*) and $(5 \xrightarrow{2} 4 \xrightarrow{2} 2 \xrightarrow{2} 0)$ curve (*d*). A temperature scale is included for curves (*a*) and (*d*), $J = 5$, on the assumption that the magnetic moment of ^{60}Co is 3·00 nuclear magnetons. The effective value of H is known from the hyperfine splitting in ^{59}Co (Bleaney 1951) and the magnetic moment of ^{59}Co (Mack 1950).

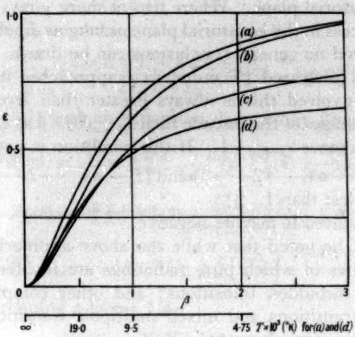

Variation of anisotropy, $\epsilon = [I(\pi/2) - I(0)]/I(\pi/2)$, with β. (*a*) $(5 \xrightarrow{1} 4 \xrightarrow{2} 2 \xrightarrow{2} 0)$, (*b*) $(4 \xrightarrow{0} 4 \xrightarrow{2} 2 \xrightarrow{2} 0)$, (*c*) $(4 \xrightarrow{1} 4 \xrightarrow{2} 2 \xrightarrow{2} 0)$, (*d*) $(5 \xrightarrow{2} 4 \xrightarrow{2} 2 \xrightarrow{2} 0)$. The temperature scale refers to curves (*a*) and (*d*) only.

The figure of course represents uniaxial alignment. In the experiment of Daniels *et al.* (1951) a crystal was used which gave biaxial alignment, the two axes intersecting at an angle of approximately 76°. Intensity measurements were made in the meridian plane defined by the bisector of the axis and their common perpendicular. This arrangement reduces the anisotropy at saturation from 100% to 38·6% ($\cos^4 38°$) in the case of the $(5 \xrightarrow{1} 4 \xrightarrow{2} 2 \xrightarrow{2} 0)$ transition. It should be noted that in this case since Bleaney's method was used M is not strictly a 'good' quantum number so that the theoretical curves given here require correction which is expected to be slight.

§ 6. DISCUSSION

Certain features of the angular distribution are common to all decay schemes. First if $J = 0$ or $\tfrac{1}{2}$ no angular effect can be observed for any emission, if $J_1 = 0$ or $\tfrac{1}{2}$ no angular effect can be observed from a second particle and so on.

Secondly, if an angular effect can be observed, from eqn. (8) it can be seen that for small values of β, ϵ varies with β^2 or T^{-2}, the slope of the curve of ϵ against T^{-2} being

$$\frac{d\epsilon(T)}{d(T^{-2})} = -\frac{1}{4}\left(\frac{H\mu}{kJ}\right)^2 \sum_n \delta_n{}' \alpha(L_n) C_n,$$

where C_n is the product of the appropriate constants, and the summation is over all observed γ-rays. If only one γ-ray is observed, and if it is a dipole, it can be seen that since $\alpha(1)=\frac{1}{10}$ and $\epsilon<0$ there will be an excess of radiation along the axis of alignment. For all higher multipoles $\alpha(L)<0$ so that $\epsilon>0$ and the excess is in the equatorial plane. Where two or more γ-rays are observed there will always be an excess in the equatorial plane as long as dipoles are not involved. If dipoles are involved no general conclusions can be drawn.

Thirdly, as β is increased (T reduced) ϵ approaches its saturation value. If dipoles are not involved this is always greater than zero. If furthermore, $J_{n-1}-J_n=j_n$ for all stages of the cascade then $I_{\beta\to\infty}(0)=0$ as can be seen from the $I_L^L(\theta)$ listed in §3, whence $\epsilon_{\beta\to\infty}=1$. If this condition is not met, (e.g. in such decay schemes as ($4\xrightarrow{1}4\xrightarrow{2}2\xrightarrow{2}0$) and ($5\xrightarrow{2}4\xrightarrow{2}2\xrightarrow{2}0$) the anisotropy at saturation will be less than 1.

If dipoles are involved it may be negative.

Finally it should be noted that while the above approach has been applied only to decay schemes in which pure radiations are involved it would appear difficult to include forbidden transitions* and other complex decay schemes such as branching transitions and mixed multipole transitions. These would then involve nuclear matrix elements.

ACKNOWLEDGMENTS

The author is indebted to the Royal Commission for the Exhibition of 1851 for an Overseas Scholarship which made this work possible, and to Dr. J. A. Spiers for his advice and guidance.

APPENDIX I

THE EXPANSION OF $I_m^L(\theta)$

$A_\sigma^{Lm}(\theta\phi)$ can be written (see Goertzel 1946),

$$A_{-\sigma}^{Lm}(\theta\phi) = C_{m,\ m-\sigma,\ \sigma}^{L\ \ L\ \ \ 1} f_L(r) Y_L^{m-\sigma}(\theta\phi)$$

where $Y_L^{m-\sigma}(\theta\phi)$ is a normalized spherical harmonic and $f_L(r)$ is a function of r which can be disregarded. This can in turn be written

$$A_{-\sigma}^{Lm}(\theta\phi) = L_{-\sigma} Y_L^m(\theta\phi),$$

where $L_{\pm 1} = \pm(L_x \pm iL_y)/[2L(L+1)]^{1/2}$, $L_0 = L_z/[L(L+1)]^{1/2}$ and L_x, L_y, L_z are the differential operators representing angular momentum. Similarly $\bar{A}_{-\sigma}^{Lm}(\theta\phi) = -(-1)^\sigma L_\sigma \bar{Y}_L^m(\theta\phi)$. Consider the expression $\Sigma_\sigma \bar{A}_{-\sigma}^{Lm}(\theta_j\phi_j) A_{-\sigma}^{Lm}(\theta_i\phi_i)$ which reduces to $\Sigma_\sigma |A_{\sigma-}^{Lm}(\theta)|^2$ when θ_j, ϕ_j is put equal to θ_i, ϕ_i. Now

$$\Sigma_\sigma A_{-\sigma}^{Lm}(i) \bar{A}_{-\sigma}^{Lm}(j) = -\Sigma_\sigma(-1)^\sigma L_{-\sigma}^{(i)} L_\sigma^{(j)} Y_L^m(i) \bar{Y}_L^m(j).$$

* Allowed β-transitions under all selection rules involve only one value of the angular momentum j of the β–ν system. Forbidden transitions may involve as many as three different values of j. See for example Blin-Stoyle and Spiers (1951).

But $\overline{Y}{}^m_L(j)=(-1)^m Y^m_L(j)$ and the product $Y_L^{-m}(j)Y^m_L(i)$ can be written

$$Y_L^{-m}(j)Y^m_L(i)=\sum_{K=0}^{2L} C^{K\,L\,L}_{0,\,m,\,-m}\,F^0_K(i,j), \qquad \ldots\ldots(\mathrm{A}\,1)$$

where F^0_K is an eigenfunction of $(\mathbf{L}^{(i)})^2, (\mathbf{L}^{(j)})^2$ and of the differential operator $\mathbf{K}^2$ which corresponds to an angular momentum $\mathbf{K}$ which is the vector sum of $\mathbf{L}^{(i)}$ and $\mathbf{L}^{(j)}$. The eigenvalues are $L^{(i)}(L^{(i)}+1)$, $L^{(j)}(L^{(j)}+1)$ and $K(K+1)$ respectively. Operating with

$$\sum_\sigma (-1)^\sigma L^{(j)}_\sigma L^{(i)}_{-\sigma}=\frac{\mathbf{L}^{(i)}.\mathbf{L}^{(j)}}{L(L+1)}=\frac{1}{2L(L+1)}[\mathbf{K}^2-\mathbf{L}^{(i)2}-\mathbf{L}^{(j)2}]$$

and, putting $\theta_j, \phi_j=\theta_i, \phi_i$ we obtain

$$\sum_\sigma |A^{LM}_{-\sigma}(\theta)|^2=\sum_{K=0}^{2L}\left\{\frac{2L(L+1)-K(K+1)}{2L(L+1)}\right\}(-1)^m C^{K\,L\,L}_{0,\,m,\,-m}\,F^0_K(\theta).$$

On comparing eqn. (A 1) with an expansion deduced by Blin-Stoyle (1951),

$$Y_L^{-m}(\theta\phi)Y^m_L(\theta\phi)=\sum_{K=0}^{2L} C^{K\,L\,L}_{0,\,m,\,-m}\,C^{K\,L\,L}_{0,\,0,\,0}\,Y^0_K(\theta)\,\frac{(2L+1)}{[4\pi(2K+1)]^{1/2}}$$

we can write $$F^0_K(\theta)=C^{K\,2\,L}_{0,\,0,\,0}\,Y^0_K(\theta)\,\frac{(2L+1)}{[4\pi(2K+1)]^{1/2}}.$$

Noting that $$C^{K\,L\,L}_{0,\,m,\,-m}=(-1)^{L-m}\,C^{L\,K\,L}_{m,\,0,\,m}\left(\frac{2K+1}{2L+1}\right)^{1/2}$$

the final result is, dropping a factor $1/4\pi$,

$$I^L_m(\theta)=\sum_\sigma |A^{Lm}_\sigma(\theta)|^2=1+\sum_{K=2}^{2L}\left\{1-\frac{K(K+1)}{2L(L+1)}\right\}(2K+1)\,C^{L\,K\,L}_{m,\,0,\,m}\,C^{L\,K\,L}_{0,\,0,\,0}\,P_K(\cos\theta).$$

APPENDIX II

The scalar factors $S_K(J,J-L,L)$ and $S_K(J,J-L+1,L)$ are readily derived. It has been shown that

$$\Sigma_m\,|C^{J\ \ J_1\ \ L}_{M,\,M-m,\,m}|^2\,\Pi_K(m,L)=S_K(J,J_1,L)\,\Pi_K(M,J).$$

(*a*) $J_1=J-L$.

If we put $M=J$ the Wigner coefficients reduce to $|C^{J\ \ J-L,\ L}_{J,\,J-m,\,m}|^2=\delta_{mL}$ and therefore

$$S_K(J,J-L,L)=\frac{\Pi_K(L,L)}{\Pi_K(J,J)}=\frac{(2L)!\,(2J-K)!}{(2L-K)!\,(2J)!}.$$

(*b*) $J_1=J-L+1$.

For $M=J$, m takes only the values L and $L-1$ whence

$$\begin{aligned}S_K(J,J-L+1,L)&=[\Pi_K(J,J)]^{-1}\{|C^{J\ \ J-L+1\ \ L}_{J,\,J-L,\ \ L}|^2\,\Pi_K(L,L)\\&\quad+|C^{J\ \ J-L+1\ \ L}_{J,\,J-L+1,\,L-1}|^2\,\Pi_K(L-1,L)\}\\&=S_K(J,J-L,L)\left[1-\tfrac{1}{2}K(K+1)\frac{(J-L+1)}{L(J+1)}\right].\end{aligned}$$

It is evident how this procedure would extend to $S_K(J,J-L+2,L)$ and so forth.

The remaining cases are considerably more involved, and the derivation will be merely sketched.

(*c*) $J_1 = J + L$.

$\Pi_K(mL)$ is rewritten in the equivalent form

$$\Pi_K(mL) = \sum_{\mu=-K/2}^{K/2} \frac{(-1)^{\mu+K/2}(L+m)!\,(L-m)!\,K!}{[(\tfrac{1}{2}K+\mu)!\,(\tfrac{1}{2}K-\mu)!]^2(L-\tfrac{1}{2}K+m-\mu)!\,(L-\tfrac{1}{2}K-m+\mu)!}.$$

Then by writing $|C^{J,\,J+L,\,L}_{M,\,M-m,\,m}|^2$ explicitly, interchanging the order of summation, and some manipulation of factors the following result is obtained:

$$\Sigma_m |C^{J,\,J+L,\,L}_{M,\,M-m,\,m}|^2\,\Pi_K(m, L)$$

$$= N_1 P_1^{-1} \sum_{\mu} \frac{(-1)^{\mu+K/2}K!\,(J'+M-\mu)!\,(J'-M+\mu)!}{[(\tfrac{1}{2}K+\mu)!\,(\tfrac{1}{2}K-\mu)!]^2(J+M)!\,(J-M)!} \sum_{\lambda=-L'}^{L'} |C^{J',\,J+L,\,L'}_{M',\,M'-\lambda,\,\lambda}|^2$$

where $J' = J + \tfrac{1}{2}K$, $M' = M - \mu$, $L' = L - \tfrac{1}{2}K$, $\lambda = m - \mu$, and N_1, P_1 are the normalizing coefficients of $|C^{J,\,J+L,\,L}_{M,\,M-m,\,m}|^2$ and $|C^{J',\,J+L,\,L'}_{M',\,M'-\lambda,\,\lambda}|^2$ respectively.

$$N_1 = \frac{(2J+1)!\,(2L)!}{(2J+2L+1)!}, \qquad P_1 = \frac{(2J+K+1)!\,(2L-K)!}{(2J+2L+1)!}.$$

The summation over λ is unity. Putting $M = J$ and rewriting the summation over μ in an equivalent form, we are left with the result

$$N_1 P_1^{-1}(-1)^K \sum_{\nu=0}^{K} \frac{(-1)^{\nu}(2J+\nu)!\,(K-\nu)!\,K!}{[(K-\nu)!\,\nu!]^2(2J)!} = S_K(J, J+L, L)\,\Pi_K(J, J).$$

We now note that $\Pi_K(J,J) = (-1)^K(2J)!/K!\,(2J-K)!$ is the coefficient of x^K in the binomial expansion of $(1+x)^{-(2J-K+1)}$. By rewriting $(1+x)^{-(2J-K+1)}$ as $(1+x)^{-(2J+1)}(1+x)^K$ and expanding the latter expression, the coefficient of x^K is also found to be

$$\sum_{\nu=0}^{K} \frac{(-1)^{\nu}(2J+\nu)!\,K!}{(K-\nu)!\,(\nu!)^2(2J)!}.$$

Whence $S_K(J, J+L, L) = (-1)^K N_1 P_1^{-1} = \dfrac{(-1)^K(2L)!\,(2J+1)!}{(2L-K)!\,(2J+K+1)!}$.

(*d*) $J_1 = J + L - 1$.

$S_K(J, J+L-1, L)$ is found by a procedure similar to (*c*) above.

REFERENCES

Arnold, W. R., 1950, *Phys. Rev.*, **80**, 34.

Bleaney, B., 1951, *Proc. Phys. Soc.* A, **64**, 315.

Blin-Stoyle, R. J., 1951, *Thesis*, Oxford University.

Blin-Stoyle, R. J., and Spiers, J. A., 1951, *Phys. Rev.*, **82**, 969.

Brady, E. L., and Deutsch, M., 1950, *Phys. Rev.*, **78**, 558.

Condon, E. U., and Shortley, G. H., 1935, *The Theory of Atomic Spectra* (Cambridge: University Press).

Daniels, J. M., Grace, M. A., and Robinson, F. H., 1951, *Nature, Lond.*, **168**, 780.

Deutsch, M., and Scharff-Goldhaber, G., 1951, *Phys. Rev.*, **83**, 1059.

Goertzel, G., 1946, *Phys. Rev.*, **70**, 897.

Gorter, C. J., Poppema, O. J., Steenland, M. J., and Beun, J. A., 1951, *Physica*, **17**, 1050.

Heitler, W., 1936, *Proc. Camb. Phil. Soc.*, **32**, 112.

Mack, J. E., 1950, *Rev. Mod. Phys.*, **22**, 64.

Pound, R. V., 1949, *Phys. Rev.*, **76**, 1410.

Spiers, J. A., 1949, *Directional Effects in Radioactivity* (Ontario: Nat. Res. Ccl. of Canada).

Steenberg, N. R., 1951, *Phys. Rev.*, **84**, 1051.

A Formulation of Beta-decay Theory for Forbidden Transitions of Arbitrary Order
I: Selection Rules and Energy Spectra

By J. A. SPIERS and R. J. BLIN-STOYLE
Clarendon Laboratory, Oxford

MS. received 21*st March* 1952; *read before the Society at Southampton on* 19*th December* 1951

ABSTRACT. The matrix elements of beta-decay theory are expressed in a way which not only gives the beta-spectra and angular distributions for arbitrary degree of forbiddenness, but also yields very simply the selection rules appropriate to any type of interaction.

Results for the energy spectra confirm those found by Greuling by inspection ; angular distributions and electron–neutrino correlations are considered in a subsequent paper.

§ 1. INTRODUCTION

In the theory of beta-decay an investigation is made of the matrix elements associated with nuclear transitions which result in the emission of an electron (or positron) and a neutrino. The properties of these matrix elements lead to the classification of beta-emissions by ' degrees of forbiddenness ' and to the corresponding spin and parity selection rules, energy spectra and angular distribution properties.

The states of the emitted particles are expressed as plane waves or spherical waves (Dirac central field solutions) and the selection rules, etc., are then usually found by expanding these wave functions in powers of the coordinates near the origin (nucleus). From these expressions vectors and tensors are constructed whose complexity increases with each degree of forbiddenness (Marshak 1942, Konopinski 1943).

It is the purpose of this paper to give a method of writing the matrix elements which avoids this process by using eigenstates of the total angular momentum $J=0, 1, 2, \ldots$ of the system 'electron plus neutrino' treated as a whole. Matrix elements so written are then expressed as a sum of terms specified by quantities $L=0, 1, 2, \ldots$ and $S=0, 1$ which play the part respectively of total orbital and total spin angular momentum of the system.

Consideration of these terms (matrix elements for the creation of the system electron plus neutrino in a state specified by J, L, S) leads to simple rules for the degree of forbiddenness of a beta-emission between nuclear states of given spin and parity and to expressions for the energy spectrum and angular distribution properties of the emitted particles for arbitrary degree of forbiddenness.

To anticipate, let a particular interaction (Fermi, tensor, etc.) be chosen; then for each Dirac operator of that interaction the non-vanishing matrix terms can be picked out and classified by degree of forbiddenness as follows:

(i) If the nuclear spin change is $J_i \rightarrow J_f$, the possible values of J are $|J_i - J_f|$ to $J_i + J_f$ in integral steps.

(ii) For the scalar operators $1, \beta, \gamma_5, \beta\gamma_5$, $S=0$ only; for the vector operators $\boldsymbol{\alpha}, \beta\boldsymbol{\alpha}, \boldsymbol{\sigma}, \beta\boldsymbol{\sigma}$, $S=1$ only (electron and neutrino emitted with spins antiparallel and parallel respectively).

.A
5
2

(iii) For given J, $L=|J-S|$ to $J+S$ in integral steps.

(iv) The degree of forbiddenness f of a transition creating the system electron plus neutrino in the state JLS is numerically equal to L for the operators 1, β, $\boldsymbol{\sigma}$, $\beta\boldsymbol{\sigma}$, while $f=L+1$ for the 'velocity dependent' operators $\boldsymbol{\alpha}$, $\beta\boldsymbol{\alpha}$, γ_5, $\beta\gamma_5$ (0 = allowed, 1 = first forbidden, etc.).

(v) If there is (is not) a nuclear parity change on emission, only states of the system electron plus neutrino with odd (even) f can be created.

Table 1 is constructed using rules (ii) to (v). Using rule (i) and selecting the Dirac operators of the chosen interaction we can enumerate the f-values of all terms contributing to the beta-emission; the least f-value among these gives the degree of forbiddenness F of the emission as a whole.† Thus, for example, for a nuclear spin change $0 \rightarrow 0$, $J=0$ only, and table 1 shows that on the Fermi interaction, $F=0$ (allowed) for parity change 'No' and completely forbidden for 'Yes'. For $1 \rightarrow 1$, $J=0$, 1, 2, and on the Fermi interaction $F=0$ ('No') and 1 ('Yes').

Table 1

Interaction	Operators	S	$J=0$		1			2			3			4		
			$L=0$	1	0	1	2	1	2	3	2	3	4	3	4	5
Scalar																
	1, β	0	$f=0$	$\underline{*}$	*	$\underline{1}$	*	*	2	*	*	$\underline{3}$	*	*	4	*
Fermi																
	$\boldsymbol{\alpha}$, $\beta\boldsymbol{\alpha}$	1	$f=\underline{*}$	2	$\underline{1}$	2	($\underline{3}$)	2	$\underline{3}$	(4)	$\underline{3}$	4	($\underline{5}$)	4	$\underline{5}$	(6)
Tensor																
	$\boldsymbol{\sigma}$, $\beta\boldsymbol{\sigma}$	1	$f=*$	$\underline{1}$	0	$\underline{1}$	(2)	$\underline{1}$	2	($\underline{3}$)	2	$\underline{3}$	(4)	$\underline{3}$	4	($\underline{5}$)
Axial vector																
	γ_5, $\beta\gamma_5$	0	$f=\underline{1}$	*	*	2	*	*	$\underline{3}$	*	*	4	*	*	$\underline{5}$	*
Pseudo-scalar																

Degrees of forbiddenness f of transitions creating the system electron–neutrino in states JSL. Even values refer to parity change 'No,' odd values (underlined) to parity change 'Yes.' * denotes that the term vanishes, ( ) that the term represents a small correction to other terms.

§ 2. FORMAL DEVELOPMENT

For convenience in considering angular momentum relations we write the matrix elements of beta-decay as

$$M=\int(\Psi_f^{*}\mathbf{K}\Psi_i)(\psi\,\mathbf{Q}\phi)^{*}\,d\tau \qquad \ldots\ldots(1)$$

where Ψ_i, Ψ_f are initial and final nuclear wave functions, ψ, ϕ are wave functions of the emitted electron and neutrino, $\mathbf{K}$ is a Dirac operator and $\mathbf{Q}=(\mathbf{K}D^{*})^{*}$, D being the operator defined by Furry (1937, 1938).

Spherical wave solutions of Dirac's equation for a central field have been conveniently listed by Rose (1937). Inspection of these solutions shows that the wave function of a state of total angular momentum j, m may be written in the form

$$\psi_{jm\alpha}(\mathbf{r}\sigma\beta)=C^{j,\,j+\frac{1}{2}\alpha\beta,\,\frac{1}{2}}_{m,\,m-\sigma,\,\sigma}F^{\beta,\,\alpha}_{j+\frac{1}{2}\alpha\beta}(pr)\,Y^{m-\sigma}_{j+\frac{1}{2}\alpha\beta}(\theta,\phi). \qquad \ldots\ldots(2)$$

Here the C's are Wigner coefficients used in the theory of addition of quantized angular momenta (Racah 1942) and the spherical harmonics are defined with the Condon–Shortley (1935) choice of phase factors. The four Dirac components of each solution are characterized by the variables $\beta=\pm 1$ ('small' and 'large' components respectively) and $\sigma=\pm\frac{1}{2}$; a takes the values ± 1, corresponding to the two types of solution (Rose's 'type a' and 'type b' respectively); p is the momentum of the electron. For r equal to or greater than nuclear radius, the radial functions F become coulomb field functions; the relation to Rose's notation is $F_l^{1,1}=if_{l-1}$, $F_l^{-1,1}=g_l$, $F_l^{1,-1}=if_{-l-2}$, $F_l^{-1,-1}=g_{-l-1}$.

---

† Except that for the pure pseudo-scalar interaction $\beta\gamma_5$, F is counted as one unit less owing to the absence of any terms with $f=0$.

Note that for given values of a and β, (2) has the form of the wave function of a particle of spin $\frac{1}{2}$ and orbital angular momentum $j+\frac{1}{2}a\beta$ combined to give a total angular momentum j with z-component m.

The neutrino wave functions will have the same form as (2), but with radial functions G appropriate to the case of $Z=0$ and negligible mass, thus: for $pr \ll 1$,

$$\left(\frac{W}{W-1}\right)^{1/2} F_l^{1,\pm 1}(Z=0)=G_l^{1,\pm 1}=\frac{-ip(pr)^l}{(2l+1)!!} \qquad \ldots\ldots(3)$$

$$\left(\frac{W}{W+1}\right)^{1/2} F_l^{-1,\pm 1}(Z=0)=G_l^{-1,\pm 1}=\frac{\pm p(pr)^l}{(2l+1)!!} \qquad \ldots\ldots(4)$$

where

$$(2l+1)!!=1.3.5\ldots.(2l+1)=\frac{(2l+1)!}{2^l l!}. \qquad \ldots\ldots(5)$$

Here p is electron or neutrino momentum; to avoid confusion the latter will subsequently be denoted by q.

§ 3. THE DIRAC OPERATORS

The operators $\mathbf{Q}=(\mathbf{K}D^*)^*$ will act on the variables σ and β in the wave functions of the electron and of the neutrino, and must therefore be written as outer products of 2×2 matrices with matrix elements denoted by $\mathbf{Q}_{\beta\beta'}^{\sigma\sigma'}$. This is done in table 2, where†

$$\sigma_x=\begin{pmatrix}0&1\\1&0\end{pmatrix},\quad \sigma_y=\begin{pmatrix}0&-i\\i&0\end{pmatrix},\quad \sigma_z=\begin{pmatrix}1&0\\0&-1\end{pmatrix},\quad \delta=\begin{pmatrix}1&0\\0&1\end{pmatrix}, \qquad \ldots\ldots(6)$$

$$w_1=-i\sqrt{2}\begin{pmatrix}0&1\\0&0\end{pmatrix},\quad w_0=i\begin{pmatrix}0&1\\1&0\end{pmatrix},\quad w_{-1}=-i\sqrt{2}\begin{pmatrix}1&0\\0&0\end{pmatrix}. \qquad \ldots\ldots(7)$$

Table 2

Interaction	Main term		Velocity term	
	K	$Q_{\beta\beta'}^{\sigma\sigma'}$	K	$Q_{\beta\beta'}^{\sigma\sigma'}$
Scalar	β	$-i(\sigma_x)_{\beta\beta'}(\sigma_y)^{\sigma\sigma'}$	—	—
Fermi	1	$+(\sigma_y)_{\beta\beta'}(\sigma_y)^{\sigma\sigma'}$	$\boldsymbol{\alpha}$	$+i(\sigma_z)_{\beta\beta'}(w_\lambda)^{\sigma\sigma'}$
Tensor	$\beta\boldsymbol{\sigma}$	$+i(\sigma_x)_{\beta\beta'}(w_\lambda)^{\sigma\sigma'}$	$\beta\boldsymbol{\alpha}$	$-i(\delta)_{\beta\beta'}(w_\lambda)^{\sigma\sigma'}$
Axial vector	$\boldsymbol{\sigma}$	$-(\sigma_y)_{\beta\beta'}(w_\lambda)^{\sigma\sigma'}$	γ_5	$-i(\sigma_z)_{\beta\beta'}(\sigma_y)^{\sigma\sigma'}$
Pseudo-scalar	—	—	$\beta\gamma_5$	$-i(\delta)_{\beta\beta'}(\sigma_y)^{\sigma\sigma'}$

Note that, for any of the interactions listed, we can factorize Q thus

$$(Q_\lambda)_{\beta\beta'}^{\sigma\sigma'}=(Q)_{\beta\beta'}(Q_\lambda)^{\sigma\sigma'}, \qquad \ldots\ldots(8)$$

the first part of the product being independent of λ.

---

† We use the notation $A_\lambda=A_1$, A_0, A_{-1} for the components of any vector $\mathbf{A}$, where $A_1=-(A_x+iA_y)/\sqrt{2}$, $A_0=A_z$, $A_{-1}=(A_x-iA_y)/\sqrt{2}$. In this notation the scalar product

$$\mathbf{A}\cdot\mathbf{B}=-\sqrt{3}\,\Sigma_\lambda C_{0\ \lambda\ -\lambda}^{0\ 1\ \ 1} A_\lambda B_{-\lambda}.$$

§4. STATES OF THE SYSTEM ELECTRON PLUS NEUTRINO

By the usual theorem of vector addition, we construct states of the system electron plus neutrino with total angular momentum quantum numbers J, M, thus

$$\psi_{JMja}(\mathbf{r}\sigma\beta, \mathbf{r}'\sigma'\beta') = \sum_{m, m'} C^{Jjj'}_{Mmm'}\psi_{jma}\phi_{j'm'a'} \qquad \ldots\ldots(9)$$

where primes are used to distinguish neutrino variables from electron variables, and ja stands for $jj'aa'$.

The matrix element for creation of the system in such a state is then

$$M^{M_iM_f}_{JMja} = -\sqrt{3}C^{011}_{0\lambda-\lambda}\int (\Psi_f{}^*K_\lambda\Psi_i)[(Q_{-\lambda})^{\sigma\sigma'}_{\beta\beta'}\psi_{JMja}]^* d\tau \qquad \ldots\ldots(10)$$

where summation over σ, σ', β, β', λ is implied; the suffix λ and the expression $-\sqrt{3}C^{011}_{0\lambda-\lambda}$ are to be omitted if K, Q are scalar.

Now, using (2) and (9),

$$\psi_{JMja}(\mathbf{r}\sigma\beta, \mathbf{r}\sigma'\beta') = \sum_{m, m'} C^{Jjj'}_{Mmm'}C^{jl\frac{1}{2}}_{mm-\sigma\sigma}C^{j'l'\frac{1}{2}}_{m'm'-\sigma'\sigma'}Y^{m-\sigma}_{l}Y^{m'-\sigma'}_{l'}F^{\beta a}_{l}G^{\beta' a'}_{l'} \qquad \ldots\ldots(11)$$

where l, l' stand for the quantities $j+\frac{1}{2}a\beta$, $j'+\frac{1}{2}a'\beta'$; and by a theorem proved in the Appendix this can be written as

$$\sum_{L,S} A^{ll'}_{jj'}(JLS)C^{JLS}_{MM-\Sigma\Sigma}C^{S\frac{1}{2}\frac{1}{2}}_{\Sigma\sigma\sigma'}Y^{M-\Sigma}_{L}F^{\beta a}_{l}G^{\beta' a'}_{l'} \qquad \ldots\ldots(12)$$

with $L=l+l'$ to $|l-l'|$ in integral steps, $S=0$ or 1, $\Sigma=\sigma+\sigma'$, and the A's are constants.

Inserting (12) in (10), we obtain, using the expression for $Q^{\sigma\sigma'}_{\lambda}$ given in table 2,

$$M^{M_iM_f}_{JMja} = \sum_{LS} M^{M_iM_f}_{JMja(LS)} = \sum_{LS}\int \Psi_f{}^*[T^{JLS}_{M}R^{ja}_{JLS}]^*\Psi_i\, d\tau \qquad \ldots\ldots(13)$$

where

$$R^{ja}_{JLS}(p, q, r) = r^{-L}\sum_{\beta\beta'} A^{ll'}_{jj'}(JLS)F^{\beta a}_{l}G^{\beta' a'}_{l'}Q_{\beta\beta'} \qquad \ldots\ldots(14)$$

and for the scalar operators $K=1, \beta, \gamma_5, \beta\gamma_5$,

$$\begin{cases} T^{JL0}_{M} = i\sqrt{2}r^{L}Y^{M}_{L}(\theta\phi)K \\ T^{JL1}_{M} = 0 \end{cases} \qquad \ldots\ldots(15)$$

while for the vector operators $\mathbf{K}=\boldsymbol{\alpha}, \beta\boldsymbol{\alpha}, \boldsymbol{\sigma}, \beta\boldsymbol{\sigma}$

$$\begin{cases} T^{JL0}_{M} = 0 \\ T^{JL1}_{M} = i\sqrt{2}\sum_{\lambda} C^{JL1}_{MM-\lambda\lambda}r^{L}Y^{M-\lambda}_{L}(\theta\phi)K_\lambda. \end{cases} \qquad \ldots\ldots(16)$$

It is evident from the form of T^{JLS}_{M} that it transforms under a spatial rotation according to the D^J group; accordingly the matrix elements vanish unless $J=|J_i-J_f|$ to J_i+J_f (rule (i) of §1) and can be written

$$M^{M_iM_f}_{JMja(LS)} = C^{J_iJ_fJ}_{M_iM_fM}M_{Jja(LS)} \qquad \ldots\ldots(17)$$

where $M_{Jja(LS)}$ is independent of M, M_i, M_f.

The factors r^L in T and r^{-L} in R are introduced in order that T^{JLS}_{M} may be equivalent (except for normalizing factors) to the $2J+1$ independent components (for $M=-J, -J+1, \ldots\ldots, +J$) of the various Cartesian vectors and tensors (linear in K, homogeneous of order L in $\mathbf{r}$, and transforming according to the D^J group) used in the standard treatment.

The 'average over a sphere' (Greuling 1942) of T_M^{JLS} is

$$\left.\begin{aligned}\sum_M \int |\, T_M^{JLS} \,|^2_{r=\rho} \frac{d\Omega}{4\pi} &= \frac{2J+1}{2\pi}\rho^{2L}(K)^2 && \text{(scalar operator)}\\ &= \frac{2J+1}{2\pi}\rho^{2L}\tfrac{1}{3}(\mathbf{K})^2 && \text{(vector operator)}\end{aligned}\right\} \qquad \ldots\ldots(18)$$

§ 5. PARITY SELECTION RULE

From the form of T_M^{JLS} and the invariance of the matrix terms (13) under reflection of axes, it follows that if there is (is not) a nuclear parity change on emission, then L must be odd (even) for the operators 1, β, $\boldsymbol{\sigma}$, $\beta\boldsymbol{\sigma}$, and even (odd) for $\boldsymbol{\alpha}$, $\beta\boldsymbol{\alpha}$, γ_5, $\beta\gamma_5$. Since $f=L$ for the former and $L+1$ for the latter (see below), rule (v) of § 1 follows.

§ 6. THE ENERGY SPECTRUM AND DEGREE OF FORBIDDENNESS

From standard time-dependent perturbation theory, the probability per unit time of ejection of an electron with energy between E and $E+dE$ is

$$P(E)\,dE = \frac{2g^2}{\pi}\Sigma_{\substack{M_iM_f\\ JMja}}\frac{1}{2J_i+1}\left|\sum_K\sum_L M_{JMja(LS)}^{M_iM_f}\right|^2\frac{E}{p}\,dE \qquad \ldots\ldots(19)$$

g is the Fermi constant. Σ_K denotes summation over the matrix elements for the various Dirac operators of the chosen interaction, with the appropriate value of $S=0$, 1.

In order to obtain relative orders of magnitude ('degrees of forbiddenness') of transitions between initial and final nuclear states of various spins and parities, and to obtain explicit expressions for the energy spectrum $P(E)$, we write

$$M_{JMja(LS)}^{M_iM_f} \simeq \left[\int \Psi_f{}^* T_M^{JLS*}\Psi_i\,d\tau\right]R_{JLS}^{ja}(p,q,\rho)^* \qquad \ldots\ldots(20)$$

$$= [C_{M_iM_fM}^{J_iJ_fJ}M_{JLS}]R_{JLS}^{ja}(p,q,\rho)^* \qquad \ldots\ldots(21)$$

where ρ is the nuclear radius, and the 'nuclear matrix elements' M_{JLS} are independent of p, q, M_i, M_f, M, j, j', a, a'; in estimating orders of magnitude, they are assumed to have roughly equal values for the operators 1, β, $\boldsymbol{\sigma}$, $\beta\boldsymbol{\sigma}$, and values of order $v/\mathbf{c}$ smaller than these for $\boldsymbol{\alpha}$, $\beta\boldsymbol{\alpha}$, γ_5, $\beta\gamma_5$, the latter being classified as one degree of forbiddenness higher than the former.

Substituting in (19) and using properties of Wigner coefficients, we have

$$P(E)\,dE = \frac{2g^2}{\pi}\sum_{Jja}\left|\sum_K\sum_{L=|J-S|}^{J+S}M_{JLS}R_{JLS}^{ja}\right|^2\frac{E}{p}. \qquad \ldots\ldots(22)$$

For the sake of brevity we ignore cross-terms resulting from different K and L values which may occur in transitions such that more than one state of the electron–neutrino system exists with the same J and same (lowest) degree of forbiddenness f (table 1).

Substituting (14) and using the form of G for $q\rho \ll 1$, we obtain after some algebra

$$P_{JLS}(E) = \frac{2g^2}{\pi}|\,M_{JLS}|^2\,.\,2Epq^2\sum_{\nu=0}^{L}\{\alpha_\nu^{JLS}f_\nu^{(1)}(p)q^{2(L-\nu)-2}$$

$$\mp\beta_\nu^{JLS}f_\nu^{(2)}(p)q^{2(L-\nu)-1}+\gamma_\nu^{JLS}f_\nu^{(3)}(p)q^{2(L-\nu)}\} \qquad \ldots\ldots(23)$$

.A
5
2

where*

$$
\begin{aligned}
f_\nu^{(1)} &= [\,|F_{\nu+1}^{1,1}|^2 + |F_{\nu+1}^{-1,-1}|^2](2p^2\rho^{2\nu+2})^{-1} \rightarrow p^{2\nu+2}(2\nu+3\,!!)^{-2}\\
f_\nu^{(2)} &= -i[F_{\nu+1}^{1,1}F_\nu^{-1,1} - F_\nu^{1,-1}F_{\nu+1}^{-1,-1}](2p^2\rho^{2\nu+1})^{-1} \rightarrow -\frac{p}{E}p^{2\nu+1}(2\nu+1\,!!\;2\nu+3\,!!)^{-1}\\
f_\nu^{(3)} &= [\,|F_\nu^{1,-1}|^2 + |F_\nu^{-1,1}|^2](2p^2\rho^{2\nu})^{-1} \rightarrow p^{2\nu}(2\nu+1\,!!)^{-2} \qquad \ldots\ldots(24)
\end{aligned}
$$

and

$$
\left.
\begin{aligned}
\alpha_\nu^{JLS} &= \sum_{a=\pm1} (A_{\nu+\frac{1}{2},\,L-\nu-1-\frac{1}{2}a}^{\nu+1,\,L-\nu-1})^2[(2L-2\nu-1)\,!!]^{-2}\\
\beta_\nu^{JLS} &= 2(A_{\nu+\frac{1}{2},\,L-\nu-\frac{1}{2}}^{\nu+1,\,L-\nu-1})(A_{\nu+\frac{1}{2},\,L-\nu-\frac{1}{2}}^{\nu,\,L-\nu})[(2L-2\nu+1)\,!!\,(2L-2\nu-1)\,!!]^{-1}\\
\gamma_\nu^{JLS} &= \sum_{a=\pm1} (A_{\nu+\frac{1}{2},\,L-\nu-\frac{1}{2}a}^{\nu,\,L-\nu})^2[(2L-2\nu+1)\,!!]^{-2}.
\end{aligned}
\right\} \quad \ldots(25)
$$

The negative sign applies for 1, $\boldsymbol{\sigma}$, $\boldsymbol{\alpha}$, γ_5, and the positive for β, $\beta\boldsymbol{\sigma}$, $\beta\boldsymbol{\alpha}$, $\beta\gamma_5$. Except for this sign the expressions for the energy spectrum depend only on J, L, S (through the A coefficients). In obtaining these expressions we have ignored all terms which in the $Z=0$ approximation would lead to combined powers of $p\rho$, $q\rho$ ($\ll 1$) greater than the lowest (which is $2L$, since $A_{jj'}^{ll'}(JLS)=0$ unless $l+l' \geqslant L$. It follows that the degree of forbiddenness depends directly on L, rule (iv) of § 1).

Expansions in powers of αZ of the functions $f_\nu^{(1)}$, $f_\nu^{(2)}$, $f_\nu^{(3)}$, are given by Greuling (1942), the relation to Greuling's functions M_ν, N_ν, L_ν and F_0 being $f_\nu^{(1)} = F_0M_\nu$, $f_\nu^{(2)} = F_0N_\nu$, $f_\nu^{(3)} = F_0L_\nu$.

Using the values for the A coefficients given in the Appendix, we obtain

1. For the scalar operators ($S=0$, $J=L$),

$$
\left.
\begin{aligned}
\alpha_\nu^{L,L,0} &= U_L\,\frac{(L-\nu)(2\nu+1)\,!\,2^{L-2\nu}}{(2L-2\nu)\,!\,(\nu\,!)^2},\\
\beta_\nu^{L,L,0} &= U_L\,\frac{(L-\nu)(2\nu+1)\,!\,2^{L-2\nu}}{(2L-2\nu+1)\,!\,(\nu\,!)^2},\\
\gamma_\nu^{L,L,0} &= U_L\,\frac{(\nu+1)(2\nu)\,!\,2^{L-2\nu}}{(2L-2\nu+1)\,!\,(\nu\,!)^2}.
\end{aligned}
\right\} \quad \ldots\ldots(26)
$$

$$
U_L = \frac{(L\,!)^2 2^L}{4\pi(2L+1)\,!}. \qquad \ldots\ldots(27)
$$

2. For the vector operators ($S=1, J=L+1$ or L),†

$$
\left.
\begin{aligned}
\alpha_\nu^{L+1,L,1} &= \beta_\nu^{L+1,L,1} = 0,\\
\gamma_\nu^{L+1,L,1} &= U_L\,\frac{(2\nu+1)\,!\,2^{L-2\nu}}{(2L-2\nu+1)\,!\,(\nu\,!)^2}.
\end{aligned}
\right\} \quad \ldots\ldots(28)
$$

$$
\left.
\begin{aligned}
\alpha_\nu^{L,L,1} &= \frac{L+1}{L}\,\alpha_\nu^{L,L,0},\\
\beta_\nu^{L,L,1} &= -\frac{L+1}{L}\,\beta_\nu^{L,L,0}\\
\gamma_\nu^{L,L,1} &= \frac{L+1}{L}\left(\gamma_\nu^{L,L,0} - \frac{1}{L+1}\,\gamma_\nu^{L+1,L,1}\right).
\end{aligned}
\right\} \quad \ldots\ldots(29)
$$

These results agree with those found by Greuling (1942) by inspection, except for the factors U_L and $(L+1)/L$. The origin of these factors can be seen if we compare the 'averages over a sphere' (18) of the T_M^{JLS} with those calculated by Greuling for the corresponding Cartesian vectors and tensors, and thus obtain the relations

---

* The → indicates the values in the limit $Z=0$.

† Expressions for $J=L-1$ are only required in the special case $J=0$, $L=1$ with tensor and axial vector interaction (see table 1) and so are not considered here.

$$\left.\begin{aligned} 8\pi^2 U_L |M_{LL0}|^2_{\mathrm{av}} &= \left|\frac{Q_L(K\mathbf{r},\mathbf{r})}{L!}\right|^2_{\mathrm{av}}, \\ 8\pi^2 U_L |M_{L+1,L,1}|^2_{\mathrm{av}} &= \left|\frac{Q_{L+1}(\mathbf{K},\mathbf{r})}{(L+1)!}\right|^2_{\mathrm{av}}, \\ 8\pi^2\frac{L+1}{L} U_L |M_{LL1}|^2_{\mathrm{av}} &= \left|\frac{Q_L(\mathbf{K}\times\mathbf{r},\mathbf{r})}{L!}\right|^2_{\mathrm{av}}. \end{aligned}\right\} \qquad \ldots\ldots(30)$$

§7. ALLOWED SPECTRUM

Putting $L=0$ (hence $J=S=0$ or 1 according to the interaction), we obtain, since $\alpha_0^{S0S}=\beta_0^{S0S}=0$, $\gamma_0^{S0S}=U_0=1/4\pi$,

$$P_{S0S}(E) = \frac{g^2}{2\pi^3} 2\pi |M_{S0S}|^2 Epq^2 f_0^{(3)},$$

which is the energy spectrum for all allowed transitions and for certain first forbidden transitions with $L=0$. $f_0^{(3)}$ is the usual correction factor for $Z\neq 0$.

§8. CONCLUSIONS

We have shown that by using eigenstates of total angular momentum of the system electron–neutrino, the selection rules and energy spectra of beta-emissions between nuclear states of arbitrary spin and parity can be derived.

In a subsequent paper (Spiers and Blin-Stoyle 1952) the method used above will be applied to the derivation of angular distributions and electron–neutrino correlations for arbitrary degree of forbiddenness.

APPENDIX

A COEFFICIENTS

It is well known from the theory of atomic spectra (Condon and Shortley 1935) that a state of two particles of spin $\frac{1}{2}$ characterized in the usual notation by quantum numbers JMj_1j_2 can also be written as a linear superposition of states characterized by quantum numbers $JMLS$.

Formally, this implies that the following relation exists between Wigner coefficients:

$$C^{Jj_1j_2}_{Mm_1m_2} C^{j_1l_1\frac{1}{2}}_{m_1\mu_1\sigma_1} C^{j_2l_2\frac{1}{2}}_{m_2\mu_2\sigma_2} = \sum_{LS} B^{l_1l_2}_{j_1j_2}(JLS) C^{JLS}_{M\mu\sigma} C^{Ll_1l_2}_{\mu\mu_1\mu_2} C^{S\frac{1}{2}\frac{1}{2}}_{\sigma\sigma_1\sigma_2} \qquad \ldots\ldots(31)$$

where $\mu=\mu_1+\mu_2$, $\sigma=\sigma_1+\sigma_2$ and the constants $B^{l_1l_2}_{j_1j_2}$ (JLS) are to be determined.

Bearing in mind the following relation between normalized spherical harmonics

$$\sum_{\mu_1\mu_2} C^{Ll_1l_2}_{\mu\mu_1\mu_2} Y^{\mu_1}_{l_1} Y^{\mu_2}_{l_2} = \left[\frac{(2l_1+1)(2l_2+1)}{4\pi(2L+1)}\right]^{1/2} C^{Ll_1l_2}_{000} Y^{\mu}_{L}, \qquad \ldots\ldots(32)$$

we can then write

$$\sum_{\mu_1\mu_2} C^{Jj_1j_2}_{Mm_1m_2} C^{j_1l_1\frac{1}{2}}_{m_1\mu_1\sigma_1} C^{j_2l_2\frac{1}{2}}_{m_2\mu_2\sigma_2} Y^{\mu_1}_{l_1} Y^{\mu_2}_{l_2}$$

$$= \sum_{LS} A^{l_1l_2}_{j_1j_2}(JLS) C^{JLS}_{MM-\sigma\sigma} C^{S\frac{1}{2}\frac{1}{2}}_{\sigma\sigma_1\sigma_2} Y^{M-\sigma}_{L}, \qquad \ldots\ldots(33)$$

where $$A^{l_1l_2}_{j_1j_2}(JLS) = \left[\frac{(2l_1+1)(2l_2+1)}{4\pi(2L+1)}\right]^{1/2} C^{Ll_1l_2}_{000} B^{l_1l_2}_{j_1j_2}(JLS). \qquad \ldots\ldots(34)$$

In the theory of beta-decay, only those values of l_1 and l_2 are of interest for which $l_1+l_2=L$, and it is then easy to calculate the B coefficients by solving eqns. (31).

The following results are obtained:

For $S=0$, $J=L$,

$$\left.\begin{aligned} B^{l_1l_2}_{l_1+\frac12\, l_2+\frac12}&=\left[\frac{L+1}{(2l_1+1)(2l_2+1)}\right]^{1/2} & B^{l_1l_2}_{l_1-\frac12\, l_2+\frac12}&=-\left[\frac{l_1}{2l_1+1}\right]^{1/2}, \\ B^{l_1l_2}_{l_1+\frac12\, l_2-\frac12}&=\left[\frac{l_2}{2l_2+1}\right]^{1/2} & B^{l_1l_2}_{l_1-\frac12\, l_2-\frac12}&=0. \end{aligned}\right\} \qquad \ldots\ldots(35)$$

For $S=1$, $J=L+1$, $B^{l_1l_2}_{l_1+\frac12\, l_2+\frac12}=1$. All other coefficients vanish.

For $S=1$, $J=L$,

$$\left.\begin{aligned} B^{l_1l_2}_{l_1+\frac12\, l_2+\frac12}&=\frac{l_1-l_2}{[L(2l_1+1)(2l_2+1)]^{1/2}} & B^{l_1l_2}_{l_1-\frac12\, l_2+\frac12}&=\left[\frac{(L+1)l_1}{L(2l_1+1)}\right]^{1/2}, \\ B^{l_1l_2}_{l_1+\frac12\, l_2-\frac12}&=\left[\frac{(L+1)l_2}{L(2l_2+1)}\right]^{1/2} & B^{l_1l_2}_{l_1-\frac12\, l_2-\frac12}&=0. \end{aligned}\right\} \qquad \ldots\ldots(36)$$

REFERENCES

CONDON, E. U., and SHORTLEY, G. H., 1935, *The Theory of Atomic Spectra* (Cambridge : University Press).

FURRY, W. H., 1937, *Phys. Rev.*, **51**, 125; 1938, *Ibid.*, **54**, 36.

GREULING, E., 1942, *Phys. Rev.*, **61**, 568.

KONOPINSKI, E. J., 1943, *Rev. Mod. Phys.*, **15**, 209.

MARSHAK, R. E., 1942, *Phys. Rev.*, **61**, 431.

RACAH, G., 1942, *Phys. Rev.*, **62**, 438.

ROSE, M. E., 1937, *Phys. Rev.*, **51**, 484.

SPIERS, J. A., and BLIN-STOYLE, R. J., 1952, *Proc. Phys. Soc.* A, **65**, 809.

A Formulation of Beta-Decay Theory for Forbidden Transitions of Arbitrary Order
II: Angular Distributions

By J. A. SPIERS and R. J. BLIN-STOYLE
Clarendon Laboratory, Oxford

MS. received 21*st March* 1952; *read before the Society at Southampton on* 19*th December* 1951

ABSTRACT. The method of a previous paper is used to derive general formulae (valid for arbitrary *Z*) for the angular distributions of beta-emissions.

.A
5
2

§ 1. INTRODUCTION

In a previous paper (Spiers and Blin-Stoyle 1952, to be referred to as I), by using eigenstates of the total angular momentum of the electron–neutrino system, expressions are derived for the energy spectra of beta-emissions between nuclear states of arbitrary spin and parity.

The object of the present paper is to apply this method to the angular distributions of the beta-particles emitted in transitions between magnetic sub-levels of the initial and final nuclear states. These angular distributions are required in the theory of beta–gamma correlations (Falkoff and Uhlenbeck 1950) and of emissions from oriented nuclei (Spiers 1949), and hitherto have only been calculated for first and second forbidden transitions in the $Z=0$ approximation (Falkoff and Uhlenbeck 1950). The formulae obtained here apply to an arbitrarily forbidden transition and take account of the coulomb field of the nucleus.

§ 2. ANGULAR DISTRIBUTIONS

Consider a transition from an initial nuclear state with angular momentum quantum numbers J_iM_i to a final nuclear state J_fM_f, resulting in the emission of an electron–neutrino system specified by the total angular momentum quantum numbers J, $M=M_i-M_f$.

The state of the electron–neutrino system can then be written in the notation of I as

$$\chi_{M_iM_f}=\sum_{Jjaj'a'} g M^{M_iM_f}_{JMjaj'a'} \sum_{mm'} C^{Jjj'}_{Mmm'} \psi_{jma}(\mathbf{r}\sigma\beta)\phi_{j'm'a'}(\mathbf{r}'\sigma'\beta'). \quad \ldots\ldots(1)$$

The 'differential angular distribution' (Falkoff and Uhlenbeck 1950) of the electrons with energy between E and $E+dE$ is then given by

$$I_{M_iM_f}(\theta;E)\,d\Omega\,dE=\frac{E}{\pi p}S\,|\chi_{M_iM_f}|^2_{r=R}R^2\,d\Omega\,dE, \quad \ldots\ldots(2)$$

where S represents an integral over the neutrino coordinates and a sum over the variables $\sigma\sigma'\beta\beta'$. R is a large but constant distance.

The normalization of (2) is such that on averaging over initial and summing over final nuclear orientations

$$\frac{1}{2J_i+1}\sum_{M_iM_f}\int I_{M_iM_f}(\theta;E)\,d\Omega=P(E). \quad \ldots\ldots(3)$$

Substitution of (1) into (2), using (13) and (21) of I and the normalization properties of ϕ, gives

$$I_{M_iM_f}(\theta;E)=\frac{g^2E}{\pi p}\sum_{j'a'm}\sum_{\beta\sigma}\Big|\sum_{jaJLS}M_{JLS}C^{J_iJ_fJ}_{M_iM_fM}R^{jaj'a'}_{JLS}(p,q,\rho)^*C^{Jjj'}_{Mmm'}\psi_{jma}(R\theta\phi;\sigma\beta)\Big|^2 \qquad \ldots\ldots(4)$$

with $m'=M-m$, $M=M_i-M_f$.

The summation over J, L, S in the square modulus may lead to many cross terms involving unknown nuclear matrix elements M_{JLS} if the nuclear transition is such that a number of states J, L, S have the same (lowest) degree of forbiddenness (see table 1 of I). In order to obtain more definite results we consider here only transitions in which all but one matrix element may in fact be neglected. In this case

$$I_{M_iM_f}(\theta;E)=|C^{J_iJ_fJ}_{M_iM_fM}|^2F^{JLS}_M(\theta;E), \qquad \ldots\ldots(5)$$

where
$$F^{JLS}_M(\theta;E)=\frac{g^2E}{\pi p}|M_{JLS}|^2\sum_{j'a'\beta\sigma m}\Big|\sum_{ja}R^{jaj'a'}_{JLS}(p,q,\rho)^*C^{Jjj'}_{Mmm'}\psi_{jma}(R\theta\phi;\sigma\beta)\Big|^2 \qquad \ldots\ldots(6)$$

$F^{JLS}_M(\theta;E)$ could be obtained from (6) by a similar procedure to that used for the energy spectrum (I, § 6).

However, for beta–gamma correlation theory (Falkoff and Uhlenbeck 1950) and for the theory of emission from oriented nuclei (Spiers 1949) it is sufficient (and much easier) to calculate $F^{JLS}_M(0;E)$ only, since the properties of angular distributions under spatial rotation are such that

$$F^{JLS}_M(\theta;E)=\Sigma_{M'}|D^{(J)}_{MM'}(\theta)|^2F^{JLS}_M(0;E), \qquad \ldots\ldots(7)$$

where the matrix elements $D^{(J)}_{MM'}(\theta)$ are the irreducible representation of order J of the group of real spatial rotations. This reduces, for the special case $M=0$, to

$$F^{JLS}_0(\theta;E)=\frac{4\pi}{2J+1}\Sigma_{M'}|Y^{M'}_J(\theta)|^2F^{JLS}_M(0;E). \qquad \ldots\ldots(8)$$

Now for large R the electron wave function has the asymptotic form (Rose 1937, using the notation of I)

$$\psi_{jma}(R\theta\phi;\sigma\beta)\rightarrow\left(\frac{E-\beta}{E}\right)^{1/2}C^{j\,j+\frac{1}{2}a\beta\,\frac{1}{2}}_{m\,m-\sigma\,\sigma}Y^{m-\sigma}_{j+\frac{1}{2}a\beta}(\theta\phi)\frac{\exp i[pR+\xi_{ja}+\zeta_\beta]}{R}, \qquad \ldots\ldots(9)$$

where the phase factors ξ_{ja} and ζ_β are dependent on the variables indicated and on the screened coulomb field through which the electron moves.

In the absence of screening

$$\xi_{ja}=-\arg\Gamma(\gamma+i\alpha ZE/p)+\eta-\gamma\pi/2 \quad \text{and} \quad \zeta_\beta=(\alpha ZE/p)\ln(2pR)-\pi(1+\beta)/2$$

where $\gamma=[(j+\frac{1}{2})^2-\alpha^2Z^2]^{1/2}$ and $\exp(2i\eta)=[a(j+\frac{1}{2})+i\alpha Z/p]/[\gamma+i\alpha ZE/p]$. α is the fine structure constant.

To take screening into account these phase factors would have to be computed numerically.

Substituting from (9) into (6) and writing $\theta=0$ we obtain, after some algebra,

$$F^{JLS}_M(0;E)=\frac{4g^2pEq^2}{\pi}|M_{JLS}|^2\sum_{\nu=0}^{L}\Big\{(\alpha^{JLS}_\nu(M)\phi^{(1)}_\nu+\delta^{JLS}_\nu(M)\phi^{(4)}_\nu)p^{2(\nu+1)}q^{2(L-\nu-1)}$$
$$\pm(\beta^{JLS}_\nu(M)\phi^{(2)}_\nu+\epsilon^{JLS}_\nu(M)\phi^{(5)}_\nu)\frac{p^{2(\nu+1)}q^{2(L-\nu)-1}}{E}+\gamma^{JLS}_\nu(M)\phi^{(3)}_\nu p^{2\nu}q^{2(L-\nu)}\Big\} \qquad \ldots(10)$$

which is the required result. The positive or negative sign is to be used if the matrix element involves one of the Dirac operators 1, $\boldsymbol{\sigma}$, $\boldsymbol{\alpha}$, γ_5 or β, $\beta\boldsymbol{\sigma}$, $\beta\boldsymbol{\alpha}$, $\beta\gamma_5$ respectively. The coefficients $\alpha_\nu^{JLS}(M), \ldots . \epsilon_\nu^{JLS}(M)$ are given in the Appendix.†

The $\phi_\nu^{(n)} (n=1, \ldots, 5)$ are functions of p, ρ related to the radial solutions of Dirac's equation for a central field. They are so defined as to reduce to unity in the limit $Z=0$.

In the notation of I:

$$\left.\begin{aligned}
\phi_\nu^{(1)} &= \frac{[(2\nu+3)!!]}{p^{2(\nu+1)}} f_\nu^{(1)} = \frac{[(2\nu+3)!!]^2}{2p^{2(\nu+2)}} (|F_{\nu+1}^{11}|^2 + |F_{\nu+1}^{-1-1}|^2)\rho^{-2(\nu+1)} \\
&\qquad = 1 + \frac{2\nu+3}{\nu+1}\frac{\alpha Z}{\rho E} + O(\alpha^2 Z^2) \\
\phi_\nu^{(2)} &= \frac{-E(2\nu+3)!!(2\nu+1)!!}{p^{2(\nu+1)}} f_\nu^{(2)} = \frac{iE(2\nu+3)!!(2\nu+1)!!}{2p^{2(\nu+2)}} \\
&\qquad \times (F_{\nu+1}^{11} F_\nu^{-11} - F_\nu^{1-1} F_{\nu+1}^{-1-1})\rho^{-2\nu-1} = 1 + \frac{2\nu+3}{\nu+1}\frac{\alpha Z E}{2\rho p^2} + O(\alpha^2 Z^2) \\
\phi_\nu^{(3)} &= \frac{[(2\nu+1)!!]^2}{p^{2\nu}} f_\nu^{(3)} = \frac{[(2\nu+1)!!]^2}{2p^{2(\nu+1)}} (|F_\nu^{-11}|^2 + |F_\nu^{1-1}|^2)\rho^{-2\nu} = 1 + O(\alpha^2 Z^2) \\
\phi_\nu^{(4)} &= \frac{-[(2\nu+3)!!]^2}{2p^{2(\nu+2)}} (F_{\nu+1}^{1-1} F_{\nu+1}^{11} \cos \pi_\nu - F_{\nu+1}^{-1-1} F_{\nu+1}^{-11} \cos \pi'_\nu)\rho^{-2(\nu+1)} \\
&\qquad = 1 + \frac{2\nu+3}{\nu+1}\frac{\alpha Z}{2\rho E} + O(\alpha^2 Z^2) \\
\phi_\nu^{(5)} &= \frac{-iE(2\nu+3)!!(2\nu+1)!!}{2p^{2(\nu+2)}} (F_\nu^{1-1} F_{\nu+1}^{-11} \cos \pi_\nu + F_{\nu+1}^{1-1} F_\nu^{-11} \cos \pi'_\nu)\rho^{-2\nu-1} \\
&\qquad = 1 + O(\alpha^2 Z^2)
\end{aligned}\right\} \quad \ldots\ldots(11)$$

where $\pi_\nu = \xi_{\nu+\frac{1}{2}, -1} - \xi_{\nu+\frac{1}{2}, 1}$ and $\pi'_\nu = \pi - \xi_{\nu+\frac{1}{2}, -1} + \xi_{\nu+\frac{1}{2}, 1}$.

Both these factors are zero for $Z=0$.

As shown above, the first three ϕ's are related to the f's used in the expression for the energy spectrum in paper I, and do not involve the phase factors ξ.

§ 3. RELATION TO THE ENERGY SPECTRUM

Using (3) and (7) gives

$$P^{JLS}(E) = \frac{1}{2J_i+1} \sum_{M_i M_f} \int I_{M_i M_f}(\theta; E)\, d\Omega = \frac{1}{2J+1} \sum_M F_M^{JLS}(0; E). \quad \ldots\ldots(12)$$

It is easy to show that the sums over M of the coefficients $\alpha_\nu^{JLS}(M)$, etc. are as follows:

$$\left.\begin{aligned}
&\sum_M \alpha_\nu^{JLS}(M) = \frac{2J+1}{[(2\nu+3)!!]^2}\alpha_\nu^{JLS}, \quad \sum_M \gamma_\nu^{JLS}(M) = \frac{2J+1}{[(2\nu+1)!!]^2}\gamma_\nu^{JLS} \\
&\sum_M \beta_\nu^{JLS}(M) = \frac{2J+1}{[(2\nu+3)!!(2\nu+1)!!]}\beta_\nu^{JLS}, \quad \sum_M \delta_\nu^{JLS}(M) = \sum_M \epsilon_\nu^{JLS}(M) = 0
\end{aligned}\right\} \ldots(13)$$

where the α_ν^{JLS} etc. are defined in I.

---

† Each term of the summation over ν corresponds to a total angular momentum $j=\nu+\frac{1}{2}$ of the electron.

Hence from (10)

$$P^{JLS}(E)=\frac{4}{\pi}g^2pEq^2|M_{JLS}|^2\sum_{\nu}\left\{\frac{\alpha_\nu^{JLS}}{[(2\nu+3)!!]^2}\phi_\nu^{(1)}p^{2(\nu+1)}q^{2(L-\nu-1)}\right.$$

$$\left.\pm\frac{\beta_\nu^{JLS}}{(2\nu+3)!!(2\nu+1)!!}\phi_\nu^{(2)}\frac{p^{2(\nu+1)}q^{2(L-\nu)-1}}{E}+\frac{\gamma_\nu^{JLS}}{[(2\nu+1)!!]^2}\phi_\nu^{(3)}p^{2\nu}q^{2(L-\nu)}\right\} \qquad \ldots\ldots(14)$$

From the relation of $\phi_\nu^{(n)}$ to $f_\nu^{(n)}$ $(n=1, 2, 3)$ set out in (11) we see that this agrees with eqn. (23) of I and is therefore a check on the calculations of this paper.

The expression (14) for the energy spectrum has the advantage over the one given previously (I, eqn. (23)) that the ϕ functions have a simple form for small αZ and that the numerical coefficients are sufficiently simple to be written explicitly for the three cases of importance

$$P^{LL0}(E)=\frac{4}{\pi}g^2pEq^2U_L|M_{LL0}|^2$$

$$\times\sum_{\nu=0}^{L}\left\{\frac{2^{L-1}}{(2L-2\nu-1)!(2\nu+1)!(2\nu+3)^2}\phi_\nu^{(1)}p^{2(\nu+1)}q^{2(L-\nu-1)}\right.$$

$$\pm\frac{(L-\nu)(\nu+1)2^{L+1}}{(2L-2\nu+1)!(2\nu+3)!}\phi_\nu^{(2)}\frac{p^{2(\nu+1)}q^{2(L-\nu)-1}}{E}$$

$$\left.+\frac{(\nu+1)2^{L}}{(2L-2\nu+1)!(2\nu+1)!(2\nu+1)}\phi_\nu^{(3)}p^{2\nu}q^{2(L-\nu)}\right\}$$

$$P^{L+1,L,1}(E)=\frac{4}{\pi}g^2pEq^2U_L|M_{L+1,L,1}|^2\sum_{\nu=0}^{L}\left\{\frac{2^{L}}{(2L-2\nu+1)!(2\nu+1)!}\phi_\nu^{(3)}p^{2\nu}q^{2(L-\nu)}\right\}$$

$$P^{LL1}(E)=\frac{4}{\pi}g^2pEq^2\,\frac{L+1}{L}\,U_L|M_{LL1}|^2$$

$$\times\sum_{\nu=0}^{L}\left\{\frac{2^{L-1}}{(2L-2\nu-1)!(2\nu+1)!(2\nu+3)^2}\phi_\nu^{(1)}p^{2(\nu+1)}q^{2(L-\nu-1)}\right.$$

$$-(\pm)\frac{(L-\nu)(\nu+1)2^{L+1}}{(2L-2\nu+1)!(2\nu+3)!}\phi_\nu^{(2)}\frac{p^{2(\nu+1)}q^{2(L-\nu)-1}}{E}$$

$$\left.+\frac{L(\nu+1)-\nu}{(2L-2\nu+1)!(2\nu+1)!(2\nu+1)(L+1)}\phi_\nu^{(3)}p^{2\nu}q^{2(L-\nu)}\right\},$$

with the same sign convention as for (10).

§ 4. PROPERTIES OF $F_M^{JLS}(\theta\,;E)$

Inspection of the coefficients $\alpha_\nu^{JLS}(M)$ etc. (Appendix) shows that they all possess the property $\alpha_\nu^{JLS}(M)=\alpha_\nu^{JLS}(-M)$ etc., so that $F_M^{JLS}(0;E)=F_{-M}^{JLS}(0;E)$, and hence $F_M^{JLS}(\theta;E)=F_{-M}^{JLS}(\theta;E)$; this implies that $F_M^{JLS}(\theta;E)$ is a polynomial in even powers of cos θ.

Further, the way in which θ is involved in (6) and (7) serves to limit the maximum power $2n$ of cos θ thus: n is the largest integer such that $n\leqslant L$, $n\leqslant J$.

As already mentioned, the phase factors π_ν and π_ν' occurring in $\phi_\nu^{(4)}$ and $\phi_\nu^{(5)}$ are dependent on the coulomb field through which the beta-particles move, and for a screened field would have to be computed numerically. It should be noted, however, that in the important case of $F_M^{L+1L1}(\theta;E)$ the functions $\phi_\nu^{(4)}$ and $\phi_\nu^{(5)}$ are not involved since $\alpha=\beta=\delta=\epsilon=0$. The expression for the angular distribution is then independent of any possible screening effects except in so far as these may affect the form of the Dirac radial function at $r=\rho$ (Reitz 1950). $F_M^{L+1L1}(\theta;E)$ relates to nuclear transitions in which the parity change is such that $|J_i-J_f|$

is greater by one than the degree of forbiddenness (see table 1 of paper I). These transitions have the further property that only one state $L+1$, L, 1 of the electron–neutrino system occurs with non-negligible probability; the angular distribution and energy spectrum are then uniquely defined, while for all other transitions several matrix elements may be non-negligible with unknown ratios and cross-terms result.

§ 5. PARTICULAR CASES

The following are tabulated as they constitute a generalization for $Z \neq 0$ of the angular distribution functions given by Falkoff and Uhlenbeck (1950) for use in the study of beta–gamma correlations.

We use $b=+1$ for the operators 1, $\boldsymbol{\alpha}$, $\boldsymbol{\sigma}$, γ_5 and $b=-1$ for β, $\beta\boldsymbol{\alpha}$, $\beta\boldsymbol{\sigma}$, $\beta\gamma_5$.

(i) $L=1$ (*First or Second Forbidden Transitions*)

$$
\begin{aligned}
F_0^{110}(\theta;E) &= \tfrac{1}{3}\phi_0^{(3)}q^2+(\phi_0^{(1)}/9-2\phi_0^{(4)}/9+\phi_1^{(3)}/9)p^2+b(2\phi_0^{(2)}/9-2\phi_0^{(5)}/9)p^2q/E \\
&\qquad +\cos^2\theta[(\phi_1^{(3)}/3+2\phi_0^{(4)}/3)p^2+2bp^2q\phi_0^{(5)}/3E] \\
F_0^{111}(\theta;E) &= \phi_0^{(3)}q^2/6+(\phi_0^{(1)}/9+\phi_1^{(3)}/36+\phi_0^{(4)}/9)p^2-b(2\phi_0^{(2)}/9+\phi_0^{(5)}/9)p^2q/E \\
&\qquad +\cos^2\theta[(\phi_1^{(3)}/12-\phi_0^{(4)}/3)p^2+b\phi_0^{(5)}p^2q/3E] \\
F_0^{211}(\theta;E) &= \phi_0^{(3)}q^2/3+\phi_1^{(3)}p^2/6+\tfrac{1}{2}\phi_1^{(3)}p^2\cos^2\theta .
\end{aligned}
$$

(ii) $L=2$ (*Second or Third Forbidden Transitions*)

$$
\begin{aligned}
F_0^{220}(\theta;E) &= 2\phi_0^{(3)}q^4/15+(4\phi_0^{(1)}/27+2\phi_1^{(3)}/9-4\phi_0^{(4)}/27)p^2q^2 \\
&\quad +(2\phi_1^{(1)}/75+3\phi_2^{(3)}/50+2\phi_1^{(4)}/25)p^4 \\
&\quad +b(8\phi_0^{(2)}/45-4\phi_0^{(5)}/45)p^2q^3/E+b(4\phi_1^{(2)}/45+2\phi_1^{(5)}/15)p^4q/E \\
&\quad +\cos^2\theta[(2\phi_1^{(3)}/9+4\phi_0^{(4)}/9)p^2q^2+(2\phi_1^{(1)}/25-3\phi_2^{(3)}/25-24\phi_1^{(4)}/25)p \\
&\quad +4b\phi_0^{(5)}p^2q^3/15E+b(4\phi_1^{(2)}/15-8\phi_1^{(5)}/5)p^3q/E] \\
&\quad +\cos^4\theta[(3\phi_2^{(3)}/10+6\phi_1^{(4)}/5)p^4+2b\phi_1^{(5)}p^4q/E] \\
F_0^{221}(\theta;E) &= \phi_0^{(3)}q^4/45+(\phi_0^{(1)}/27+\phi_1^{(3)}/54)p^2q^2+(\phi_1^{(1)}/150+\phi_2^{(3)}/150-\phi_1^{(4)}/75)p^4 \\
&\quad -2b\phi_0^{(2)}p^2q^3/45E+b(\phi_1^{(5)}/45-\phi_1^{(2)}/45)p^4q/E \\
&\quad +\cos^2\theta[\phi_1^{(3)}p^2q^2/18+(\phi_1^{(1)}/50-\phi_2^{(3)}/75+4\phi_1^{(4)}/25)p^4 \\
&\quad -b(\phi_1^{(2)}/15+4\phi_1^{(5)}/15)p^4q/E] \\
&\quad +\cos^4\theta[(\phi_2^{(3)}/30-\phi_1^{(4)}/5)p^4+b\phi_1^{(5)}p^4q/3E] \\
F_0^{321}(\theta;E) &= \phi_0^{(3)}q^4/30+\phi_1^{(3)}p^2q^2/15+\phi_2^{(3)}p^4/40 \\
&\quad +\cos^2\theta[2\phi_1^{(3)}p^2q^2/15-\phi_2^{(3)}p^4/20]+\cos^4\theta[\phi_2^{(3)}p^4/8].
\end{aligned}
$$

§ 6. CONCLUSIONS

By using eigenstates of the total angular momentum of the system electron–neutrino, it has been found possible to derive a general formula (valid for arbitrary Z) for the angular distribution of the charged beta-particles in a transition between magnetic sub-levels of nuclear states of arbitrary spin and parity. We have considered explicitly only cases where all but one nuclear matrix element may be neglected, but the method is of course applicable to the general case if required.

A subsequent paper will deal in a similar fashion with electron–neutrino correlations for arbitrary degree of forbiddenness.

APPENDIX

We give below the values of the coefficients $\alpha_\nu^{JLS}(M)\,\ldots\,\epsilon_\nu^{JLS}(M)$ used in the text.

(i) *Scalar Operators* ($S=0$, $J=L$)

$$\alpha_\nu^{LL0}(M)=\frac{U_L 2^{L-1}}{2L!}\frac{(L+M)!(L-M)!}{[(2\nu+3)\nu!]^2}\times\left\{\frac{1}{(L+M-\nu-1)!(L-M-\nu)!}+\frac{1}{(L-M-\nu-1)!(L+M-\nu)!}\right\}$$

$$\beta_\nu^{LL0}(M)=\frac{2\nu+3}{2L-2\nu+1}\alpha_\nu^{LL0}(M)$$

$$\gamma_\nu^{LL0}(M)=\left(\frac{2\nu+3}{2L-2\nu+1}\right)^2\alpha_\nu^{LL0}(M)+\frac{U_L 2^{L-1}}{2L!}\frac{(L+M)!(L-M)!}{[(2\nu+1)(2L-2\nu+1)\nu!]^2}\times\left\{\frac{(L-M-2M\nu+1)^2}{(L+M-\nu)!(L-M-\nu+1)!}+\frac{(L+M+2M\nu+1)^2}{(L-M-\nu)!(L+M-\nu+1)!}\right\}$$

$$\delta_\nu^{LL0}(M)=\frac{U_L 2^{L}}{2L!}\frac{(L+M)!(L-M)!}{[(2\nu+3)\nu!]^2(\nu+1)(2L-2\nu-1)}\times\left\{\frac{L-3M-2M\nu+1}{(L+M-1-\nu)!(L-M-\nu)!}+\frac{L+3M+2M\nu+1}{(L-M-1-\nu)!(L+M-\nu)!}\right\}$$

$$\epsilon_\nu^{LL0}(M)=\frac{2\nu+3}{2L-2\nu+1}\delta_\nu^{LL0}(M).$$

(ii) *Vector Operators* ($S=1$, $J=L+1$ *or* L)

$$\alpha_\nu^{L+1L1}(M)=\beta_\nu^{L+1L1}(M)=\delta_\nu^{L+1L1}(M)=\epsilon_\nu^{L+1L1}(M)=0$$

$$\gamma_\nu^{L+1L1}(M)=\frac{U_L 2^{L}}{2L!}\frac{(L+1+M)!(L+1-M)!}{(L+1)(2L+1)(\nu!)^2}\times\left\{\frac{1}{(L+M-\nu)!(L-M-\nu+1)!}+\frac{1}{(L-M-\nu)!(L+M-\nu+1)!}\right\}$$

$$\alpha_\nu^{LL1}(M)=\frac{L+1}{L}\alpha_\nu^{LL0}(M),\quad \beta_\nu^{LL1}(M)=-\frac{L+1}{L}\beta_\nu^{LL0}(M)$$

$$\gamma_\nu^{LL1}(M)=\left(\frac{2\nu+3}{2L-2\nu+1}\right)^2\alpha_\nu^{LL1}(M)+\frac{U_L 2^{L-1}}{2L!}\frac{(L+M)!(L-M)!(2\nu-L)^2}{[(2\nu+1)(2L-2\nu+1)(L+1)\nu!]^2}\times\left\{\frac{(L-M-2M\nu+1)^2}{(L+M-\nu)!(L-M-\nu+1)!}+\frac{(L+M+2M\nu+1)^2}{(L-M-\nu)!(L+M-\nu+1)!}\right\}$$

$$\delta_\nu^{LL1}(M)=-\frac{2\nu+2-L}{L}\delta_\nu^{LL0}(M),\quad \epsilon_\nu^{LL1}(M)=\frac{2\nu+2-L}{L}\epsilon_\nu^{LL0}(M).$$

REFERENCES

FALKOFF, D. L., and UHLENBECK, G. E., 1950, *Phys. Rev.*, **79**, 323.
REITZ, J. R., 1950, *Phys. Rev.*, **77**, 10.
ROSE, M. E., 1937, *Phys. Rev.*, **51**, 484.
SPIERS, J. A., 1949, *Directional Effects in Radio-Activity* (Ontario : Nat. Res. Ccl. of Canada).
SPIERS, J. A., and BLIN-STOYLE, R. J., 1952, *Proc. Phys. Soc.* A, **65**, 801.

Studies in Graphite and Related Compounds
I: Electronic Band Structure in Graphite

By C. A. COULSON* and R. TAYLOR†
Wheatstone Physics Department, King's College, London

MS. received 24th March 1952

ABSTRACT. The Bloch (tight-binding) approximation is applied to a study of graphite. The mean energy per atom and the internuclear distance are calculated in good agreement with experiment. Previous accounts are extended by including certain overlap integrals and by dealing with a set of parallel layer planes instead of only one plane. The shape of the band due to the π-electrons is calculated, and the experimental x-ray emission spectrum of graphite is interpreted. It is concluded that the role of σ-electrons is greater than is often supposed.

§1. INTRODUCTION

The fact that in graphite the individual planes are separated by about 3·35 Å, whereas the interatomic distance within any one plane is only 1·42 Å, shows conclusively that we regard each hexagonal plane as a large 'aromatic' molecule, and the binding between the planes as essentially van der Waals in character. Current theories of aromatic molecules divide the bonds into two types—first there are the σ-bonds, localized in the region between two adjacent nuclei, and described by electronic wave functions with approximately axial symmetry: second there are the π-bonds due to π-electrons. These latter are the metallic electrons, since we represent them by orbitals extending over the complete plane. It is these latter, and not the former, which give graphite its characteristic properties. Discussions of the electronic structure of graphite, with the solitary exception of some early calculations by Hund and Mrowka (1937), have dealt only with the π-electrons. We may regard these as having energies lying within a band, the π-band, and as contributing to the observed interatomic distance and heat of sublimation. In two following papers we shall see that (*a*) these π-electrons contribute to the x-ray scattering in a characteristic manner, and (*b*) in the boron nitride crystal, which may be regarded as derived from graphite by alternately increasing and decreasing the nuclear charges by unity, these electrons exhibit certain differences from graphite.

A preliminary account of this work has already been given (Coulson 1947). Since then a paper by Wallace (1947) has shown how the π-electron distribution is related to the electrical conductivity, though he did not attempt to draw the band distribution, and a further paper by Barriol and Metzger (1950) has reproduced part of the work reported by Coulson (1947). This will enable us to abbreviate the first part of the present discussion though, as we shall show, there is one serious inaccuracy in this earlier work. In the later part of this paper we shall show the influence on the band shape of an overlap factor previously neglected, and the way in which the presence of other planes modifies the details of this shape. We conclude with a discussion of the relationship between our calculated energy–density curve and the observed x-ray emission bands.

---

* Now at Mathematical Institute, Oxford. † Now at T.R.E., Malvern, Worcs.

§ 2. TIGHT-BINDING APPROXIMATION WAVE FUNCTIONS FOR AN INFINITE SHEET

Figure 1 shows a unit cell, which contains two atoms. Let us represent the normalized π-orbital of atom (j, k) by ϕ_{jk} and that of atom $[j, k]$ by $\psi_{j,k}$. We may consider a plane array such as that of fig. 2 in which there are altogether $2UV$ atoms. Later both U and V will tend to infinity. It can be seen from fig. 2 that the allowed values of j and k are

$$j=-u,-u+1,\ldots.-1,0,1,\ldots.u, \qquad \overline{\overline{U}}=2u+1,$$
$$k=-v,\ -v+1,\ldots.-1,0,1,\ldots.v, \qquad \overline{\overline{V}}=2v+1.$$

If we introduce Born's cyclic condition (or, alternatively, bend the large sheet of fig. 2 into a closed torus) we can use symmetry conditions to give us nearly all that we require about the Bloch wave functions. Let us introduce the auxiliary functions

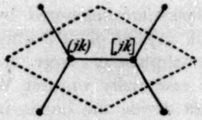

Fig. 1. Nomenclature for atoms in a unit cell of a graphite layer.

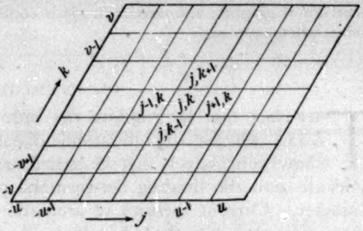

Fig. 2. Nomenclature for the unit cells in a graphite layer.

$$\Phi_{m,n}=\sum_{j=-u}^{+u}\sum_{k=-v}^{+v}\phi_{jk}\exp 2\pi i\left\{\frac{jm}{\overline{\overline{U}}}+\frac{kn}{\overline{\overline{V}}}\right\},$$
$$\Psi_{m,n}=\sum_{j=-u}^{+u}\sum_{k=-v}^{+v}\psi_{jk}\exp 2\pi i\left\{\frac{jm}{\overline{\overline{U}}}+\frac{kn}{\overline{\overline{V}}}\right\}, \qquad \ldots\ldots(1)$$

where $-u\leqslant m\leqslant u,\ -v\leqslant n\leqslant v$. These auxiliary functions are such that the only combining pairs are $\Phi_{m,n}$ and $\Psi_{m,n}$ with the same m and n. This means that each molecular wave function (or molecular orbital, m.o.) is of the form

$$(\Psi)_{mn}=N_{mn}^{-1}\{\Psi_{mn}+c_{mn}\Phi_{mn}\}, \qquad \ldots\ldots(2)$$

where N_{mn} is a normalizing constant and c_{mn} is a complex quantity, of modulus unity, whose value, for given m and n, has to be found from the secular equations.

Let E_{mn} be the energy associated with $(\Psi)_{mn}$, and E_0 the energy of a separate atomic orbital ϕ_{jk}; further let β be the resonance integral across a bond. This means that if H is the one-electron Hamiltonian, then

$$\beta=\int\phi_{jk}H\psi_{jk}\alpha\tau=\int\phi_{jk}H\psi_{j+1,k}\,d\tau=\text{etc.} \qquad \ldots\ldots(3)$$

We require two other quantities. The first is the overlap integral between adjacent pairs of atomic orbitals, defined by

$$S=\int\phi_{jk}\psi_{jk}\,d\tau=\int\phi_{jk}\psi_{j+1,k}\,d\tau=\text{etc.} \qquad \ldots\ldots(4)$$

The second is closely related to the resonance integral. It is the quantity introduced first by Mulliken, Rieke and Brown (1941) and defined by

$$\gamma = \beta - E_0 S. \qquad \ldots\ldots(5)$$

Resonance and overlap integrals between other than nearest neighbours are temporarily neglected.

We are now in a position to write down the secular equations, which are quadratics. A quite straightforward analysis gives

$$E_{mn} = E_0 + \frac{g}{1+Sg}\gamma, \qquad \ldots\ldots(6)$$

where

$$[g(m,n)]^2 = 3 + 2\cos\frac{2\pi m}{\overline{U}} + 2\cos\frac{2\pi n}{\overline{V}} + 2\cos 2\pi\left(\frac{m}{\overline{U}} - \frac{n}{\overline{V}}\right). \qquad \ldots\ldots(7)$$

It may be seen that g^2 ranges continuously from 0 to 9. The details of the corresponding wave function are given by

$$c_{mn} = \left\{1 + \exp\frac{2\pi i m}{\overline{U}} + \exp\frac{2\pi i n}{\overline{V}}\right\} \Big/ g(m,n), \qquad \ldots\ldots(8)$$

so that $\quad c_{mn}c_{mn}{}^{*} = 1 \ldots\ldots(9) \quad$ and $\quad N_{mn}{}^2 = 2\overline{U}\overline{V}(1+gS). \quad \ldots\ldots(10)$

If we assume, as is often done, that the overlap integral S is zero, these results simplify to

$$E_{mn} = E_0 + g\beta, \qquad N_{mn}{}^2 = 2\overline{U}\overline{V}. \qquad \ldots\ldots(11)$$

These last two equations are implicit in the work of Wallace, and of Barriol and Metzger. Since, however, the numerical value of S is known (Wheland 1941) to be approximately $\frac{1}{4}$, it is undesirable to omit it completely as these authors did. Furthermore, as Wheland (1941) and Mulliken, Rieke and Brown (1941) have shown for aromatic and conjugated molecules, agreement between theory and experiment for the heats of sublimation and energies of spectral transitions is impossible without its inclusion. We shall find that in our case the shape of the complete band of π-electron energies is greatly affected by the presence of S. In numerical work we shall put

$$S = 0{\cdot}25. \qquad \ldots\ldots(12)$$

This value is obtained by direct evaluation of the integral (4) when Slater-type atomic orbitals are used (Slater 1930), together with the observed value of the interatomic distance. The same is true for the inter-layer overlap ($\bar{0}{\cdot}034$, see p. 821) between atoms facing each other in adjacent planes. Explicit formulae for these integrals may be found in Coulson (1942) and numerical tables in Mulliken, Rieke, Orloff and Orloff (1949).

§ 3. MEAN ENERGY AND BOND LENGTH

Equations (6)–(11) enable us, without great difficulty, to estimate the mean energy per atom and the internuclear distance, or bond length. Since there is exactly one π-electron per carbon atom it is simple to see from (6) and (7) that the occupied levels are just those for which $g(m,n)$ is positive. These occupy orbitals which, in molecular language, would be called bonding. The others, for which $g(m,n)$ is negative, are antibonding. In the ground state, at absolute zero of temperature, they will all be empty. Thus the mean energy per atom is

$\bar{E}=2\Sigma_{m,n}E_{mn}/2UV$, where the factor 2 is introduced on account of the two spin assignments, and the summation is over all m and n, choosing the positive g in eqn. (7).

It is simplest, as Coulson and Rushbrooke (1948) have shown for graphitic strips, to deal with the simpler case of $S=0$ first. Then, on letting $\bar{U}$, $\bar{V}$ tend to ∞, we have

$$\bar{E}-E_0=\frac{\beta}{4\pi^2}\iint\{3+2\cos x+2\cos y+2\cos(x-y)\}^{1/2}\,dx\,dy,\ldots \qquad \ldots\ldots(13)$$

where the range of integration is $-\pi\leqslant x,\ y\leqslant\pi$. This reduces to

$$\bar{E}-E_0=\frac{4\beta}{\pi^2}\int_0^{\pi/2}E(k)(1+2\cos t)\,dt, \qquad \ldots\ldots(14)$$

where $k^2=8\cos t/(1+2\cos t)^2$, and $E(k)$ is the complete elliptic integral of the second kind defined by

$$E(k)=\int_0^{\pi/2}\{1-k^2\sin^2\theta\}^{1/2}\,d\theta.$$

Tables of $E(k)$ are available, but it does not appear possible to complete the integration in (14) analytically. Numerical integration gives

$$\bar{E}-E_0=1{\cdot}576\beta. \qquad \ldots\ldots(15)$$

This is the same as the value given without proof by Wheland (1934) and Coulson (1947). It agrees to within 1% with the value obtained by Barriol and Metzger (1950) by considering particular values of $\bar{U}$ and $\bar{V}$.

If we include the overlap integral S, then the analysis is a little more complicated. The result is

$$\bar{E}-E_0=1{\cdot}08\gamma \qquad \ldots\ldots(16)$$

where γ is defined by (5).

It will be noticed that the values in (15) and (16) fit smoothly into the tables of binding energies in graphite crystallites of varying finite size as calculated by Bradburn, Coulson and Rushbrooke (1948) (see table I on page 340 and table IV on page 345). If we take conventional values for β and γ, then as shown in this latter paper, the numerical values in (15) and (16) do fit extremely well with the observed heat of sublimation of graphite.

Since all the bonds are equal and there are 3/2 bonds per atom, we can find the π-bond order (Coulson 1939) by dividing $\bar{E}-E_0$ by 3β. The result is

$$p=0{\cdot}525. \qquad \ldots\ldots(17)$$

As Chirgwin and Coulson (1950) have shown, this value is unaffected by inclusion of the overlap integral S. Assuming 1·540, 1·340 and 1·204 Å respectively for the bond lengths of C—C, C=C and C≡C the corresponding bond length for graphite is 1·42 Å. The complete agreement of this value (Bacon 1950) and that for the heat of sublimation (Jessup 1938) with the experimental values, provides strong support for the general picture that we have been describing. It also suggests that the inter-layer energy is quite small, perhaps only of the order of 5 kcal/g atom. This would be entirely reasonable, even though this is not an adequate means of calculating it, on the basis of likely van der Waals forces.

§4. DENSITY OF STATES IN THE π-BAND

According to (11), with $S=0$, the energy levels lie in a band stretching from $E_0+g_{\max}\beta$ to $E_0-g_{\max}\beta$. It is easily verified that the maximum value of $g(m,n)$ is when $m=n=0$, giving $g_{\max}=3$. Thus the band stretches from $E_0+3\beta$ to $E_0-3\beta$. So long as we put $S=0$, it will be a symmetrical band, just as with the strips discussed by Coulson and Rushbrooke (1948). The density of states within the band is easily found if we notice that as $\overline{U}$, $\overline{V}\rightarrow\infty$, the variables $m/\overline{U}$, $n/\overline{V}$ become uniformly distributed between $\pm\frac{1}{2}$. It is convenient to introduce the function $P(g)$ where $P(g)$ is the proportion of occupied states whose g-values lie between $g=3$ (the bottom of the band) and our chosen value of g. Evidently $P(3)=0$, $P(0)=1$. It can also be shown that $P(1)=\frac{3}{4}$. Other values of P can be found, if desired, by numerical integration in the plane defined by the continuous variables $m/\overline{U}$ and $n/\overline{V}$. The following asymptotic expressions are available:

Near bottom of band $P(g)=\dfrac{\sqrt{3}}{2\pi}(3-g)+\ldots=0{\cdot}276(3-g)+\ldots.$

Near top occupied region $P(g)=1-g^2/\sqrt{3}\pi+\ldots=1-0{\cdot}184g^2+\ldots.$ ......(18)

The variation of $P(g)$ is shown in fig. 3, together with the above asymptotic forms.

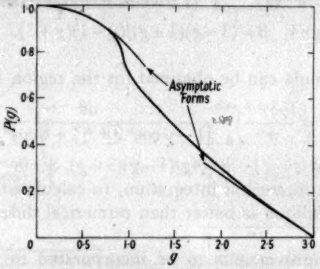

Fig. 3. The shape of the curve $P(g)$, where $P(g)$ is the probability that the function $g(x, y)$ lies between g and 3.

Since $P(g)$ is the proportion of occupied states for which $(E-E_0)/\beta>g$, it follows that $-dP/dg$ is the actual density of energies per carbon atom per unit range of $(E-E_0)/\beta$. Thus at the bottom of the band the density of states is 0·276, and near the top of the occupied region, where $E-E_0$ and g are small, the density is $0{\cdot}368g$. The complete density curve $N(E)$ is shown in fig. 4(a). Clearly $N(E)=-(1/\beta)\,dP/dg$. This curve includes both the occupied and unoccupied parts (at zero temperature). It is possible, however, to obtain an integral representation for $P(g)$ and, which is more important, dP/dg, as follows. If we restrict ourselves, for the moment, to the two-dimensional layer with $S=0$, then we know from (11) that $E_{mn}=E_0+g\beta$, where g is given by (7). If we let $x(=2\pi m/\overline{U})$ and $y(=2\pi n/\overline{V})$ be current variables appropriate to the infinite layer for which $\overline{U}$, $\overline{V}\rightarrow\infty$ as in (13), then $E-E_0=g(x,y)\beta$, where

$$[g(x,y)]^2=3+2\cos x+2\cos y+2\cos(x-y). \qquad \text{......(19)}$$

The range of allowed values may be taken to be $|x|\leqslant\pi$, $|y|\leqslant\pi$. $E-E_0$ is a function of x, y represented by the contours shown in fig. 5. Then $P(g)$ is equal to $1/4\pi^2$ times the area between the origin and the contour g. Let us first suppose that $g>1$ so that the contour is single, and of approximately elliptical shape. Then on rotating the axes through 45° in an anti-clockwise direction we have

$$g^2=\{1+4\cos(Y/2^{1/2})\cos(X/2^{1/2})+4\cos^2(X/2^{1/2})\}. \qquad \ldots\ldots(20)$$

Then $P(g)=\dfrac{1}{4\pi^2}\times 4\displaystyle\int_0^{X_{\max}} Y\,dX$, where $X_{\max}=2^{1/2}\cos^{-1}\{(g-1)/2\}$, and X and Y are related by (20). A certain amount of algebra enables this to be put in the form

$$P(g)=\frac{2}{\pi^2}\int_{(g-1)/2}^{1}\cos^{-1}\left(\frac{g^2-1-4t^2}{4t}\right)\frac{dt}{(1-t^2)^{1/2}}.$$

From this, by differentiation under the integral sign, it follows that

$$-\frac{dP}{dg}=\frac{4g}{\pi^2}\int_{(g-1)/2}^{1}\frac{dt}{[(1-t^2)\{(2t+1)^2-g^2\}\{g^2-(2t-1)^2\}]^{1/2}}.$$

The substitution $t^2=\sin^2\theta+\{\frac{1}{2}(g-1)\}^2\cos^2\theta$ allows this to be expressed as

$$-\frac{dP}{dg}=\frac{g}{\pi^2}\left(\frac{\beta}{\alpha}\right)^{1/2}\int_0^{\pi/2}\frac{d\theta}{[1-\alpha\cos^2\theta]^{1/2}[1+\beta\cos^2\theta]^{1/2}}, \qquad \ldots\ldots(21)$$

where $\alpha=(3-g)(1+g)/4$, $\beta=(3-g)(1+g)/(g-1)(g+3)$. Both α and β are positive.

An analogous formula can be obtained for the region $1>g\geqslant 0$. It is

$$-\frac{dP}{dg}=\frac{(\gamma\delta)^{1/2}}{\pi^2}\int_0^{\pi/2}\frac{d\theta}{[1-\gamma\cos^2\theta]^{1/2}[1+\delta\cos^2\theta]^{1/2}}, \qquad \ldots\ldots(22)$$

where $\gamma=4g/(1+g)^2$, $0\leqslant\gamma\leqslant 1$; $\delta=4g/(1-g)(3+g)$, $\delta>0$. From (21) and (22) it is possible, by simple numerical integration, to calculate $N(E)$ for any selected value of g. This technique is better than numerical differentiation of the $P(g)$ curve.

There are two improvements to be incorporated in this treatment. The first concerns the inclusion of S, the second involves the consideration of more than one layer plane.

§ 5. INCLUSION OF OVERLAP INTEGRAL

It is possible, as shown by Coulson and Rushbrooke (1948), to change from the case $S=0$ to the case $S\neq 0$ extremely easily. The new density function, which we may call $N_\gamma(E)$, is related to the former one $N_\beta(E)$ by the relation

$$N_\gamma(E)=(1+gS)^2N_\beta(E). \qquad \ldots\ldots(23)$$

$N_\gamma(E)$ is the number of electrons that can be accommodated per carbon atom per unit range of $(E-E_0)/\gamma$. We show, in fig. 4 (*b*), the graph of $N_\gamma(E)$. It is at once clear that the previous symmetry around the centre $E=E_0$ is no longer present. Just as in the earlier work of Coulson and Rushbrooke, the occupied part of the band is much compressed as compared with the unoccupied. But the characteristic drop to zero at the top of the occupied part, which formed the basis of Wallace's discussion of conductivity, is unaffected. Indeed, a combination of (18) and (23) shows that not even the slope of the $N(E)$ curve is changed at $E=E_0$.

§6. INTRODUCTION OF THE THIRD DIMENSION

The second improvement in our calculated band shape is the result of introducing the whole set of layer planes instead of concentrating solely on one of them. Let us first consider a somewhat idealized structure in which each carbon atom has other carbon atoms directly above and below it. (In the real graphite this is true for only half the atoms.) Then in the conventional Bloch treatment we modify the wave functions (1) by introducing a further exponential factor to deal with motion across the planes. The energy splits into two parts —one part is the two-dimensional energy given in (6) and (7): the other part is an energy due to the interplanar momentum. This latter part is, formally, just the same as for a linear chain of atoms, except that, on account of the fact that the overlapping lobes of π-orbitals on adjacent planes have opposite algebraic signs, the sign of the resonance integral is altered. Thus for any fixed $m/\overline{U}$, $n/\overline{V}$ there is now a band of energies. This band is quite thin, since its width depends on the numerical value of the resonance integral. This is not known at all precisely, but if, following suggestions of Mulliken, we suppose that the resonance integral is proportional to the corresponding overlap integral, we get for the ratio of the inter-layer resonance integral to the intra-layer resonance integral a value 0·034 : 0·25. If we consider, for simplicity, the case where $S=0$, and denote the resonance integrals by $\beta_\perp$ and $\beta_\parallel$ respectively, then the total width of the two-dimensional part is $6\beta_\parallel$, and of the part due to the third dimension it is $4\beta_\perp$.

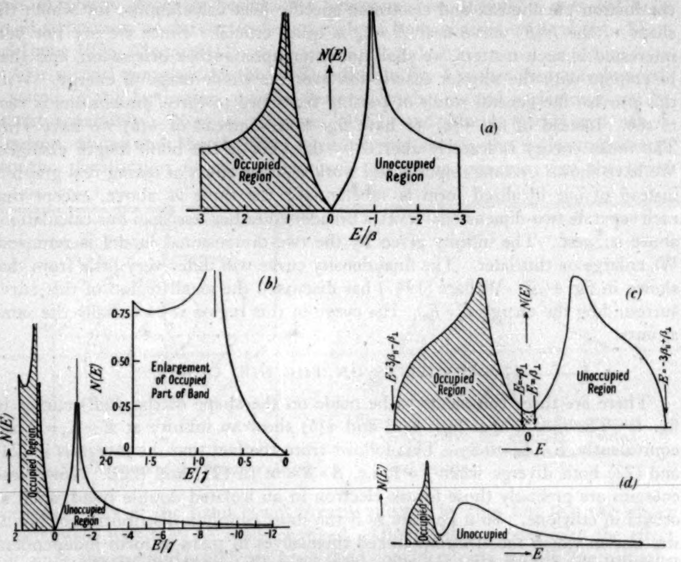

Fig. 4. (*a*) Graph of $N(E)$ for a single layer with conventional neglect of overlap integrals.
(*b*) Graph of $N(E)$ for a single layer taking account of overlap integrals.
(*c*) Graph of $N(E)$ for three-dimensional crystal, with neglect of overlap integrals.
(*d*) Graph of $N(E)$ for three-dimensional crystal, taking account of overlap integrals.

This width is less than one-tenth of the other. This means that we can pass from the diagrams in figs. 4 (*a*) and 4 (*b*) to corresponding three-dimensional distributions by replacing each separate level by a thin band, centred at the same energy value and spreading a small, but constant, distance on either side. More accurate calculations than this can be made formally, but they are not justified until we know more about the values of $\beta_\perp$ and are prepared to include $\beta_\parallel$ for second-nearest neighbours as well as nearest ones. Such more detailed calculations are, of course, necessary in discussing the shape of the band near the point $E=E_0$, where the spreading of each two-dimensional level into a band of constant width is no longer a quite fair description. This would apply to conduction phenomena and electronic specific heat calculations, for which the shape of the $N(E)$ curve near $E=E_0$ is quite crucial. Since we are not here interested in such matters, we shall not enter upon such a discussion, and shall be content with the simpler description over the whole range of energy. With this proviso the general result of passing from two to three dimensions is easy to see. Instead of fig. 4 (*a*) we have fig. 4 (*c*); instead of 4 (*b*) we have 4 (*d*). The mean energy is scarcely altered by this, nor is the bond length changed. We have shown in some unpublished work that the effect of taking real graphite instead of our idealized form is substantially the same as above, except that each separate two-dimensional level is broadened rather less than our calculations above suggest. The infinity given by the two-dimensional model is removed. We enlarge on this later. The final density curve will differ very little from that shown in fig. 4 (*d*). Wallace (1947) has discussed the small region of this curve surrounding the energy $E=E_0$. His curve in this region is essentially the same as ours.

§ 7. COMMENTS ON THE N(E) CURVE

There are three comments to be made on the shape of the $N(E)$ curves in fig. 4. The first is that figs. 4 (*a*) and 4 (*b*) show an infinity at $E-E_0=\beta$, or, equivalently, $E-E_0=0{\cdot}8\gamma$. This follows from the fact that the integrals in (21) and (22) both diverge when $g=1$, i.e. $\beta=\delta=\infty$ in (21) and (22). Now these energies are precisely those for an electron in an isolated double bond, such as occurs in ethylene. So it appears as if the most common distribution of bonds was one in which the electrons linked themselves in pairs to form independent C=C units. In this way we relate our work to that of Pauling, Brockway and Beach (1935) who determined the bond order of graphite by considering resonance of Heitler–London type among a large number of canonical structures in which the bonds were all either single or double. This resonance, it would appear, has the effect of spreading out the energies into a band, but the maximum density is still located at its value for any one of the unexcited canonical structures.

Both of the previously published $N(E)$ curves are wrong because they failed to take account of this infinity at $E-E_0=\pm\beta$. It is worth while following our argument a little further, with a view to seeing whether additional refinements would remove the infinity; and if so, which ones would do so. We shall merely report the results of our analysis here, without proof. First, on account of (23) the introduction of S is irrelevant in this respect. But we might expect that some difference would result if, in addition to β between nearest neighbours (now called β_1) we introduced β_2 between next-nearest neighbours. Instead of (19) we now find that $E-E_0=\pm g\beta_1-(g^2-3)\beta_2$. Thus the shapes of the contours in the (x, y) plane are entirely unchanged, though their labelling is slightly altered.

The infinity in $N(E)$ still remains. However, if we introduce third-nearest neighbours, with corresponding $\beta = \beta_3$, we discover that

$$\{(E-E_0)+(g^2-3)\beta_2\}^2 = \beta_1^2 g^2(x, y) + \beta_3^2 g^2(2x, 2y) + \beta_1\beta_3[(g^2-3)+4\cos(x+y)\{1+\cos x+\cos y\}].$$

It can be shown that the infinity still remains, though it occurs at a slightly different value of E than before. We have shown that an infinite value of $N(E)$ will always occur, however many neighbours we consider, provided that we consider only a two-dimensional layer. However, as soon as we go to a three-dimensional structure, the infinity disappears. This is true for several other types of crystal structure besides the hexagonal one, though it does not hold for all structures, as the particular example of body-centred-cubic shows (Mott and Jones 1936, Chapter III).

Our second comment on the $N(E)$ curves in fig. 4 is that they are obtained, as stated in the beginning, on the assumption that σ- and π-electrons can be treated separately. Now as Altmann (1952) and March (1952) and others (Coulson, Higgs and March 1951) have recently shown, the π-electrons merge into the distribution of the σ-electrons. It seems possible that the lower (occupied) part of the band is not greatly affected by this, but that the upper (unoccupied) part may be more changed. Our third comment is to the effect that since the method which we have used considers only atomic $2p\pi$ orbitals, there will be mixing of the states which we have found with the band of states arising from $3p\pi$ atomic orbitals. The matter has been referred to, for molecules, by Coulson, Craig and Jacobs (1951). Again the conclusion seems to be that the lower half of the band is unlikely to suffer much alteration, but that the upper half may be more affected.

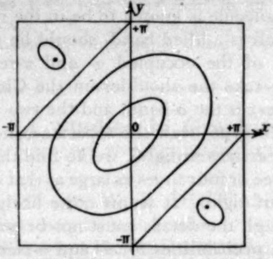

Fig. 5. Contours of the function $g(x, y)$.

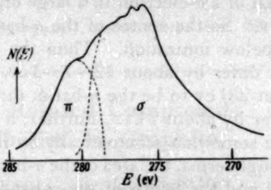

Fig. 6. Full line: Chalklin's experimental $N(E)$ curve for graphite. Dotted lines: proposed separation into σ- and π-parts.

§ 8. COMPARISON OF BAND SHAPE WITH EXPERIMENT

It is possible to compare our predicted band shape in graphite with the experimental one, as found by emission experiments in which an electron in the occupied part of the band falls into an empty K orbital. If we may suppose, for lack of any better knowledge, that the transition probability from any part of the occupied band is the same, then the observed intensity distribution is a direct measure of the band density $N(E)$. The best measurements for graphite are those of Chalklin (1948) whose $N(E)$ curve, on this assumption, is shown in fig. 6. At first sight this appears to agree excellently with the theoretical shape of fig. 4 (*d*). But the agreement is partly deceptive, for the total width of this observed band is about 15 volts. The theoretical width should be $1 \cdot 7\gamma \simeq 5$ ev, since the resonance integral γ has a value of about 3 ev. Our confusion arises from having overlooked the σ-band which must be superimposed on the π-band. Now σ-electrons have lower energy (greater binding energy) than π-electrons. So the region on the left of fig. 6 should relate to π-electrons, that on the right to σ-electrons. As there are three times as many σ-electrons as there are π-electrons we shall not expect the π-electrons to show up clearly resolved from the σ-electrons. The situation is very similar to that found for the charge distribution in benzene by March (1952). It may therefore be significant that the most noticeable difference between the $N(E)$ diagrams obtained by Chalklin for diamond (all σ-bonds) and graphite, is that in the latter there is a substantial shoulder at about 281 ev which does not appear in the former. Now this is just where the π-band would be expected, as the following figures show.

The ionization potential (work function) of graphite is about 4·3 ev. This corresponds to the removal of the top electron, and shows that for graphite $E_0 = 4 \cdot 3$ ev. The calculated width of the occupied π-region is about 5 ev, as we have seen, so that the π-band would be expected to stretch from 4·3 to about 10 ev below ionization level, with an average at about 7 ev. Now the ionization potential of a σ-electron in a large organic molecule is known to be in the region of 12 ev. So the centre of the σ-band, which is a filled band, should lie about 12 ev below ionization. Thus the centres of the occupied σ- and π-regions should differ by about $12 - 7 = 5$ ev. If we take the shoulder on the Chalklin curve at 281 ev to be the π-band, then the rest is the σ-band, and the two peaks do differ by about 5 ev. Further, if we attempt to draw the separate bands, as is done somewhat schematically by the dotted lines in fig. 6, we do find that, in very rough terms, the area of the σ-band is three or four times as large as that of the π-band and the width of the π-band is about right. It seems quite likely that our interpretation is essentially correct, though the details must not be pressed too closely. In the first place the transition probabilities for σ- and π-electrons are unlikely to be equal, and in the second place, as Altmann (1952) has shown for benzene and ethylene, there is no rigorous division into σ- and π-bands. Mixing of the two component bands would 'smudge' the separation attempted in fig. 6. But it should still be true that the left-hand (small wavelength) end of the emission band should be predominantly polarized with the electric vector perpendicular to the layer planes and the right-hand (long wavelength) end should be polarized in the layer planes.

Consideration of figs. 4 and 6 suggests that, although the main conclusions are probably correct, it would be very desirable to discuss both the σ-band and the resulting hybrid more carefully.

ACKNOWLEDGMENTS

We should like to acknowledge the provision of a calculating machine by the British Iron and Steel Research Association. We have also to thank Professor G. W. Wheland and Professor Sir John Lennard-Jones for helpful discussions on the earlier part of this work (which was done in 1937). One of us (R.T.) would like to acknowledge a research grant from the Caird Scholarship Trustees.

REFERENCES

Altmann, S. L., 1952, *Proc. Roy. Soc.* A, **210,** 327, 343.
Bacon, G. E., 1950, *Acta Crystallogr.*, **3,** 137.
Barriol, J., and **Metzger**, J., 1950, *J. Chim. Phys.*, **47,** 432.
Bradburn, M., **Coulson**, C. A., and **Rushbrooke**, G. S., 1948, *Proc. Roy. Soc. Edinb.* A, **62,** 336.
Chalklin, F. C., 1948, *Proc. Roy. Soc.* A, **194,** 42.
Chirgwin, B. H., and **Coulson**, C. A., 1950, *Proc. Roy. Soc.* A, **201,** 196.
Coulson, C. A., 1939, *Proc. Roy. Soc.* A, **169,** 413; 1942, *Proc. Camb. Phil. Soc.*, **38,** 210; 1947, *Nature, Lond.*, **159,** 265.
Coulson, C. A., **Craig**, D. P., and **Jacobs**, J., 1951, *Proc. Roy. Soc.* A, **206,** 297.
Coulson, C. A., **Higgs**, P. W., and **March**, N. H., 1951, *Nature, Lond.*, **168,** 1039.
Coulson, C. A., and **Rushbrooke**, G. S., 1948, *Proc. Roy. Soc. Edinb.* A, **62,** 350.
Hund, F., and **Mrowka**, B., 1937, *Ber. verh. Akad. Wiss. Lpz. math. phys. Kl.*, **87,** 185, 325.
Jessup, R. S., 1938, *Bur. Stand. J. Res., Wash.*, **21,** 475.
March, N. H., 1952, *Acta Crystallogr.*, **5,** 187.
Mott, N. F., and **Jones**, H., 1936, *The Theory of the Properties of Metals and Alloys* (Oxford : University Press).
Mulliken, R. S., **Rieke**, C. A., and **Brown**, W. G., 1941, *J. Amer. Chem. Soc.*, **63,** 41.
Mulliken, R. S., **Rieke**, C. A., **Orloff**, D., and **Orloff**, H., 1949, *J. Chem. Phys.*, **17,** 1248.
Pauling, L., **Brockway**, L. O., and **Beach**, J. Y., 1935, *J. Amer. Chem. Soc.*, **57,** 2705.
Slater, J. C., 1930, *Phys. Rev.*, **36,** 57.
Wallace, P. R., 1947, *Phys. Rev.*, **71,** 622.
Wheland, G. W., 1934, *J. Chem. Phys.*, **2,** 474; 1941, *J. Amer. Chem. Soc.*, **63,** 2025.

Studies in Graphite and Related Compounds II : Momentum Distribution in Graphite

By W. E. DUNCANSON* and C. A. COULSON†

* University College, London

† Wheatstone Physics Department, King's College, London; now at Mathematical Institute, Oxford

MS. received 24*th March* 1952

ABSTRACT. The space wave functions for the π-electrons in a graphite layer, as found in Part I, are transformed into momentum coordinates, and the radial distribution function, including σ-electrons and π-electrons, is calculated. Using the theory of Jauncey and DuMond the shape of the Compton profile in x-ray scattering is predicted. Both this, and the momentum distribution, are in excellent agreement with experimentally determined values. The introduction of a plausible scale factor in the atomic wave functions would make the agreement almost perfect.

§1. INTRODUCTION

The present authors have shown, in a series of papers, how the momentum distribution of electrons in various atoms and molecules may be calculated (a complete set of references is given by Duncanson 1943). In view of the difficulty of handling the wave equation in momentum coordinates, we found it more convenient to adopt the Dirac transformation theory to derive the momentum wave functions from the corresponding space functions. Even this procedure is exceedingly complex, if any but the simplest approximate wave functions are used, as the example of H_2^+ showed. Now the momentum distribution cannot be determined directly by experiment, but it can be deduced from the detailed shape of the Compton line in x-ray scattering, and from the energy distribution of inelastically scattered electrons. In order that the experiments may be directly comparable with the theoretical work, the atoms or molecules must be effectively isolated from each other, as in a gas, with the result that the intensity of the scattered x-ray or electron beam is weak. In addition, in the x-ray measurements, an extremely high dispersion is necessary. It is for this reason that only a limited amount of experimental work has been done which is at all suitable for comparison with theory.

In view of this situation it seems desirable to consider the corresponding problem in relation to the solid state. The theoretical aspect is rather more forbidding, since at least some of the electrons will now be described in terms of non-atomic wave functions (or possibly combinations of more than one atomic orbital on different centres). We have thought it wise to discuss the case of graphite first, partly because some careful work by Kirkpatrick and DuMond (1938) has yielded a more accurate shape for the Compton line than is available for other solids, and partly also because the layer structure of graphite is such that it is a good approximation to treat it as a two-dimensional problem by neglecting the influence of one plane on its neighbours. The analysis in Part I (Coulson and Taylor 1952, to be referred to as I) justifies this procedure. The effect of adjacent layers can be calculated in a quite straightforward manner, but it does not seem to us worth the extra labour involved, until our knowledge of the distribution of the bonding electrons in any one plane is more complete than it is at present.

Our procedure in this paper is (i) to discuss the hypothetical case of an infinite straight chain of carbon atoms, (ii) to generalize this and compare it with the true hexagonal layer, (iii) to deduce the shape of the Compton profile and compare with experiment. Our symbols and general model are the same as in I. There are three types of electron orbit to be considered. First there are the carbon K-shell electrons, in undistorted atomic orbitals; next there are the σ-electrons of the localized σ-bonds, and finally there are the π-electrons whose orbitals extend over the whole crystal. The first two types of electron have been dealt with in our previous papers, since they have just the same form as in ordinary atoms and molecules. The new features occur with the π-electrons, with which, therefore, most of our analysis will have to be concerned. As a guide in dealing with the two-dimensional problem, we have first studied the momentum distribution of the π-electrons in an infinite straight chain of carbon atoms, where each atom provides just one π-electron. The directions of all these π-electron orbits are supposed to be parallel, and perpendicular to the direction of the chain.

§2. MOMENTUM FUNCTIONS FOR THE π-ELECTRONS IN AN INFINITE CHAIN

If the chain is long enough, end effects are negligible and we may apply the Born cyclic condition. In this particular problem the use of this simplifying assumption is not necessary, for it may be shown rigorously to make no effective difference to the momentum distribution. But it is useful and, as we saw in I, it is necessary in the two-dimensional problem.

Let us suppose that the repeating unit consists of n similar atoms. Then the molecular orbitals (Bloch functions) for the π-electrons are

$$\Psi_k = \frac{1}{N_k}\sum_{j=1}^{n} c_j{}^k \psi_j, \qquad \ldots\ldots(1)$$

where

$$c_j{}^k = \exp(2\pi ijk/n), \qquad \ldots\ldots(2)$$

N_k is a normalizing factor and ψ_j is the normalized atomic orbital of the p_z electron at the jth atom. The analytical form of ψ_j is taken to be

$$\psi_j = \sqrt{\frac{\alpha^5}{\pi}}\, z_j \exp(-\alpha r_j), \qquad \ldots\ldots(3)$$

and the exponent α has the ordinary Slater value $\alpha = 1{\cdot}625$. If we neglect all overlap integrals except those between nearest neighbours, then

$$N_k{}^2 = n(1 + 2S\cos 2\pi k/n), \qquad \ldots\ldots(4)$$

where S is the overlap integral defined by

$$S = \int \psi_j \psi_{j+1}\, d\tau. \qquad \ldots\ldots(5)$$

A knowledge of the space wave functions (1) enables us without difficulty to deduce the corresponding momentum functions.

Adopting the Dirac transformation theory, and remembering that atomic units are being used throughout, the momentum function, corresponding to Ψ_k is χ_k, where

$$\chi_k = (2\pi)^{-3/2}\int \exp\{-i(\mathbf{p}\,.\,\mathbf{r})\}\Psi_k\, d\tau. \qquad \ldots\ldots(6)$$

If we substitute for Ψ_k from (1) and choose appropriate origins for each of the separate resulting integrals, this may be written

$$\chi_k = \frac{A}{N_k}\sum_{j=1}^{n} \exp ij\left(\frac{2\pi k}{n} - \rho p_x\right), \qquad \ldots\ldots(7)$$

where p_x is the component of the momentum $\mathbf{p}$ along the chain, ρ is the interatomic distance and A is the atomic momentum wave function

$$A = (2\pi)^{-3/2}\int \exp\{-i(\mathbf{p}\,.\,\mathbf{r})\}\psi_j\, d\tau. \qquad \ldots\ldots(8)$$

The summation in (7) is straightforward, giving us

$$\chi_k = \frac{A}{N_k}\exp i\left\{\frac{2\pi k}{n} - \rho p_x\right\}\cdot\frac{1-\exp(-in\rho p_x)}{1-\exp\{i(2\pi k/n - \rho p_x)\}}. \qquad \ldots\ldots(9)$$

The corresponding momentum density function is

$$\chi_k\chi_k{}^* = \frac{AA^*}{N_k{}^2}\,\frac{\sin^2 n\rho p_x/2}{\sin^2(2\pi k/n - \rho p_x)/2}. \qquad \ldots\ldots(10)$$

To find the mean momentum density function $\chi\chi^*$ we must sum terms such as (10) for all π-electrons and divide by the number n of electrons. These occupy the $\frac{1}{2}n$ lowest energy orbitals, in pairs. These orbitals correspond to the range $-n/4 < k \leqslant +n/4$. So

$$\chi\chi^* = 2AA^*\sum_{k=-n/4}^{n/4}\frac{\sin^2(n\rho p_x/2)}{n^2\sin^2(2\pi k/n - \rho p_x)/2}\,\frac{1}{1+2S\cos(2\pi k/n)}. \qquad \ldots\ldots(11)$$

(Strictly there are $\frac{1}{2}n+1$ terms in the sum (11) and we only need $\frac{1}{2}n$. But when we let n tend to ∞ the extra term is irrelevant.) This summation is difficult. But as $n \to \infty$ it simplifies. For the first fraction after the summation sign in (11) which we shall denote by $f(\rho p_x)$ has the value zero except when $\rho p_x = 2\pi k/n \pm$ any even multiple of π. Thus

$$\chi\chi^* = \frac{2AA^*}{1+2S\cos\rho p_x} f(\rho p_x), \qquad \ldots\ldots(12)$$

where, after some rather tedious algebra, which we shall not reproduce, it may be shown that

$$\begin{aligned} f(\rho p_x) &= 1 \text{ if } p_x \text{ lies between } (4l \pm 1)\pi/2,\ l \text{ integral} \\ &= 0 \text{ otherwise.} \end{aligned}$$

If we call these ranges 1 and 2 respectively, then

$$\begin{aligned} \chi\chi^* &= 2AA^*/(1+2S\cos\rho p_x) && \text{range 1,} \\ &= 0 && \text{range 2.} \end{aligned} \qquad \ldots\ldots(13)$$

In this formula A is the atomic momentum function corresponding to any of the ψ_j. It may be found by use of (8) and straightforward integration. The result is

$$AA^* = \frac{128\alpha^7}{\pi^2} \frac{p_z^2}{(\alpha^2+p^2)^6}. \qquad \ldots\ldots(14)$$

For comparison with experiment it is more useful to average over all angles. If we call the resulting function $I(p)$, then $I(p)$ is the mean radial momentum distribution. After some reduction this may be put in the form

$$I(p) = \frac{512\alpha^7 p}{\pi(\alpha^2+p^2)^6} \int_0^p \frac{p^2 - p_x^2}{1+2S\cos\rho p_x}\, dp_x, \qquad \ldots\ldots(15)$$

except that all values of p_x in range 2 are excluded from the integration. We found it easiest to perform the integration graphically. From a knowledge of $I(p)$ the Compton profile for scattered x-rays is soon found. We shall return to this later.

§3. MOMENTUM FUNCTION FOR THE TWO-DIMENSIONAL GRAPHITE LAYER

It is not difficult to generalize the preceding discussion to deal with the two-dimensional graphite layer. Again, let us concentrate first on the π-electrons. Both the nature of the unit cell, and the molecular-orbital wave functions, have been described in I. Thus we write for a typical Bloch function

$$(\Psi)_{mn} = N_{mn}^{-1}\{\Psi_{mn} + c_{mn}\Phi_{mn}\}, \qquad \ldots\ldots(16)$$

where Ψ_{mn} and Φ_{mn} are defined by I, eqn. (1); c_{mn} is a coefficient given by I (8) and N_{mn} is a normalizing constant defined by I (10). The Dirac transformation theory leads to a momentum wave function (cf. eqns. (6) to (8)) which may be written

$$\chi_{mn} = N_{mn}^{-1}\{\xi_{mn} + c_{mn}\zeta_{mn}\} \qquad \ldots\ldots(17)$$

where

$$\left.\begin{aligned} \xi_{mn} &= (2\pi)^{-3/2}\int \Psi_{mn} \exp(-i\mathbf{p}\,.\,\mathbf{r})\, d\tau, \\ \zeta_{mn} &= (2\pi)^{-3/2}\int \Phi_{mn} \exp(-i\mathbf{p}\,.\,\mathbf{r})\, d\tau. \end{aligned}\right\} \qquad \ldots\ldots(18)$$

If we use the expansion I (1) of Ψ_{mn}, and the definition II (8) of A, we can write

$$\xi_{mn} = A \sum_{j=-u}^{+u} \sum_{k=-v}^{+v} \exp 2\pi i\left\{\frac{jm}{\overline{U}} + \frac{kn}{\overline{V}}\right\} \exp\{-i\mathbf{p}\,.\,[\mathbf{r}]_{jk}\} \qquad \ldots\ldots(19)$$

where $[\mathbf{r}]_{jk}$ is the vector position of carbon atom numbered $[jk]$. A similar formula exists for ζ_{mn} except that $(\mathbf{r})_{jk}$ replaces $[\mathbf{r}]_{jk}$. This means that (17) can be written in the form

$$\chi_{mn}=N_{mn}^{-1}\{1+c_{mn}\exp(-i\mathbf{p}\cdot\boldsymbol{\rho})\}\xi_{mn}, \qquad \ldots\ldots(20)$$

where $\boldsymbol{\rho}$ is the vector joining $[jk]$ to (jk). This means that ρ is the C–C bond length. The momentum density is

$$\chi_{mn}\chi_{mn}^{*}=2N_{mn}^{-2}\left\{1+\left[\cos\mathbf{p}\cdot\boldsymbol{\rho}+\cos\left(\frac{2\pi m}{\bar{U}}-\mathbf{p}\cdot\boldsymbol{\rho}\right)\right.\right.$$
$$\left.\left.+\cos\left(\frac{2\pi n}{\bar{V}}-\mathbf{p}\cdot\boldsymbol{\rho}\right)\right]g^{-1}\right\}\xi_{mn}\xi_{mn}^{*}. \qquad \ldots\ldots(21)$$

So far we have only needed to treat $\mathbf{p}$ as a vector. When its components are required, it is most convenient to express them relative to the reciprocal lattice. The relationship of this lattice to the unit cell is exhibited in fig. 1.

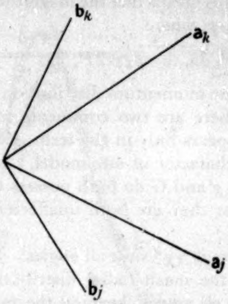

Fig. 1. Lattice vectors a and reciprocal vectors b for a graphite layer.

Here the three fundamental space vectors are $\mathbf{a}_j$, $\mathbf{a}_k$, $\mathbf{a}_z$, where $\mathbf{a}_j$ and $\mathbf{a}_k$ are each of length $\sqrt{3}\rho$ directed at an angle of 60°, and $\mathbf{a}_z$ is a vector, conveniently taken to be of unit length, perpendicular to the layer plane. The reciprocal vectors are $\mathbf{b}_j$, $\mathbf{b}_k$, $\mathbf{b}_z$ where the magnitudes are $2/3\rho$, $2/3\rho$ and 1 respectively: $\mathbf{b}_z$ is parallel to $\mathbf{a}_z$; $\mathbf{b}_j$ and $\mathbf{b}_k$ are perpendicular to $\mathbf{a}_k$ and $\mathbf{a}_j$ and make an angle of 120°.

Relative to these axes let us write

$$\mathbf{p}=\mathbf{b}_jP_j+\mathbf{b}_kP_k+\mathbf{b}_zP_z. \qquad \ldots\ldots(22)$$

Then $[\mathbf{r}]_{jk}=[\mathbf{r}]_{00}+j\mathbf{a}_j+k\mathbf{a}_k$, and $\mathbf{p}\cdot[\mathbf{r}]_{jk}=\mathbf{p}\cdot[\mathbf{r}]_{00}+jP_j+kP_k$. $\qquad\ldots\ldots(23)$

If we substitute from (23) into (19), it becomes possible to complete the summations over j and k. Each separate summation is similar to that involved in passing from (7) to (9). The corresponding density function $\xi_{mn}\xi_{mn}^{*}$ is similar to (10) except that there are two 'diffraction' factors instead of one. An analysis entirely similar to that which led from (10) to (13) shows that in the summation

$$\chi\chi^{*}=\frac{1}{\bar{U}\bar{V}}\sum_{mn}\chi_{mn}\chi_{mn}^{*},$$

which is needed to give the mean momentum density function, when $\overline{U}, \overline{V} \to \infty$, the previous range 2 in eqn. (13) disappears, and for all values of the momentum $\mathbf{p}$ it turns out that we may write

$$\chi\chi^* = AA^* \frac{G(P_j, P_k)}{1 + Sg(P_j, P_k)}. \qquad \ldots\ldots(24)$$

In this expression $A(p)$ is the momentum function for a single atomic orbital, as in (8) and (14), $g(P_j, P_k)$ is our previous g-function written in terms of the momentum coordinates, so that

$$[g(P_j, P_k)]^2 = 3 + 2\cos P_j + 2\cos P_k + 2\cos(P_j - P_k), \qquad \ldots\ldots(25)$$

and $G(P_j, P_k)$ is a function defined by

$$G(P_j, P_k) = 1 + \frac{1}{g}[\cos \tfrac{1}{3}(P_j + P_k) + \cos \tfrac{1}{3}(2P_j - P_k) + \cos \tfrac{1}{3}(2P_k - P_j)]. \qquad \ldots(26)$$

If we recall that P_j, P_k, P_z are components of the momentum in the reciprocal space, we shall recognize that the units in which they are measured are $2/3\rho$, $2/3\rho$ and 1 respectively. This means that the magnitudes of the three components, in ordinary units, are p_j, p_k, p_z where

$$p_j = 2P_j/3\rho, \qquad p_k = 2P_k/3\rho, \qquad p_z = P_z. \qquad \ldots\ldots(27)$$

This analysis gives us the momentum distribution for the π-electrons. Before going further, however, there are two comments to make. In the first place the third component p_z appears only in the term AA^* of (24). This is a direct result of the single-layer character of our model. In the second place, despite appearances, the functions g and G do both possess trigonal symmetry. It may be shown algebraically that they are both unaffected by a rotation of the axes through 120°.

Our next task is to average $\chi\chi^*$ over all angles. Just as in passing from (13) to (15) this will give us the mean radial distribution function $I(p)$. In fact $I(p) =$ integral of (24) over all angles, keeping the magnitude of p constant. If we imagine a series of concentric spheres drawn in p-space, then $I(p)\,dp =$ integral of (24) over all space between the spheres p, $p + dp$. Now the element of volume may be put in the form $\tfrac{1}{2}\sqrt{3}\,dp_j\,dp_k(p/p_z)\,dp$. This shows us that

$$I(p) = 2\iint A(p)A^*(p) \frac{G}{1 + Sg} \frac{p}{p_z} \frac{\sqrt{3}}{2}\,dp_j\,dp_k. \qquad \ldots\ldots(28)$$

The initial factor of 2 is inserted to take account of both top and bottom halves of the sphere $p =$ constant. If we now insert the value (14) for AA^* this gives

$$I(p) = \frac{128\sqrt{3}\alpha^7}{\pi^2} \frac{p}{(\alpha^2 + p^2)^6} \iint p_z \frac{G}{1 + Sg}\,dp_j\,dp_k, \qquad \ldots\ldots(29)$$

where the integration is taken over the whole of the inside of a circle of radius p lying in the jk plane. The relation between p_z and the other components is

$$p_z^2 = p^2 - p_j^2 - p_k^2 + p_j p_k. \qquad \ldots\ldots(30)$$

Also, when using (25) to obtain the value of g, the positive root is to be taken. The nature of the integrand in (29) shows that numerical, and not algebraic, methods are simplest for evaluating the integral.

This stage of our work is now complete. To obtain the total momentum distribution, we must add to (29) the contributions from the σ-bonds and from the carbon ls electrons. Since these contributions are purely atomic and molecular, and have been discussed in our earlier papers (e.g. Duncanson and Coulson 1941) we do not reproduce the analysis here.

§ 4. CALCULATIONS

It is necessary to decide what value shall be taken for the exponent α in (29). As we stated in (3) this has been given the ordinary Slater value 1·625. The same exponent is used for the basic σ-bonds. There is some doubt concerning the suitability of this value. We shall return to the matter a little later. The internuclear distance is known to be 1·421 Å which is almost equal to the rounded-off value 2·7 atomic units. We have therefore put $\rho = 2{\cdot}7$ A.U.

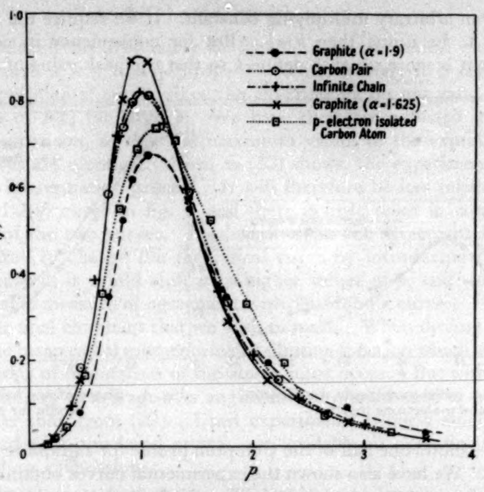

Fig. 2. Mean radial momentum distribution. Comparison of the radial momentum distribution of the p-electrons (or π-electrons where relevant) in an isolated carbon atom, a carbon pair, an infinite chain of carbon atoms, a graphite layer with parameter $\alpha = 1{\cdot}625$ and the same but with parameter $\alpha = 1{\cdot}9$.

Figure 2 shows the mean radial momentum distribution $I(p)$ for several sets of π-electrons. This includes a graphite layer, an infinite carbon chain, a pair of carbon atoms as in ethylene and an isolated carbon atom. In all four cases $\alpha = 1{\cdot}625$ and (apart from the last one) $\rho = 2{\cdot}7$. It will be seen that as we move to systems of greater complexity the maximum in the $I(p)$ curve moves to a smaller p, and the spread of the curve decreases. In passing from the infinite chain to the two-dimensional layer there is only a small change in the peak value, though the spread of the curve is reduced. We may reasonably suppose, on account of the large interlayer spacing, that the inclusion of other planes than the one we have considered would scarcely change the $I(p)$ curve any more.

In fig. 3 we have drawn curves for the total momentum distribution, including the σ-bonds and 1s electrons, weighted according to their number. This curve does not differ greatly from that appropriate to an isolated carbon atom. Just as in earlier papers we may use the curve of fig. 3 to calculate the shape of the Compton profile, using the type of argument advanced first by Jauncey. It has been shown (e.g. by DuMond 1933) that all incident wavelengths and all angles of scatter may be included in one formula, by use of a suitable 'reduced' variable. Thus the intensity J of the scattered x-rays is defined in terms of a variable q, where in DuMond's notation $q=l/2\lambda^*$, and l is the wavelength displacement from the centre of the Compton line, and λ^* is a quantity, with the dimensions of a wavelength, depending only on the primary wavelength and the angle of scattering. The formula for $J(q)$ is

$$J(q)=k\int_q^\infty \frac{I(p)}{p}\,dp, \qquad \ldots\ldots(31)$$

where k is an arbitrary multiplying constant. If we require the total area of the $J(q)$ curve to be unity, then $k=\frac{1}{2}$. But for convenience in comparison with experiment it is more usual to define k so that the peak value of $J(q)$ is given by $J(0)=1$.

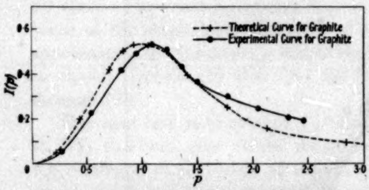

Fig. 3. Mean radial momentum distribution, σ- and π-electrons together.

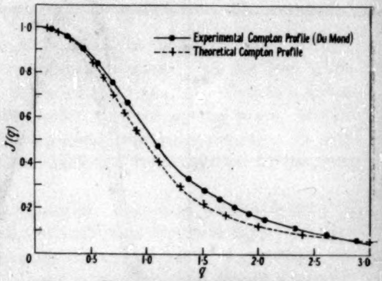

Fig. 4. Shape of one half of the Compton profile for graphite.

Figure 4 shows one half of the Compton profile for a graphite layer calculated in this way. We have also shown the experimental curves obtained by DuMond. The two curves are very similar, and differ chiefly in the fact that the half intensity is calculated to occur at $q=0{\cdot}96$, whereas it is found experimentally at $q=1{\cdot}06$. The difference is only 10%, a surprisingly good agreement in view of the approximations which we have been obliged to make in our model.

The greater half-width of the $J(q)$ curve is in complete accord with what we have found before with molecules. The matter has been discussed in some detail by ourselves (Coulson and Duncanson 1942) for methane CH_4. It is true that there are no π-electrons in this molecule, but there is no reason to doubt that similar conclusions would be obtained with them. It was found that if the Slater values for the exponents in the atomic orbitals for the 2s and 2p electrons of carbon and for the hydrogen 1s electrons were each multiplied by a parameter β, then the half-width of the Compton profile was increased by about 10% if β was changed from 1·0 to 1·1. The change in half-width was almost linear in β at least up to $\beta=1{\cdot}2$. In the case of methane reasons were given for taking $\beta=1{\cdot}1$.

Chiefly these are an acknowledgment of the fact that an electron in a molecule is under attraction to two or more centres of force instead of only one, as with an atom. And, as specific calculations for several simple molecules have shown convincingly, this contracts the charge-cloud. This is precisely what happens if β is increased. Now it would be rather laborious to repeat all our numerical integrations for several values of α; we have, however, made as careful an estimate as we could of the shape of the $I(p)$ curve when $\alpha = 1{\cdot}9$. This is shown in fig. 2. Its relationship to the previous curve, which was appropriate to the case of $\alpha = 1{\cdot}625$, is of the required type to make agreement with experiment almost perfect. This may therefore be regarded as a further justification for the increased value of α as a result of bonding.

DuMond also gives a curve for the mean radial momentum distribution $I(p)$ in graphite. This he deduces from his experimental $J(q)$ curve by means of the inverse relation to (31), viz.

$$kI(p) = p[dJ(q)/dq]_{q=p}. \qquad \ldots\ldots(32)$$

We have reproduced his $I(p)$ curve in fig. 3. Our theoretical curve here is normalized in such a way that $\int I(p)\,dp = 1$. Unfortunately it is difficult to do this for the experimental curve, since the experiments do not yield sufficiently accurate values of $I(p)$ for large p. We have therefore adjusted its scale, for purposes of comparison, so that the maximum values of the experimental and theoretical curves are identical. Now, as (32) shows, the experimental curve is obtained by a differentiation process. It will therefore be less reliable than the undifferentiated $J(q)$ curve in fig. 4, and there is little point in comparing the detailed shape of the two curves. In general terms the agreement is good. If we were prepared to change the theoretical curve by introducing the factor β previously discussed, it would shift it to higher values of p, and would lead to a quite remarkable measure of agreement with DuMond's curve.

There is one final comment that we wish to make. When dealing with atoms it is certainly the mean radial momentum distribution function which is important, since all directions of orientation of the atoms must occur. But with crystals, it may not be necessary to average over angles and we should need to work directly from (24) rather than from (29). Until experiments using a single crystal of graphite, instead of a powdered crystal, are available, it does not seem worth while making these calculations.

REFERENCES

Coulson, C. A., and Duncanson, W. E., 1942, *Proc. Camb. Phil. Soc.*, **38**, 100.

Coulson, C. A., and Taylor, R., 1952, *Proc. Phys. Soc.* A, **65**, 815.

DuMond, J. W. M., 1933, *Rev. Mod. Phys.*, **5**, 1.

Duncanson, W. E., 1943, *Proc. Camb. Phil. Soc.*, **39**, 180.

Duncanson, W. E., and Coulson, C. A., 1941, *Proc. Camb. Phil. Soc.*, **37**, 406.

Kirkpatrick, H. A., and DuMond, J. W. M., 1938, *Phys. Rev.*, **54**, 802.

Studies in Graphite and Related Compounds
III: Electronic Band Structure in Boron Nitride

By R. TAYLOR* and C. A. COULSON†
Wheatstone Physics Department, King's College, London

MS. received 24th March 1952

ABSTRACT. An analysis is made of the distribution of π-electrons in the crystal of boron nitride. The insulating character of this substance is shown by the fact that these electrons completely occupy one band, of width approximately 2·4 ev, separated from the next higher band by a gap of about 4·6 ev. The density of states in the band is calculated, accurately for a single layer plane, and approximately for the three-dimensional crystal. Until the energies of the σ-electrons are better known, further progress in understanding this substance will be difficult.

§1. INTRODUCTION

Boron nitride bears the same relationship to graphite as borazole ($B_3N_3H_6$) does to benzene (C_6H_6). Thus (see for example Bauer 1938) borazole, which has sometimes been called 'inorganic benzene' has a regular plane structure just like that of benzene, and boron nitride (Hassel 1926, Pease 1950) consists of parallel layer planes in each of which the boron and nitrogen atoms occupy alternate sites on a regular hexagonal lattice. The distance which separates the planes is almost the same (3·30 Å) as in graphite (3·35 Å) and the interatomic distances are 1·45 Å (boron nitride) and 1·42 Å (graphite). There are, however, two essential differences between graphite and boron nitride. The first is that on account of the greater electronegativity of nitrogen as compared with boron there will be an uneven distribution of the electrons, giving a partly ionic character to the lattice. The second is that, as Pease has recently shown, successive layers are stacked with their hexagons lying directly above and below each other, in such a way (fig. 1) that boron atoms lie between nitrogen atoms, and vice versa. This differs from graphite, where there is an additional parallel displacement between successive layers. The boron nitride arrangement has the advantage that atoms with a net positive charge are completely surrounded by atoms with a net negative charge, and vice versa. It is doubtless the increased electrostatic attractive energy which makes this configuration the stable one. It is our intention, in this paper, to study the electron distribution in boron nitride, in much the same way that we studied graphite in Part I (Coulson and Taylor 1952 to be referred to as I). We shall interpret the nature of the forces that cause the bonding, and estimate the band distribution (or, at least, that part of it which is due to the π-electrons). A good deal of the analysis in I may be adapted without difficulty to apply to our present problem.

§2. TYPES OF BONDING ELECTRON

The hexagonal structure of a single layer suggests strongly that there is sp^2 hybridization at the boron and nitrogen atoms. This would lead to a σ-bond distribution precisely as in graphite. But it would leave two π-electrons on each nitrogen atom and none on each boron atom. If we suppose that ionic structures exist, in which one of the π-electrons on a nitrogen atom moves into one of the empty π-orbitals of an adjacent boron atom, then a double bond may be formed. In borazole, for example, we can imagine that the true wave function is a resonance hybrid of functions corresponding to structures such as (*a*), (*b*) and (*c*) below.

---

* Now at T.R.E., Malvern, Worcs. † Now at Mathematical Institute, Oxford.

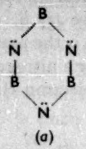

(*a*)

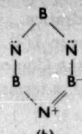

(*b*)

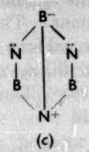

(*c*)

The stability of borazole may be attributed to the possibility of such resonance. Presumably the same situation will occur in boron nitride. If so, we may describe the bonding as due to a combination of (i) localized σ-bonds joining adjacent BN atoms and (ii) π-orbitals which, in molecular-orbital language, would cover the whole set of boron and nitrogen atoms. Just as with graphite in I, there would be a σ-band and a π-band. Arguments similar to those used before show that the distinction between σ and π is somewhat blurred; and also, that the main characteristics of the band structure can be obtained by considering a single layer plane, since the effect of including adjacent planes will be to widen out each separate energy level into a thin band. This widening, just as in I, will exert only a small influence on the shape of the complete band.

§3. THE π-BAND SYSTEM

Let us begin by considering the π-electron bands, and fix our attention on one plane. The unit cell is identical with that in I, fig. 1, except that the (jk) atoms may be taken to be all boron, and the $[jk]$ atoms all nitrogen, as in fig. 2 of the present paper. It will be convenient again to consider an array of $\overline{U}\,\overline{V}$ cells, containing $2\overline{U}\,\overline{V}$ π-electrons, just as in I, fig. 3. Later we shall let both $\overline{U}$ and $\overline{V}$ tend to infinity.

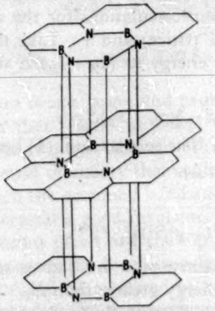

Fig. 1. The BN lattice.

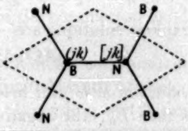

Fig. 2. Nomenclature of atoms in the unit cell of a layer plane.

Our analysis closely resembles that in I. Thus we form auxiliary functions Φ_{mn} and Ψ_{mn} exactly as in I(1), except that Φ_{mn} contains only orbitals of boron atoms and Ψ_{mn} contains only orbitals of nitrogen atoms. The Bloch orbitals $(\Upsilon)_{mn}$ can be written, entirely as I (2), in the form

$$(\Upsilon)_{mn} = N_{mn}^{-1}\{\Psi_{mn} + c_{mn}\Phi_{mn}\}. \qquad \ldots\ldots(1)$$

The coefficients c_{mn} and the energy E_{mn} of this orbital must be found from the secular equations. These are quadratics. They involve (i) β, which is the resonance integral for a B–N bond, as in I (3), (ii) S which is the overlap integral, as in I (4), and (iii) α_N, α_B which are the Coulomb terms for a nitrogen and boron atom respectively. These are defined in terms of the one-electron Hamiltonian H by the relations

$$\alpha_N = \int \psi_{jk}^* H \psi_{jk}\, d\tau, \qquad \alpha_B = \int \phi_{jk}^* H \phi_{jk}\, d\tau. \qquad \ldots\ldots(2)$$

We neglect all overlap integrals and resonance integrals except between nearest neighbours.

The secular equation whose roots are the two values of E_{mn} is easily written down. It is

$$\begin{vmatrix} \alpha_B - E & (\beta - ES)\{1 + \exp(2\pi i m/\bar{U}) + \exp(2\pi i n/\bar{V})\} \\ (\beta - ES)\{1 + \exp(-2\pi i m/\bar{U}) + \exp(-2\pi i n/\bar{V})\} & \alpha_N - E \end{vmatrix} = 0. \qquad \ldots\ldots(3)$$

When expanded, this may be written in the form

$$(\alpha_B - E)(\alpha_N - E) - g^2(\beta - ES)^2 = 0, \qquad \ldots\ldots(4)$$

where g is the same function as in I (7) and is given by

$$[g(m,n)]^2 = 3 + 2\cos\frac{2\pi m}{\bar{U}} + 2\cos\frac{2\pi n}{\bar{V}} + 2\cos 2\pi\left(\frac{m}{\bar{U}} - \frac{n}{\bar{V}}\right). \qquad \ldots\ldots(5)$$

g^2 ranges continuously from 0 up to 9.

It is interesting that eqn. (4) is identical with the equations obtained by Roothaan and Mulliken (1948) in their equivalent calculations for the molecule borazole, provided that g^2 is given the values 1 (twice) and 4. Like them, we shall find it convenient to change the origin for energy to $(\alpha_N + \alpha_B)/2$, which we call E_0. Let us put

$$E - E_0 = Z, \qquad \tfrac{1}{2}(\alpha_B - \alpha_N) = \delta, \qquad \beta - \tfrac{1}{2}(\alpha_N + \alpha_B)S = \gamma. \qquad \ldots\ldots(6)$$

These equations are the generalizations of I (5). The secular eqn. (4) becomes

$$Z^2 - \delta^2 - g^2(\gamma - SZ)^2 = 0 \qquad \ldots\ldots(7)$$

and the explicit solutions are

$$Z = (1 - g^2S^2)^{-1}\{-g^2\gamma S \pm \gamma[g^2 + (1 - g^2S^2)\delta^2/\gamma^2]^{1/2}\}. \qquad \ldots\ldots(8)$$

For any values of $m/\bar{U}$ and $n/\bar{V}$ (i.e. of g^2) the positive sign in (8) gives an energy value less than E_0; the negative sign gives an energy greater than E_0. We may call these $Z_+(g)$ and $Z_-(g)$. As g^2 increases from 0 up to 9, Z_+ decreases from $-\delta$ to some other definite negative value, and Z_- increases from $+\delta$ to some other definite positive value. In saying this we have implicitly assumed that δ is positive. This follows from the fact that nitrogen is more electronegative than boron, so that, as Roothaan and Mulliken (1948) have shown, $\alpha_N < \alpha_C < \alpha_B < 0$.

The argument above shows that the complete π-electron band is divided into two sub-bands, separated by an energy gap of magnitude 2δ. Now there are just sufficient π-electrons completely to fill the lower sub-band. Boron nitride would therefore be an insulator. If we put $\delta = 0$ in (8), we recover the energy distribution found for graphite in I, where the two sub-bands just move to touch each other. The separation of the two sub-bands depends only on the existence of a non-vanishing δ. It would not be affected (except to a very minor extent) either by including second-nearest neighbour interactions, or more than one layer plane, or the distribution due to the σ-bonds.

We have tried to estimate suitable numerical values in order to draw the $N(E)$ curve, as in I. The important parameters are the overlap integral S, the electronegativity difference term δ and the 'reduced' resonance integral γ. The value of S is easily calculated (cf. I) if we accept the usual Slater atomic wave functions. We find that $S = 0{\cdot}22$. This is very much the same as its value $0{\cdot}25$ in graphite. For δ and γ the most sensible procedure is to adopt the values which Roothaan and Mulliken (1948) have found most suitable in their discussion of the energy and spectrum of borazole. This would make $\delta = 2{\cdot}3$ ev, and $\gamma = -2{\cdot}3$ ev also. A possible alternative set of values suggested by Roothaan and Mulliken is $\delta = 2{\cdot}7$ ev and $\gamma = -1{\cdot}8$ ev. The resulting difference in the $N(E)$ curves is not large, and probably lies within the reliability of the method itself. For that reason we select the first set of values. Then the energy gap between the two sub-bands is $4{\cdot}6$ ev. This would be expected to represent the lowest amount of energy that could be absorbed electronically. A gap as large as this between the occupied band and the beginning of the conduction band would make the crystal a good insulator.

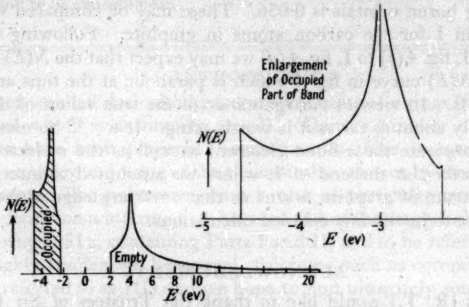

Fig. 3. Graph of $N(E)$ for a single layer, overlap integrals included.

For reasons given in I the top of the conduction band is most unlikely to be adequately predicted by this analysis. But the calculated width of the occupied sub-band would be expected to be more reliable. According to (8) this width is $2{\cdot}4$ ev, which we may compare with the value of about 5 ev predicted similarly for graphite.

The detailed shape of the $N(E)$ curve is easily found by combining (8) with the shape already calculated for graphite in I. This is because the expression $g(m, n)$ is the same both in (8) and in I, figs. 4 (*a*) and 4 (*b*), and in each case the variables are distributed uniformly in the range $-\frac{1}{2}$ to $+\frac{1}{2}$. Thus the distribution function for Z is simply $1/Z'(g)$ times the distribution function for g. Now this distribution function is, apart from a scale factor β, precisely the quantity

.A
5
2

which is plotted in I, fig. 4 (*a*). But dZ/dg is easily obtained from (8), or (7), and by this means the $N(E)$ curve in fig. 3 is drawn. The two regions, which we have previously called Z_+ and Z_-, give rise to the two sub-bands shown. Normally only the Z_+ band is occupied, and this band is full. The infinity present in the graphite case still persists, and is removed in a perfectly analogous way by taking into account other neighbours in all directions.

It is quite straightforward to include the parallel layer-planes in this analysis. The overlap integral between corresponding nitrogen orbitals on adjacent planes, calculated according to the prescription in I, is 0·011, and that between corresponding boron orbitals is 0·056. These may be compared with the value 0·034 found in I for the carbon atoms in graphite. Following the argument that led from I, fig. 4 (*b*) to I, fig. 4 (*d*) we may expect that the $N(E)$ curve in fig. 3 becomes the $N(E)$ curve in fig. 4 which is parabolic at the tops and bottoms of both sub-bands. In view of our ignorance of the true values of the parameters this is probably about as far as it is worth going. It would be more satisfying if we could incorporate the σ-bond electrons as well as the π-electrons. But the situation described at the end of I, where we attempted to interpret the x-ray emission spectrum of graphite, warns us that our knowledge of these σ-bonds is still inadequate to justify any detailed calculations.

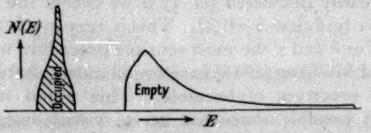

Fig. 4. Graph of $N(E)$ for three-dimensional crystal, overlap integrals included.

ACKNOWLEDGMENTS

One of us (R. T.) would like to thank the Trustees of Sir James Caird's Travelling Scholarships Trust for a grant which made this work possible. We also wish to acknowledge the provision of a calculating machine by the British Iron and Steel Research Association.

REFERENCES

Bauer, S. H., 1938, *J. Amer. Chem. Soc.*, **60**, 524.
Coulson, C. A., and Taylor, R., 1952, *Proc. Phys. Soc.* A, **65**, 815.
Hassel, O., 1926, *Norsk. Geol. Tidskr.*, **9**, 266.
Pease, R. S., 1950, *Nature, Lond.*, **165**, 722.
Roothaan, C. C. J., and Mulliken, R. S., 1948, *J. Chem. Phys.*, **16**, 118.

The Diamagnetic Anisotropy of Large Aromatic Systems
IV: The Polyacenes

By R. McWEENY
Department of Physical Chemistry and Coke Research, University of Durham,
King's College, Newcastle-upon-Tyne

MS. received 10*th April* 1952

ABSTRACT. The π-electron diamagnetic susceptibilities of polyacenes of up to ten rings are calculated by a method introduced in an earlier paper: the method, which involves only a single numerical integration, is simplified. An alternative method of calculation, which has certain attractions and is widely applicable, is sketched in an Appendix.

The relationship between the diamagnetic anisotropy and the number of rings in the molecule is found to be almost linear.

§ 1. INTRODUCTION

In this paper we shall deal with hydrocarbon chains of n rings (fig. 1), a typical member of which is anthracene ($n=3$). Quite a number of molecules of this series have been prepared; consequently there is every prospect of assessing the accuracy and value of the theoretical treatment by direct comparison with experiment. The polyacene chain is also of particular interest since the degree of condensation is intermediate between that of the singly linked polyphenyl chain (McWeeny 1951 a, containing Parts I and II, and to be referred to as I, II) and of the highly condensed, hexagonal structures such as coronene (McWeeny 1951 b, to be referred to as III) and we hope to find ultimately some relationship between degree of condensation and magnetic anisotropy.

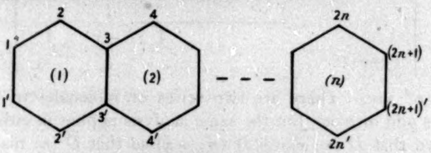

Fig. 1. Polyacene of n rings.

The method of calculation employed is essentially that of previous papers, involving expansion of the field-dependent secular determinant and a subsequent numerical integration (III), but a quite distinct approach (using second-order perturbation theory) exists and is briefly sketched in an Appendix. The second approach is immediately applicable to any molecule whose zero-field energy levels and wave functions are already known and does not involve expansion of the secular determinant; but in the present paper, where a whole series of related molecules is considered, the expansion may easily be systematized, using recurrence relations, and the second method loses its particular attractions.

§ 2. EXPANSION OF THE SECULAR DETERMINANT

Using the numbering shown in fig. 1 and taking the centre of symmetry of the molecule as the origin of the magnetic vector potential it is possible to factorize the $2(2n+1)$th degree secular equation by choosing as basis functions the sets

$$p_r=\phi_r+\phi_{(2n+2-r)'}, \qquad q_r=\phi_r-\phi_{(2n+2-r)'}$$

for these functions span subspaces providing different representations of the symmetry group of the system, C_2.

Thus, using the notation of II, with $x=(E-\alpha)/\beta$ and $k=\exp(2\pi i\alpha HS/12)$, S being the area of one benzene ring, we find the secular determinant of the n-ring molecule

$$\Delta(n)=D^+(n)\,D^-(n), \qquad \ldots\ldots(1)$$

where, for example,

$$D^\pm(4)=\begin{vmatrix} -x & k^5 & & & & & & & \pm k^{*8} \\ k^{*5} & -x & k^* & & & & & & \\ & k & -x & k^3 & & & \pm k^{*4} & & \\ & & k^{*3} & -x & k & & & & \\ & & & k^* & \pm 1-x & k & & & \\ & & & & k^* & -x & k^3 & & \\ & & \pm k^4 & & & k^{*3} & -x & k^* & \\ & & & & & & k & -x & k^5 \\ \pm k^8 & & & & & & & k^{*5} & -x \end{vmatrix} \qquad \ldots\ldots(2)$$

By suitable multiplications of rows and columns the k-factors may be removed from all elements except those lying on the 'second diagonal'; in what follows we shall assume D is in this form. With this reduction it is possible to write

$$D^\pm(n+2)=\begin{vmatrix} -x & 1 & & & \pm z^{n+2} \\ 1 & -x & 1 & & \\ & 1 & \boxed{D^\pm(n)} & & \\ & & & 1 & \\ & & 1 & -x & 1 \\ \pm z^{*n+2} & & & 1 & -x \end{vmatrix} \qquad \ldots\ldots(3)$$

where $z=k^{*6}=e^{i\theta}$ say. There are two series of molecules to be considered according as n is odd or even, but the same analysis applies in either case. It is also easily shown that $D^-(n;\,x)=-D^+(n;\,-x)$ so that $D^-(n)$ may be obtained from $D^+(n)$ simply by reversing the sign of every even power of x: we need now only consider $D^+(n)$ and the superscript + or − may be omitted.

Let $D_0(n)$ be the determinant remaining when z^n and z^{*n} are struck out from $D(n)$ and define also the following minors:

$D_1(n)$—by striking out from $D(n)$ the first row and the last column,
$D_2(n)$—by striking out from $D(n)$ the last row and the first column,
$D_3(n)$—by striking out from $D(n)$ the first row and the first column,
$D_4(n)$—by striking out from $D(n)$ the last row and the last column,
$D_5(n)$—by striking out from $D(n)$ the first and last rows and the first and last columns.

From the symmetry of the array it follows that

$$D_2(n)^* = D_1(n) = D'(n), \quad \text{say,}$$

and

$$D_3(n) = D_4(n) = {}^{\backprime}D(n), \quad \text{say,} \quad (= {}^{\backprime}D_0(n)).$$

With this notation and with $D_5(n) = D''(n)$, $(= D_0''(n))$ it is possible to expand $D(n)$ in the form

$$D(n) = D_0(n) + z^n D_0'(n) + z^{*n} D_0'(n)^* - D_0''(n). \qquad \ldots\ldots(4)$$

In order to construct a series of D's by recursion it is necessary to express each of the terms with suffix 0 as a combination of corresponding quantities associated with the preceding member of the series: the following relationships, derived by simple expansions, serve this purpose.

$$\left.\begin{aligned} D_0'(n+2) &= D_0'(n) - z^{*n} D_0''(n), \\ D_0''(n+2) &= x^2 D(n) + 2x\,{}^{\backprime}D_0(n) + D_0''(n), \\ {}^{\backprime}D_0(n+2) &= -xD_0''(n+2) + xD(n) + {}^{\backprime}D_0(n), \\ D_0(n+2) &= x^2 D_0''(n+2) - (2x^2-1)D(n) - 2x\,{}^{\backprime}D_0(n). \end{aligned}\right\} \qquad \ldots\ldots\ldots(5)$$

Thus, from $D_0'(n)$, $D_0''(n)$, ${}^{\backprime}D_0(n)$, $D_0(n)$, we may construct $D_0'(n+2) \ldots\ldots D_0(n+2)$, using (4) to get $D(n)$ and $D(n+2)$. The 'starting values' are, for the even ring molecules,

$$D_0'(0) = 1, \quad D_0''(0) = 0, \quad {}^{\backprime}D_0(0) = 1, \quad D_0(0) = (1-x) \qquad \ldots\ldots(6)$$

(being fixed by convention so that $D(2)$ is given correctly) and, for the odd ring molecules,

$$D_0'(1) = 1, \quad D_0''(1) = -x, \quad {}^{\backprime}D_0(1) = (x^2-1), \quad D_0(1) = -x(x^2-2). \qquad \ldots\ldots(7)$$

It is possible to make quite rapid progress by this method: thus five recursions would yield $D(11)$, the expansion of a determinant of 23 rows and columns.

§ 3. EXPRESSION FOR THE SUSCEPTIBILITY

In (III, § 3) it is shown that the π-electron susceptibility may be determined from $\Delta(x)$ by a numerical integration (III, (10)). Whilst this method is applicable generally, it would be extremely cumbersome in the present case owing to the form of the integrand (the various polynomials involved reach the forty-second degree if completely expanded, and expansion would be desirable since various derivatives occur). The integration may, however, be thrown into more elegant form and the subsequent numerical treatment greatly simplified.

Suppose the polynomial $\Delta(n;\, x) = f(x)$, say, is written

$$f(x) = f_0(x) + \theta^2 g(x). \qquad \ldots\ldots(8)$$

When Δ refers to the *whole* molecule (or represents a factor whose roots include all members of any initially degenerate set of levels) this form is quite general since no terms in θ can occur: this follows easily from I, Appendix I†.

Also ,for alternant hydrocarbons of the type we consider, Δ is an even function of x (Coulson and Rushbrooke 1940). Starting from the result (III, (7)) for the sum of the positive roots of $f(x)$,

$$\Sigma x = -\frac{1}{2\pi}\int_{-\infty}^{+\infty} \left\{\frac{iyf'(iy)}{f(iy)} - n\right\} dy, \qquad \ldots\ldots(9)$$

---

† In this connection an error in the published equations for coronene (III) should be noted: the equation labelled Γ_4 should differ from Γ_3 only in the sign of the θ term and similarly with Γ_6 and Γ_5.

we put, f being an even function, $f(iy) = F(y)$ (a *real* function of y) and have $iyf'(iy) = yF'(y)$. In anticipation of subsequent manipulations of the integrand we then write (9), more cautiously, as

$$\Sigma x = -\frac{1}{\pi}\lim_{R\to\infty}\int_0^R \left\{\frac{yF'(y)}{F(y)} - n\right\} dy. \qquad \ldots\ldots(10)$$

Integrating by parts

$$\Sigma x = -\frac{1}{\pi}\lim_{R\to\infty}\left\{|y \log F(y)|_0^R - \int_0^R \log F(y)\, dy - nR\right\}, \qquad \ldots\ldots(11)$$

and with $F(y) = F_0(y) + \theta^2 G(y)$, $\theta^2 G(y)$ being always very much less than $F_0(y)$, we find, on expanding the logarithms and carrying out the limiting process,

$$\Sigma x = \Sigma x_0 + \left(\frac{1}{\pi}\int_0^\infty \frac{G(y)}{F_0(y)}\, dy\right)\theta^2, \qquad \ldots\ldots(12)$$

Σx_0 denoting the sum of the roots in the limit $\theta \to 0$.

Thus, in appropriate units, the π-electron susceptibility, and hence the diamagnetic anisotropy $\Delta\chi$, is given by

$$\Delta\chi = \frac{1}{\pi}\int_0^\infty \frac{G(y)}{F_0(y)}\, dy. \qquad \ldots\ldots(13)$$

Since no derivatives occur in the integrand, there is no need to expand completely the polynomials $G(y)$ and $F_0(y)$: in the present application, for example, these quantities are conveniently expressed in terms of polynomials of lower degree.

The Effect of Overlap

The inclusion of non-orthogonality of amount δ between adjacent atomic orbitals leads only to slight modifications of (13). Starting from (III, (7)) it is a simple matter to show that

$$\Delta\chi = (\Delta\chi)_{\delta=0} - \frac{3\delta^2}{\pi}\int_0^\infty \frac{1+\frac{1}{3}\delta^2 y^2}{(1+\delta^2 y^2)^2}\,\frac{y^2 G(y)}{F_0(y)}\, dy. \qquad \ldots\ldots(14)$$

Here $(\Delta\chi)_{\delta=0}$ is a purely formal quantity since when overlap is included a change is implied in the empirical parameter β which determines the units of $\Delta\chi$: the terms in δ^2 are therefore not to be regarded as *corrections* to $(\Delta\chi)_{\delta=0}$. Nevertheless, the form of $G(y)/F_0(y)$ (fig. 2) allows us to conclude that the term involving the overlap directly makes only a small* contribution to $\Delta\chi$ and will, therefore, have little effect on *comparisons* of $\Delta\chi$ between two molecules: in fact, in all the cases considered the second term in (14) never exceeded 5% of the first.

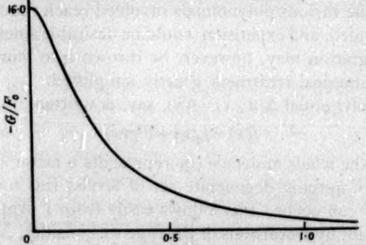

Fig. 2. G/F_0 for $n=6$.

---

* With the overlap usually assumed, $\delta^2 = 0{\cdot}0625$.

§4. RESULTS

The numerical integrations involved in (13) and (14) are easily performed using simple integration rules, the form of the $G(y)/F_0(y)$ curve being particularly satisfactory for this purpose (cf. III, where the integrand exhibits a sharp peak in the middle of the range).

It is interesting to note that the method of calculation commonly employed in previous papers (London 1937), where modifications of the *individual* energy levels are separately considered, becomes impracticable when the degree of the polynomial $\Delta(x)$ becomes sufficiently high, as in the present case: the quantities determining the perturbations of a level (e.g. $\Delta'(x)$) then occur as the differences of very large and nearly equal terms, with the result that seven- or eight-figure accuracy of the unperturbed roots may give only two-figure accuracy in $\Delta\chi$. This difficulty never arises in the contour integral method and, in addition to the fact that no zero-field energy levels need be calculated, the accuracy of the final result is limited only by that of the numerical integration; for practical purposes only three or four figures need be carried.

n	1	2	3	4	5	6	8	10
$\Delta\chi$ (without overlap)	1·0	2·19	3·45	4·75	6·06	7·39	10·07	12·81
$\Delta\chi$ (with $\delta=0{\cdot}25$)	1·0	2·22	3·53	4·88	6·26	7·64	10·46	13·33

Our calculations are summarized in the table where $\Delta\chi$ is given for a number of molecules (with and without overlap). No discussion will be attempted at this point, for it is more illuminating to make a wider survey of the results obtained in these papers and elsewhere (e.g. Berthier *et al.* 1951, 1952); this will appear in a short concluding paper.

It is worth noting here, however, that $\Delta\chi$ is an almost linear function of n, the linearity improving as n increases. Over a limited range the curve may be accurately fitted by $\Delta\chi = a + bn + cn^2$: the coefficient c, which measures the departure from linearity, then falls from 0·04 in the range $1 < n < 4$ to 0·007 in the range $4 < n < 10$. With overlap $\delta = 0{\cdot}25$, the data in the table may be fitted to within less than 1% by the formula

$$\Delta\chi = -0{\cdot}47 + 1{\cdot}31n + 0{\cdot}007n^2 \qquad (n \geqslant 4).$$

APPENDIX

A Perturbation Method

The π-electron energy levels and wave functions in the absence of a magnetic field are known for a great many molecules: in some instances they may be very easily obtained using symmetries which are destroyed by the field. The molecules considered in this paper come within this latter category and it seems worth while, in view of other possible applications, to outline a perturbation treatment based upon a knowledge of the zero-field solutions. It also seems worth while recording the complete solutions (eigenvalues and eigenvectors) for the general polyacene, on crude molecular orbital theory. In the absence of the field the secular determinant of an n-ring polyacene is conveniently factorized using a plane of symmetry and, choosing basis functions

$$u_r = \phi_r + \phi_{r'}, \qquad v_r = \phi_r - \phi_{r'},$$

Coulson (1948) has shown how the factors may be evaluated: but in our case the eigenvectors, $U_k=\Sigma_r u_r a_{rk}$, $V_k=\Sigma_r v_r b_{rk}$ are required and it is more profitable to examine the difference equations for the coefficients a_{rk}, b_{rk}. By suitable manipulations the equations may be thrown into a form satisfied by

$$\left.\begin{aligned} a_{rk} &= \sin\frac{rk\pi}{2(n+1)}\bigg/ x_k^{1/2} \qquad (r \text{ even}), \\ &= \sin\frac{rk\pi}{2(n+1)}\bigg/ (x_k-1)^{1/2} \qquad (r \text{ odd}), \end{aligned}\right\} \quad \ldots\ldots(15)$$

where x_k is a root of $x_k(x_k-1)=4\cos^2 k\pi/2(n+1)$, with rather similar solutions b_{rk}. These equations give $2n$ U's and $2n$ V's, two more solutions resulting from the special cases $k=n+1$ and completing the full set of $2(2n+1)$.

Now the field-dependent determinant factorizes only when we choose the basis functions p_r, q_r (see § 2). If $\mathbf{H}$ is the matrix of the array remaining when the x's are struck out of D^+ (and similarly with D^-) then $D^+=0$ expresses the compatibility of the equations, in matrix form, $\mathbf{HC}=x\mathbf{C}$ and a perturbation treatment must be based on a knowledge of the solutions of $\mathbf{H}_0\mathbf{C}=x\mathbf{C}$, $\mathbf{H}_0$ being the form taken by $\mathbf{H}$ when $\theta\to 0$. It is, therefore, necessary to express the zero-field eigenvectors (15) as combinations of the new basis functions p_r, q_r: it is easily seen that this in fact involves only a re-classification of the eigenvectors U_k, V_k (i.e. the number sets a_{rk}, b_{rk}) as P's or Q's.

Arranging the zero-field eigenvectors into square matrices

$$\mathbf{P}=\left[\begin{array}{c|c|c} P_1 & P_2 & \ldots \end{array}\right] \qquad \mathbf{Q}=\left[\begin{array}{c|c|c} Q_1 & Q_2 & \ldots \end{array}\right]$$

and writing $\mathbf{H}=\mathbf{H}_0+i\theta\mathbf{H}'+\theta^2\mathbf{H}''$ (expanding the complex exponentials) the perturbation of the rth energy level x_r may be written, to the second order in θ,

$$\Delta x_r=\theta^2\mathscr{H}_{rr}''+\theta^2\sum_s{}'\frac{(\mathscr{H}_{rs}')^2}{x_r-x_s},$$

where $\mathfrak{H}'=\mathbf{P}^\dagger\mathbf{H}'\mathbf{P}$, $\mathfrak{H}''=\mathbf{P}^\dagger\mathbf{H}''\mathbf{P}$, and $\mathbf{P}^\dagger$ is, in this case, simply the transpose of $\mathbf{P}$.

In the present case the matrix elements are easily written down:

$$\mathscr{H}_{rs}'=\pm 2[nP_{1r}P_{1s}+(n-2)P_{3r}P_{3s}+\ \ldots\ +P_{(n-1)r}P_{(n-1)s}]$$

(the upper or lower sign being taken according as (r odd, s even) or (r even, s odd), $\mathscr{H}_{rs}'$ vanishing otherwise)

$$\mathscr{H}_{rr}''=\pm[n^2P_{1r}^2+(n-2)^2P_{3r}^2+\ \ldots\ +P_{(n-1)r}^2]$$

(according as r is even or odd). It should be noted that the number of terms in these expressions is quite small (e.g. five terms for the 42-atom molecule) so that the computation is not unduly cumbersome; this result appears to be fairly generally true, i.e. by manipulation of the original determinant the number of complex elements may always be enormously reduced, only a few elements then remaining in $\mathbf{H}'$ and $\mathbf{H}''$ and the calculation being kept within manageable dimensions.

The perturbation of a root of $D^-=0$ is calculated in exactly the same way, with a sign reversal in $\mathbf{H}'$ and $\mathbf{H}''$ and the substitution of $\mathbf{Q}$ for $\mathbf{P}$: actually no new matrix elements need be calculated, the resultant matrices being identical with those already computed (except for a reversal of order of the rows and columns).

Finally, in the same units as in § 3, $\Delta\chi = \Sigma_r \Delta\chi_r$ where the summation extends over all the (doubly) occupied energy levels and

$$\Delta\chi_r = \mathscr{H}_{rr}'' + \sum_s{}' \frac{(\mathscr{H}_{rs}')^2}{x_r - x_s}.$$

REFERENCES

Berthier, C., Mayot, M., Pullman, A., and Pullman, B., 1952, *J. Phys. Radium*, **13**, 15.
Berthier, G., Mayot, M., and Pullman, B., 1951, *J. Phys. Radium*, **12**, 652, 717.
Coulson, C. A., 1948, *Proc. Phys. Soc.*, **60**, 257.
Coulson, C. A., and Rushbrooke, G. S., 1940, *Proc. Camb. Phil. Soc.*, **36**, 193.
London, F., 1937, *J. Phys. Radium*, **8**, 397.
McWeeny, R., 1951 a, *Proc. Phys. Soc.* A, **64**, 261 ; 1951 b, *Ibid.*, 921.

Strong Coupling in Inelastic Collisions of Electrons with Atoms

By H. S. W. MASSEY* and C. B. O. MOHR†

* Department of Physics, University College, London
† Department of Physics, University of Melbourne

MS. received 9*th May* 1952

ABSTRACT. The various approximations which have been used to calculate the probability of excitation of an atom by impact with an electron whose energy is not greatly in excess of the threshold are known to fail under certain conditions. This is especially true in the important cases in which the excitation proceeds mainly through electron exchange. In these cases the exchange coupling is too strong for approximate methods, which assume weak coupling, to be valid. By using a schematic model exact solutions for strong exchange coupling are obtained and compared with the results of different weak coupling approximations. It is found that the Born–Oppenheimer approximation is never reliable at low electron energies but if distortion of the incident and scattered waves by the atomic field is allowed for correctly much better results may be obtained.

§ 1. INTRODUCTION

It was first pointed out by Mott (1932) that the contribution to the cross section for an inelastic collision between two interacting systems which arises from impacts in which their relative angular momentum is $\{l(l+1)\}^{1/2}\hbar$ can never exceed $(2l+1)\lambda^2/4\pi$ where λ is the wavelength of the initial relative motion. This follows from quite general arguments and is the quantum theory version of the obvious classical result that, if the relative angular momentum lies between J and $J+dJ$, the target area is $2\pi J\, dJ/M^2v^2$ where v is the relative velocity and M the reduced mass.

Many applications (see Mott and Massey 1949) of this limit theorem have been made in the interpretation of nuclear collision phenomena in which the interaction is strong and the usual perturbation theory (Born's approximation) breaks down completely. For collisions of electrons with atoms the interaction is weaker and comes into play more gradually and more reliance has been placed on methods such as that of Born in these cases. Recently, however, it has been pointed out by Bates, Fundaminsky, Leech and Massey (1950) that there are many instances in which calculations of cross sections for excitation of atoms by electrons, based on current approximations, have given results in excess of the allowed maximum. In all these cases the large values obtained are associated with the possibility of electron exchange occurring in the collision and arise at electron energies near the threshold for the process. It appears in fact that a calculation, in which the usual approximations are made, is likely to give more than the allowed maximum value for the cross section near the threshold of excitation of one level from another if both belong to the same electron configuration and may do so in other cases in which there is no change of azimuthal quantum number of the atomic electron concerned in the process.

Unfortunately it is just under these conditions that information about excitation cross sections is required for the interpretation of astrophysical and geophysical phenomena. Thus of the examples of failure noted by Bates *et al.* (1950) the excitation of O^{2+}, O^{+} and He (2^1S and 2^3S) are of major importance in the interpretation of nebular spectra while the deactivation of $O(^1S)$ and $O(^1D)$ by electron impact would, if rapid enough, be important in the emission of the air glow and aurora. Another excitation process which is important in this connection is the dissociation of hydrogen by electron impact due to excitation of the $^3\Sigma_u$ and $^3\Sigma_g$ states. This process provides the most effective means of obtaining atomic hydrogen. A knowledge of its probability under different conditions would be very valuable, but here again calculations carried out using the Born–Oppenheimer approximation give results exceeding the possible maximum.

Before proceeding further it is necessary to distinguish between the various approximations which have been used in the calculation of inelastic cross sections for electron–atom collisions. In the Born approximation it is assumed that all matrix elements of the interaction between the electron and atom, whether diagonal or non-diagonal, are small and the possibility of electron exchange is ignored. The cross section is then proportional to the square of the matrix element of the interaction between initial and final states in which the free electron wave functions are plane waves and the overall wave function is simply an unsymmetrical product.

The Born–Oppenheimer approximation includes the possibility of electron exchange but still assumes that all matrix elements are small. The overall wave functions used to calculate the probability amplitude are properly symmetrized combinations of plane waves and atomic wave functions.

As a next step it may be assumed that only the non-diagonal matrix elements are small. The plane waves which represent the initial and final free electron wave functions are then replaced by waves distorted by the mean interaction with the atom in the initial and final states respectively. If exchange effects are ignored in calculating the distortion we shall call the approximation the distorted wave Born (D.W.B.) approximation. This is to be distinguished from the distorted wave Born–Oppenheimer (D.W.B.O.) approximation in which the effect of exchange in producing distortion is allowed for.

Of the cases cited by Bates *et al.* in which the calculations yielded cross sections in excess of the possible maxima, $H_2(^1\Sigma_g^+ \rightarrow {}^3\Sigma_u^+)$, $He(1^1S - 2^3S)$ and $Hg(6^1S \rightarrow 6^3P)$ were calculated using the Born–Oppenheimer and $O(2^3P \rightarrow 2^1D$ and $2^1S)$, $O^+(2^4S \rightarrow 2^2D)$ and $O^{2+}(2^3P \rightarrow 2^1D$ and $2^1S)$ using the D.W.B. approximations. It is natural to enquire whether, in general, there is any advantage gained by using the D.W.B. or the D.W.B.O. method and whether, if the cross section as calculated by either method comes out to be in excess of the maximum, the true cross section is actually close to the maximum. The same question can be put in a slightly different way.

We may measure the strength of the interaction by a parameter A. Both the Born–Oppenheimer and D.W.B.O. approximations will give a cross section Q increasing as A^2 but the constant of proportionality will in general be different with the two methods. Which of these gives the best results for small A?

In any case the true cross section cannot increase indefinitely as A^2. We wish to know how Q varies with A when A is too large for the approximate formula to be valid. If it should turn out that, as A increases, either approximate formula continues to give a fair approximation until it gives $Q=Q_{\max}$ (the allowed maximum) and that for a considerable range of A beyond this the correct Q remains close to $Q_{\max}$, then we have a result of immediate application. In most actual circumstances it is probable that the effective value of A is not an order of magnitude greater than that for which the approximate $Q=Q_{\max}$, i.e. the coupling though not weak is not very strong.

A reasonable indication as to the way these questions may be answered may be obtained by studying a schematic 'model' of the process of excitation involving electron exchange. While the essential features are retained such a model may be set up which involves exactly soluble coupled integro-differential equations. In this paper an account of an investigation on these lines is given and very useful conclusions are arrived at which should make it possible to predict without serious error the cross sections for excitation processes in which electron exchange is of primary importance. It may be said in anticipation that it appears highly probable that the predictions of the D.W.B.O. method are not seriously incorrect if $Q<\frac{1}{2}Q_{\max}$ while if it predicts a value of Q considerably greater than $Q_{\max}$ the true value is close to $Q_{\max}$. On the other hand, if distortion is not allowed for, little use may be made of the results for electron energies near the threshold.

§ 2. THE INTEGRO-DIFFERENTIAL EQUATIONS FOR THE PROBLEM

The problem of the excitation of the 2s level of atomic hydrogen by electrons has recently been considered by Erskine and Massey (1952). They find that, for electron energies near the threshold, the cross section for the excitation is given by

$$Q=4\pi k_1|\beta|^2/k_0^3. \qquad \ldots\ldots(1)$$

k_0 and k_1 are the wave numbers of the initial and final motion of the electron relative to the atom. $|\beta|$ is such that the asymptotic form of the solution f_1 of a certain pair of integro-differential equations is

$$f_1 \sim \beta \exp(ik_1 r). \qquad \ldots\ldots(2)$$

Since the maximum possible value for Q is π/k_0^2 we may call $4\pi k_1|\beta|^2/k_0$ the probability of the particular inelastic collision concerned.

The integro-differential equations expressed in atomic units are of the form

$$\left.\begin{aligned}
&\left[\frac{d^2}{dr^2}-2V_{00}(r)+k_0^2\right]f_0+\int_0^\infty K_{00}(r,r')f_0(r')\,dr' \\
&\qquad\qquad =2V_{01}(r)f_1(r)-\int_0^\infty K_{01}(r,r')f_1(r')\,dr', \\
&\left[\frac{d^2}{dr^2}-2V_{11}(r)+k_1^2\right]f_1+\int_0^\infty K_{11}(r,r')f_1(r')\,dr' \\
&\qquad\qquad =2V_{01}(r)f_0(r)-\int_0^\infty K_{10}(r,r')f_0(r')\,dr',
\end{aligned}\right\} \ldots(3)$$

and the solutions must be proper functions satisfying the asymptotic conditions (2) and

$$f_0 \sim \sin k_0 r + \alpha \exp(ik_0 r). \qquad \ldots\ldots(4)$$

In these equations V_{00} and V_{11} are the direct interactions between the electron and the atom arranged over the initial and final states of the atom, K_{00} and K_{11} are interaction kernels which represent the contribution of electron exchange to the mean interaction in each case, V_{01} is the direct non-diagonal matrix element of the interaction and K_{01}, K_{10} are the corresponding contributions from exchange effects. If V_{01}, K_{01} and K_{10} are zero the probability of the transition vanishes.

If the equations (3) are solved exactly the resulting cross section should be accurate, provided that the wave numbers k_0 and k_1 are sufficiently small for the contribution to the excitation from incident electrons with angular momenta greater than zero to be ignored and provided that the influence of other excited states is also negligible. As far as the first of these is concerned it is quite clear that almost all, if not all, of the violations of the conservation law occur for electron energies near the threshold in which case the main contribution comes from head-on collisions. The second approximation amounts to a neglect of dynamic polarization effects. At the electron energies concerned these are probably not very important though it is difficult to estimate their order of magnitude.

In any case the exact solutions of eqns. (3) will certainly give cross sections which obey the conservation laws. It is only when the equations are solved by approximate methods that violation of these laws can occur. All approximate methods used hitherto proceed by solving eqns. (3) by successive approximation on the assumption that V_{01}, K_{01} and K_{10} are small. The D.W.B.O. method makes no further assumption, but the Born–Oppenheimer approximation assumes that V_{00}, V_{11}, K_{00} and K_{11} are also negligible and the Born approximation neglects K_{10} and K_{01} as well.

It is to be expected that the D.W.B.O. method will give accurate results if V_{01}, K_{01} and K_{10} are indeed small but this is clearly not sufficient to justify the Born–Oppenheimer method. In fact, for excitation of atoms by electrons with energy near the threshold the distortion introduced by V_{00} and V_{11} at least is very marked. The detailed calculations carried out by Erskine and Massey (1952) illustrate this for the excitation of the 2s level of atomic hydrogen.

To examine the usefulness of the various approximations it is very desirable to effect comparison with an exact solution of equations of the form (3). If the functions V_{00}, V_{11}, V_{01}, K_{00}, K_{11}, K_{01} and K_{10} have the actual values appropriate to an atom it is quite clear that it would be a very laborious task to obtain an exact solution. It is therefore necessary to simplify the problem by substituting simplified forms for the various interactions in (3) so that exact solution is possible in analytical terms. We now proceed to discuss the choice of such a schematic model for the equations.

§3. SCHEMATIC MODEL ASSUMED

The effect we are particularly concerned to investigate arises from the exchange terms K_{01}, K_{10}. It is this term rather than the direct non-diagonal matrix element V_{01} which is responsible for the large cross sections given by the Born–Oppenheimer method for electron energies near the threshold. For the 1s–2s excitation of atomic hydrogen

$$K_{01}(r, r') = 4\pi r\psi_0(r)\{k_{01}{}^2 - 2\gamma_0(r, r')\}r'\psi_1(r') = K_{10}(r', r), \qquad \ldots\ldots(5)$$

where ψ_0 and ψ_1 are the respective wave functions for the 1s and 2s levels of hydrogen, $k_{01}{}^2 = k_0{}^2 - \frac{1}{4}$ and $\gamma_0(r, r')$ is such that

$$|\mathbf{r}-\mathbf{r}'|^{-1} = \Sigma\gamma_n(r, r')P_n(\cos\theta). \qquad \ldots\ldots(6)$$

To represent the various features of these kernels we take

$$\left.\begin{aligned} \psi_0(r) &= (4\pi r_0{}^3)^{-1/2}, \ r<r_0; \ \psi_0(r)=0, \ r>r_0, \\ \psi_1(r) &= (4\pi r_1{}^3)^{-1/2}, \ r<r_1; \ \psi_1(r)=0, \ r>r_1. \end{aligned}\right\} \qquad \ldots\ldots(7)$$

We further ignore $k_{01}{}^2$ and multiply the whole by a constant $\frac{1}{2}A$ which is equivalent to replacing the effective interaction $\mathbf{e}^2/|\mathbf{r}-\mathbf{r}'|$ between the two electrons by $A\,\mathbf{e}^2/|\mathbf{r}-\mathbf{r}'|$. A can be taken then as the parameter which measures the strength of the coupling. Apart from A, our assumed kernel includes two other adjustable parameters r_0 and r_1 which measure the spread of the initial and final wave functions.

The direct interaction V_{01} is put equal to zero as the main effect with which we are concerned arises from exchange.

The combined effect of V_{00} and K_{00} in producing distortion of the incident electron wave is represented in the schematic model by a single function $v_0(r)$ which is such that

$$v_0(r) = -C, \quad r<r_0; \qquad v_0(r)=0, \quad r>r_0. \qquad \ldots\ldots(8)$$

A similar function $v_1(r)$ given by

$$v_1(r) = -D, \quad r<r_1; \qquad v_1(r)=0, \quad r>r_1 \qquad \ldots\ldots(9)$$

replaces V_{11} and K_{11}. Over the comparatively narrow range of electron energies concerned the constants C and D may be chosen so that the distortion produced by the potentials v_0 and v_1 approximates quite closely to the actual distortion due to V_{00} and K_{00} and to V_{11} and K_{11} respectively. In any case we are concerned here with obtaining results of general interest and application rather than studying excitation of a particular atom. It is only important that the range covered in the investigation should be that in which particular cases are likely to fall.

The equations which we use as a model representation of (3) are therefore

$$\frac{d^2f_0}{dr^2} + \nu_0{}^2 f_0 = \mathscr{A}^{1/2}\left\{\int_0^r f_1(r')r'\,dr' + r\int_r^{r_1} f_1(r')\,dr'\right\}, \qquad r<r_0, \qquad \ldots\ldots(10\,a)$$

$$\frac{d^2f_0}{dr^2} + k_0{}^2 f_0 = 0, \qquad r>r_0; \qquad \ldots\ldots(10\,b)$$

$$\frac{d^2f_1}{dr^2} + \nu_1{}^2 f_1 = \mathscr{A}^{1/2}\left\{\int_0^r f_0(r')r'\,dr' + r\int_r^{r_0} f_0(r')\,dr'\right\}, \qquad r<r_0, \qquad \ldots\ldots(10\,c)$$

$$= \mathscr{A}^{1/2}\int_0^{r_0} f_0(r')r'\,dr', \qquad r_0<r<r_1, \qquad \ldots\ldots(10\,d)$$

$$\frac{d^2f_1}{dr^2} + k_1{}^2 f_1 = 0, \qquad r>r_1. \qquad \ldots\ldots(10\,e)$$

As ψ_1 refers to the excited state we have taken $r_1 > r_0$. In these equations

$$\nu_0{}^2 = k_0{}^2 + 2C, \quad \nu_1{}^2 = k_1{}^2 + 2D, \quad \mathscr{A}^{1/2} = 3A/(r_0r_1)^{3/2}. \qquad \ldots\ldots(11)$$

Similar equations have been discussed previously by Massey and Mohr (1937) in connection with nuclear collisions. They involve an extension to inelastic collisions of a model used by Morse and Allis (1933) to discuss the importance of exchange effects in elastic scattering of electrons by atoms.

§ 4. SOLUTION OF THE EQUATIONS

For $r_0<r<r_1$ we have

$$f_1=B\sin k_1r+C\cos k_1r+I, \qquad \text{......(12)}$$

$$I=(\mathscr{A}^{1/2}/\nu_1^2)\int_0^{r_0} f_0(r')r'\,dr', \qquad \text{......(13)}$$

and, for $r>r_1$, $f_1=\beta\exp(ik_1r)$. Continuity of f_1 and df_1/dr at $r=r_1$ gives

$$B=i\beta-I\sin k_1r_1, \qquad C=\beta-I\cos k_1r_1, \qquad \text{......(14)}$$

so for $r_0<r<r_1$ $\quad f_1=\beta\exp(ik_1r)+I\{1-\cos k_1(r_1-r)\}. \qquad$ ......(15)

For $r<r_0$ we take

$$f_0=\sum_{s=1}^{4} a_s\sin\chi_s r, \qquad \text{......(16)}$$

$$f_1=\sum_{s=1}^{4} b_s\sin\chi_s r, \qquad \text{......(17)}$$

so that to satisfy (10 *a*)

$$\Sigma a_s(\nu_0^2-\chi_s^2)\sin\chi_s r=\mathscr{A}^{1/2}\left\{-r\Sigma b_s\frac{\cos\chi_s r_0}{\chi_s}+\Sigma b_s\frac{\sin\chi_s r}{\chi_s^2}+rJ\right\}, \qquad \text{......(18)}$$

where

$$\begin{aligned}J&=\int_{r_0}^{r_1}[I\{1-\cos k_1(r_1-r)\}+\beta\exp(ik_1r)]\,dr\\&=I\{r_1-r_0-k_1^{-1}\sin k_1(r_1-r_0)\}-(i\beta/k_1)\{\exp(ik_1r_1)-\exp(ik_1r_0)\} \qquad \text{...(19)}\end{aligned}$$

and, from (13) and (16),

$$I=\mathscr{A}^{1/2}\Sigma a_s\left(\frac{\sin\chi_s r_0}{\chi_s^2}-r_0\frac{\cos\chi_s r_0}{\chi_s}\right). \qquad \text{......(20)}$$

To satisfy (10 *c*)

$$\Sigma b_s(\nu_1^2-\chi_s^2)\sin\chi_s r=\mathscr{A}^{1/2}\left\{-r\Sigma a_s\frac{\cos\chi_s r_0}{\chi_s}+\Sigma a_s\frac{\sin\chi_s r}{\chi_s^2}\right\}. \qquad \text{......(21)}$$

Equating to zero the coefficients of r on the right-hand sides of (18) and of (21),

$$\begin{aligned}\Sigma b_s\frac{\cos\chi_s r_0}{\chi_s}-\mathscr{A}^{1/2}\{r_1-r_0-k_1^{-1}\sin k_1(r_1-r_0)\}\Sigma a_s\left(\frac{\sin\chi_s r_0}{\chi_s^2}-r_0\frac{\cos\chi_s r_0}{\chi_s}\right)\\=-i\beta k_1^{-1}\{\exp(ik_1r_1)-\exp(ik_1r_0)\}. \qquad \text{......(22)}\end{aligned}$$

$$\Sigma a_s\frac{\cos\chi_s r_0}{\chi_s}=0. \qquad \text{......(23)}$$

Once these equations are satisfied the complete equations will also be satisfied if

$$\left.\begin{aligned}a_s(\nu_0^2-\chi_s^2)&=\mathscr{A}^{1/2}b_s/\chi_s^2,\\ b_s(\nu_1^2-\chi_s^2)&=\mathscr{A}^{1/2}a_s/\chi_s^2,\end{aligned}\right\} \qquad \text{......(24)}$$

for $s=1$ to 4. This will be so if the χ_s^2 are the roots of the biquadratic in χ^2,

$$\chi^4(\chi^2-\nu_0^2)(\chi^2-\nu_1^2)=\mathscr{A}. \qquad \text{......(25)}$$

Having determined the χ_s from (25) the ten unknowns a_s, b_s, α and β are obtained from the four equations (24), the two equations (22) and (23) and the four continuity conditions at the boundary $r=r_0$. Since for $r>r_0$, f_0 must have the form (4) these four conditions are

$$\left.\begin{aligned}\Sigma a_s\sin\chi_s r_0&=\sin k_0r_0+\alpha\exp(ik_0r_0),\\ \Sigma a_s\chi_s\cos\chi_s r_0&=k_0\cos k_0r_0+ik_0\alpha\exp(ik_0r_0),\\ \Sigma b_s\sin\chi_s r_0&=\beta\exp(ik_1r_0)+I\{1-\cos k_1(r_1-r_0)\},\\ \Sigma b_s\chi_s\cos\chi_s r_0&=ik_1\beta\exp(ik_1r_0)-k_1I\sin k_1(r_1-r_0).\end{aligned}\right\} \qquad \text{......(26)}$$

Eliminating the b_s by the relations (24) we may obtain β in the form Δ_1/Δ_0 where Δ_1 and Δ_0 are two six-row determinants. For given values of the constants $\mathscr{A}$, k_0, k_1, ν_0, ν_1, r_0 and r_1, the procedure is to solve eqn. (25) numerically to obtain the χ_s and then proceed to the numerical evaluation of Δ_1 and Δ_0.

When $\mathscr{A}$ is small we find for β the D.W.B.O. approximation

$$\beta = \mathscr{A}^{1/2} r_0^3 \frac{KL}{k_1}\left[\frac{1}{2u_0^2}\left\{\frac{\sin(u_0-u_1)}{u_0-u_1}-\frac{\sin(u_0+u_1)}{u_0+u_1}\right\}+\frac{1}{u_0u_1}\left\{\cos u_0\left(\cos u_1-\frac{\sin u_1}{u_1}\right)\right.\right.$$
$$\left.\left.+\left(\frac{\sin u_0}{u_0}-\cos u_0\right)(\cos u_1-\cos v_1)\right\}\right], \quad \ldots\ldots(27)$$

where

$$K=\{\sin^2 u_0+(\nu_0^2/k_0^2)\cos^2 u_0\}^{-1/2}, \quad L=\{\sin^2 v_1+(\nu_1^2/k_1^2)\cos^2 v_1\}^{-1/2}.$$
$$u_0=\nu_0 r_0, \quad u_1=\nu_1 r_0 \quad \text{and} \quad v_1=\nu_1 r_1.$$

The Born–Oppenheimer approximation follows by putting $\nu_0=k_0$, $\nu_1=k_1$ in (27).

§ 5. NUMERICAL RESULTS AND DISCUSSION

Detailed numerical calculations were carried out according to the following scheme. The constants r_0 and r_1 were first chosen to correspond roughly to atomic magnitudes. Two separate cases were investigated. In the first of these, referred to as the 'hydrogen' model, the values chosen were $r_0=1$, $r_1=2$ and in the second, referred to as the 'helium' model, $r_0=0{\cdot}6$, $r_1=2$. Detailed calculation of $|\beta|$ as a function of k_0 was first carried out for the 'distortionless' cases in which C and D in (11) were put equal to zero. In this case the relevant small coupling formula is the Born–Oppenheimer approximation. The calculations were carried out for a number of different values of $\mathscr{A}$ including particularly several values of such magnitude that the small coupling approximation gives results for the inelastic collision probability $4k_1|\beta|^2/k_0$ exceeding unity, the maximum possible value. For each value of $\mathscr{A}$ the maximum value of the inelastic collision probability considered as a function of k_0 was obtained and the curves I*a* of figs. 1 and 2 illustrate the variation of this maximum value with $\mathscr{A}$ for the 'hydrogen' and 'helium' cases respectively. It will be seen that in each case the probability rises to a maximum of nearly unity at a particular value of $\mathscr{A}$ and then falls gradually at greater values. Probabilities calculated by the Born–Oppenheimer approximation are illustrated by the curves I*b* of figs. 1 and 2. They agree quite closely with the exact calculations provided the probability is less than 0·6.

In both figs. 1 and 2 the value of the coupling constant which corresponds roughly to atomic conditions is indicated. This is given by putting $A=2$ in (11) so that, in absolute units, the effective interaction between the incident and atomic electrons has the true value $\mathbf{e}^2/|\mathbf{r}-\mathbf{r}'|$.

The results obtained in the 'distortionless' cases are encouraging in that they suggest that when the weak coupling approximation gives an excessively large result the correct probability is probably fairly close to unity. This satisfactory feature remains when distortion is taken into account, the relevant weak coupling formula being now that given by the D.W.B.O. approximation (27). Detailed calculations were carried out again for a 'hydrogen' and a 'helium' model differing from the 'distortionless' cases in that C and D were no longer put equal to zero. For the 'hydrogen' case C and D were so chosen that $\nu_0^2=k_0^2+2{\cdot}2$, $\nu_1^2=k_1^2+3{\cdot}5$, and for the 'helium' case so that $\nu_0^2=k_0^2+8{\cdot}36$, $\nu_1^2=k_1^2+2{\cdot}75$. These choices were based on the following considerations. The values of ν_0 are such that, for k_0^2 in the neighbourhood of the threshold, the phase shift produced in an incident wave by the potential well assumed agrees approximately with that already calculated for the actual atomic field (Morse and Allis 1933). ν_1 was determined in the same way the phase shifts now referring to waves scattered by the respective atoms in the 2s state. For hydrogen the phase shifts are available from the calculations of Erskine and Massey (1952) but for helium they were estimated specially.

The results of the calculations, in which distortion occurs, are illustrated in figs. 1 and 2. The curves II*a* represent the exact variation of collision probability with the coupling constant $\mathscr{A}$, and the corresponding curves II*b* the values given by the D.W.B.O. approximation (27). It is clear that this approximation is a good one provided the probability is less than 0·5. As the correct probability has a very flat maximum for a coupling constant which is much greater than that which would be expected to arise in actual atomic problems it also follows that when the D.W.B.O. approximation gives a result greater than unity the exact value is between 0·5 and 1·0. Knowledge that the probability in any actual case lies between these limits would be of considerable value in many applications.

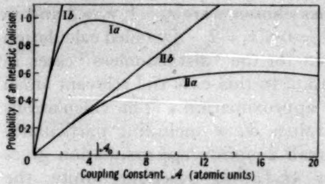

Fig. 1. Probability of an inelastic collision as a function of the coupling constant $\mathscr{A}$ (see (11))—'hydrogen' case (estimated actual value of $\mathscr{A}$ for hydrogen is indicated at $\mathscr{A}_0$).

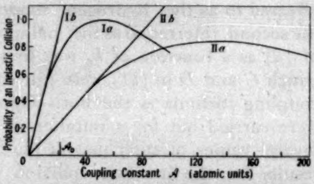

Fig. 2. Probability of an inelastic collision as a function of the coupling constant $\mathscr{A}$ (see (11))—'helium' case (estimated actual value of $\mathscr{A}$ for helium is indicated at $\mathscr{A}_0$).

Curve I*a*. Exact calculation—no distortion present.
I*b*. Born–Oppenheimer approximation.
II*a*. Exact calculation—distortion present.
II*b*. D.W.B.O. approximation.

Comparison of the curves II*a*, II*b* and I*b* shows that the Born–Oppenheimer approximation (curves I*b*) is completely unsatisfactory when distortion typical of actual atomic fields is present. Thus the curves I*b* do not give a good approximation to the actual curves II*a* for any coupling constant. Entirely misleading conclusions would be drawn from them when distortion is present. We can therefore state quite definitely that the Born–Oppenheimer approximation is wholly unreliable if appreciable distortion is present, no matter how small the coupling may be. In the cases considered it gives greater probabilities than the D.W.B.O. method but this is not a general result. Cases were easily found for which the D.W.B.O. method gives greater probabilities but remains more accurate. The following procedure may be recommended for the estimation of the probability of an inelastic collision in which electron exchange predominates: Evaluate the probability using the D.W.B.O. method. If the value obtained is less than 0·5 it is probably fairly reliable. If it gives a probability much greater than 0·5 the true value is likely to be between 0·5 and 1·0. In carrying out this prescription it is important that distortion should be fully allowed for. Thus, referring to the eqns. (3) for the excitation of atomic hydrogen, it is important to include the effect of the exchange interaction kernels K_{00} and K_{11} as well as that of the direct interactions V_{00} and V_{11}.

The way the energy variation of the inelastic cross section varies with the coupling constant $\mathscr{A}$ is also of interest. Figure 3 illustrates results obtained for the 'helium' model. There is very little change of shape until $\mathscr{A}$ exceeds 100 after which the maximum begins to move out to higher energies. This effect occurs for values of $\mathscr{A}$ greater than that for which the maximum probability of an inelastic collision is attained (see curve II*a* of fig. 2). For most atomic problems it is probable that the D.W.B.O. approximation gives a fairly good representation of the actual energy variation of the cross section.

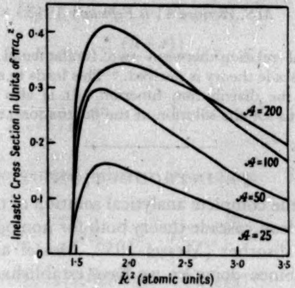

Fig. 3. Variation of the inelastic cross section with electron energy for different values of the coupling constant $\mathscr{A}$—' helium ' case (exact calculation with distortion present).

ACKNOWLEDGMENTS

We are indebted to Mrs. F. Ledsham and Miss Turner for carrying out a large part of the extensive numerical calculations.

REFERENCES

Bates, D. R., Fundaminsky, A., Leech, J. W., and Massey, H. S. W., 1950, *Phil. Trans. Roy. Soc.* A, **243**, 93.

Erskine, G. A., and Massey, H. S. W., 1952, *Proc. Roy. Soc.* A, **212**, 521.

Massey, H. S. W., and Mohr, C. B. O., 1937, *Proc. Roy. Soc.* A, **162**, 529.

Morse, P. M., and Allis, W. P., 1933, *Phys. Rev.*, **44**, 269.

Mott, N. F., 1932, *Proc. Roy. Soc.* A, **133**, 228.

Mott, N. F., and Massey, H. S. W., 1949, *The Theory of Atomic Collisions* (Oxford : Clarendon Press, 2nd edn.) Ch. VIII.

Note on the Fluctuation Problem in Cascade Theory

By H. MESSEL and R. B. POTTS
University of Adelaide, South Australia

MS. received 11*th February* 1952

ABSTRACT. A general relation between two fundamental functions appearing in fluctuation problems in cascade theory is derived. This leads to a direct method of solving for the *n*th moments of the distribution function. It is also shown that the Jánossy *G*-equations are superfluous for the solution of the fluctuation problem.

---

§ 1. INTRODUCTION

We have given the complete analytical solution of the fluctuation problem arising in nucleon cascade theory both for homogeneous nuclear matter and a finite absorber (Messel 1952, Messel and Potts 1952, to be referred to as I, II). Since doing so we have established a number of general relations which greatly simplify the previous work and which at the same time make the so-called Jánossy *G*-equations superfluous for the solution of the fluctuation problem (Jánossy 1950). It will be recalled that Jánossy introduced his *G*-equations in an attempt to solve the fluctuation problem in nucleon and electron–photon cascade theory. These equations, though appearing very simple in form, have proved to be of no value whatever in obtaining the actual distribution functions themselves (I, II). However, until the present, it appeared that differential equations for the *n*th moments of the distribution functions could only be obtained from either Jánossy's *G*-equations or Bhabha's (1950) method of utilizing the energy as a continuously varying parameter. The partial integro-differential equations for the moments so obtained have not been solved directly, though a recurrence solution may be given. On the other hand we have given in I and II the complete solution for the moments, by an indirect method with the Jánossy *G*-equations as the starting point.

It is the purpose of this paper to show that the solutions for the moments may be obtained by an alternative general method, which is straightforward and direct, using a simple relation between two fundamental functions appearing in cascade theory. No use is made of the Jánossy *G*-equations. Though throughout this paper we shall for convenience consider the distribution functions which were given in II, the arguments are of general applicability and may be applied in particular to the fluctuation problem in electron–photon cascade theory.

§ 2. FUNDAMENTAL RELATIONS

As in II we define $H_n(E_0; E_1, \dots, E_n; \theta)\, dE_1 \dots dE_n$ as the differential probability that after depth θ a primary nucleon of energy E_0 has given rise to n nucleons with energies in the ranges $E_j, E_j + dE_j, j = 1, \dots, n$ in any order, and $\phi(E_0; E, N; \theta)$ as the probability of finding N particles with energies greater than E and an arbitrary number of particles with energies less than E at a depth θ. Furthermore $J_n(E_0; E_1, \dots, E_n; \theta)\, dE_1 \dots dE_n$ is defined as the differential probability of finding n particles with energies in the ranges E_j, $E_j + dE_j, j = 1, \dots, n$

at a depth θ and any number of particles with arbitrary energies, due to a primary of energy E_0. The nth factorial moment of the distribution function ϕ is defined as $T_n(E_0;E;\theta)$.

Then by definition

$$\phi(E_0;E,N;\theta)=\sum_{b=0}^{\infty}\frac{1}{N!\,b!}\int_E^{\infty}dE_1\ldots\int_E^{\infty}dE_N\int_0^E dE_{N+1}\ldots\int_0^E dE_{N+b} \times H_{N+b}(E_0;E_1,\ldots,E_{N+b};\theta), \qquad \ldots\ldots(1)$$

$$T_n(E_0;E;\theta)=\sum_{a=0}^{\infty}\frac{(n+a)!}{a!}\,\phi(E_0;E,n+a;\theta), \qquad \ldots\ldots(2)$$

$$J_n(E_0;E_1,\ldots,E_n;\theta)=\sum_{c=0}^{\infty}\frac{1}{c!}\int_0^{\infty}dE_{n+1}\ldots\int_0^{\infty}dE_{n+c}H_{n+c}(E_0;E_1,\ldots,E_{n+c};\theta). \qquad \ldots\ldots(3)$$

We now establish the general relation we require. Substituting (1) and (2) we get

$$T_n(E_0;E;\theta)=\sum_{a=0}^{\infty}\sum_{b=0}^{\infty}\frac{1}{a!\,b!}\int_E^{\infty}dE_1\ldots\int_E^{\infty}dE_{n+a}\int_0^E dE_{n+a+1}\ldots\int_0^E dE_{n+a+b} \times H_{n+a+b}(E_0;E_1,\ldots,E_{n+a+b};\theta). \qquad \ldots\ldots(4)$$

Setting $b=c-a$ (4) becomes

$$\begin{aligned}T_n(E_0;E;\theta)&=\int_E^{\infty}dE_1\ldots\int_E^{\infty}dE_n\sum_{c=0}^{\infty}\frac{1}{c!}\sum_{a=0}^{c}\frac{c!}{a!\,(c-a)!}\\&\quad\times\int_E^{\infty}dE_{n+1}\ldots\int_E^{\infty}dE_{n+a}\int_0^E dE_{n+a+1}\ldots\ldots\int_0^E dE_{n+c}H_{n+c}(E_0;E_1,\ldots E_{n+c};\theta)\\&=\int_E^{\infty}dE_1\ldots\int_E^{\infty}dE_n\sum_{c=0}^{\infty}\frac{1}{c!}\int_0^{\infty}dE_{n+1}\ldots\int_0^{\infty}dE_{n+c}\\&\quad\times H_{n+c}(E_0;E_1,\ldots,E_{n+c};\theta).\end{aligned} \qquad \ldots\ldots(5)$$

Note that eqn. (5) gives a much simpler relation between H and T than (4).

Now using definition (3) we find the rather surprising relation

$$T_n(E_0;E;\theta)=\int_E^{\infty}dE_1\ldots\int_E^{\infty}dE_nJ_n(E_0;E_1,\ldots,E_n;\theta). \qquad \ldots\ldots(6)$$

The same relation holds between the $S^k(\epsilon,x)$ and $C_k(\epsilon_1,\ldots,\epsilon_n;x)$ in I. It should be pointed out that the relation (6) may be readily established from Ramakrishnan's (1950) product density function.

Hence equation (6) gives the nth moment expressed in terms of the distribution function J_n and is obtained from J_n by an elementary integration over the energy variables. Scott (1951) derived a similar relation for the special case of $E=0$ corresponding to the physically unimportant quantity, the nth moment of the distribution function for the total number of particles of all energies.

§ 3. FIRST-COLLISION AND LAST-COLLISION DIFFUSION EQUATIONS

It is well known that by considering just the first collision in a cascade a diffusion equation for the distribution function H may be obtained. This 'first-collision' equation is a non-linear partial integro-differential equation and has not been solved directly. By considering all possible last collisions a further diffusion equation satisfied by H_n is obtained. The 'last-collision' equation is also a partial integro-differential equation but is linear, and we have solved it directly in II.

Just as for the case of the H_n, both a first-collision and a last-collision equation may be derived for the function J_n. The last-collision equation may be solved directly and hence using (6) the general solution for T_n is obtained immediately.

In II the solution for J_n was given as

$$\begin{aligned} J_n(E_0;E_1,\dots,E_n;\theta) &= \frac{E_0^{-n}}{(2\pi i)^{n+1}}\int_{u_1-i\infty}^{u_1+i\infty} ds_1 \dots \int_{u_n-i\infty}^{u_n+i\infty} ds_n \int_{\lambda-i\infty}^{\lambda+i\infty} dp\, e^{p\theta} \\ &\quad \times \left(\frac{E_0}{E_1}\right)^{s_1+1} \dots \left(\frac{E_0}{E_n}\right)^{s_n+1} Y_n(s_1,\dots,s_n;p), \qquad \dots\dots(7) \end{aligned}$$

where Y_n is a known function.

From (6) therefore, it follows that (cf. II, eqn. (36))

$$\begin{aligned} T_n(E_0;E;\theta) &= \frac{1}{(2\pi i)^{n+1}}\int_{u_1-i\infty}^{u_1+i\infty} \frac{ds_1}{s_1} \dots \int_{u_n-i\infty}^{u_n+i\infty} \frac{ds_n}{s_n} \int_{\lambda-i\infty}^{\lambda+i\infty} dp\, e^{p\theta} \\ &\quad \times \left(\frac{E_0}{E}\right)^{s_1+\dots+s_n} Y_n(s_1,\dots,s_n;p). \qquad \dots\dots(8) \end{aligned}$$

It is now apparent that all that was required to solve the fluctuation problem was the solution of the last-collision diffusion equation for H_n and J_n. This method has also been used by us to solve the similar problem in electron–photon cascade theory.

It should be noted that in the above work, no use is made of the Jánossy *G*-equation. Since the only value of these equations originally was in obtaining the differential equation for the *n*th moments, it now appears that there is little reason for their introduction into the theory.

REFERENCES

BHABHA, H. J., 1950, *Proc. Roy. Soc.* A, **202**, 301.
JÁNOSSY, L., 1950, *Proc. Phys. Soc.* A, **63**, 241.
MESSEL, H., 1952, *Proc. Phys. Soc.* A, **65**, 465.
MESSEL, H., and POTTS, R. B., 1952, *Proc. Phys. Soc.* A, **65**, 473.
RAMAKRISHNAN, A., 1950, *Proc. Camb. Phil. Soc.*, **46**, 595.
SCOTT, W. T., 1951, *Phys. Rev.*, **82**, 893.

LETTERS TO THE EDITOR

Diffuse Reflection of Neutrons from a Single Crystal

Diffuse streaks have been found in the Laue diffraction pattern of an iron single crystal placed in a beam of neutrons from the Harwell pile.

The crystal, which had an effective irradiated volume of 0·025 cm^3, was mounted with the $[1\bar{1}0]$ zone axis vertical, and surveys of the background scattering were made at various fixed crystal settings. The intensity near the 110 reflection is illustrated in the figures. Figure 1 shows the counting rates along the equatorial layer line, on both sides of the Laue position, fig. 2 the counting rates on a line at right angles through A. The Laue reflection is seen to be accompanied by substantial wings, which cannot be attributed to instrumental broadening. By subtracting the disordered scattering and the Laue peak, whose outline is known from the later studies, the excess counting rate resolves into the long hump of intensity shown. This is the (110) diffuse streak: it contributes up to 140 counts per minute from vibrational and magnetic inelastic scattering processes.

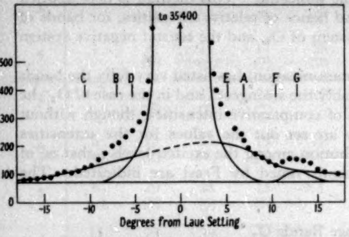

Fig. 1. The equatorial distribution of background intensity around the Laue reflection 110 of iron. Experimental points are indicated by circles. The residual intensity above the level of the disordered scattering is shown resolved into the Laue contour and the associated diffuse streak. The small peak at G is a Laue reflection from a disoriented inclusion in the iron crystal. $\theta_B(110) = 19° 41'$.

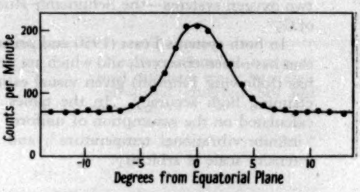

Fig. 2. A transverse survey through A of fig. 1. Taken at $\theta_B\ (110) = 26° 50'$.

As the Bragg angle of (110) is increased from zero, the diffuse streak first appears displaced towards the side of greater scattering angle and, in accordance with theory, gradually passes through the Laue reflection position.

The intensity of the extra scattering is, as with X-rays, a few thousandths that of the elastic reflection. Between 292° K and 585° K it is observed to be closely proportional to temperature, as required by the equations of Weinstock (1944) and Moorhouse (1951).

The wavelength changes which take place on scattering have been detected by absorption measurements at the settings A and B (with $\theta_B(110) = 32° 41'$). It may be deduced from the geometry of scattering theory that neutrons undergoing first-order inelastic scattering associated with a given set of lattice planes gain energy if they are too slow for Bragg reflection, and lose energy if they are too fast. This is strictly true for the vibrational scattering of slower-than-sound neutrons, and true for the predominant type of scattering in other processes. It follows that the equatorial survey of fig. 1 should almost completely separate out the two cases, accelerated neutrons going to the right of the Laue peak and decelerated neutrons to the left. The readings at A and B have verified this theorem.

Weinstock's theory of the vibrational scattering component predicts counting rates at C, D, E and F of about 40, 75, 105 and 55 per minute respectively. The observed streak is slightly more intense, and also of greater transverse breadth, than thus estimated.

The difference corresponds to an inelastic scattering cross section of about ten millibarns. It is of the magnitude required by the theory of magnetic inelastic scattering, as discussed by Halpern and Johnson (1939) and by Moorhouse.

Full details will be published in due course.

Atomic Energy Research Establishment,
Harwell.
19th June 1952.
R. D. Lowde.

Halpern, O., and Johnson, M. H., 1939, *Phys. Rev.*, **55**, 898.
Moorhouse, R. G., 1951, *Proc. Phys. Soc.* A, **64**, 1097.
Weinstock, R., 1944, *Phys. Rev.*, **65**, 1.

Intensities in Band-Systems of O_2 and O_2^+

In a note published recently (Pillow 1951) an improved method was suggested for distorting wave functions for a simple harmonic oscillator in order to give approximations to the vibrational wave functions for a diatomic molecule. This method is here applied to the calculation of transition probabilities, and hence of relative intensities, for bands of two oxygen systems—the Schumann–Runge system of O_2, and the second negative system of O_2^+.

In both systems Feast (1950 and private communication) has listed very fully the bands that have been observed, and which are presumably the strongest; and in the case of O_2^+ he has (following Johnson) given visual estimates of comparative intensities, though without claiming high accuracy. In the tables below are set out the values for the intensities calculated on the assumption of uniform distribution among the excited levels—that is, of 'infinite vibrational temperature', and the bands noted by Feast are indicated. The intensity scale is arbitrary.

Schumann–Runge Bands O_2

Excited State (constants calculated from data of Knauss and Ballard (1935)). *
$\omega_e' = 801{\cdot}7$, $x'\omega_e' = 19{\cdot}27$, $r_e' = 1{\cdot}604 \times 10^{-8}$ cm.

Ground State (constants from Herzberg (1950)).
$\omega_e'' = 1580$, $x''\omega_e'' = 12{\cdot}07$, $r_e'' = 1{\cdot}207 \times 10^{-8}$ cm.

Calculated intensities at $T \to \infty$

v' \ v''	5	6	7	8	9	10	11	12	13	14	15	16
0			0·5	1·2	2·4 F	4·2 F	6·3 F	8·3 F	10·0 F	8·2 F	7·8 F	6·2 F
1		0·7	2·0	4·1 F	6·6 F	9·2 F	7·3 F	7·1 F	3·6	0·9	0·1	1·9
2	0·8	2·2 F	5·0 F	7·4 F	9·2 F	9·1 F	5·5	1·4		1·1	4·0 F	3·0 F
3	1·7 F	4·3 F	7·8 F	9·8 F	9·3 F	5·6	1·3		2·1	3·5	2·4	

F = bands listed by Feast as having been observed.

* The method of distortion requires a potential function of the Morse form, and hence a quadratic expression for the energy levels. In most cases the measured values give such an expression to a very close approximation. For the excited state of the Schumann–Runge system the levels given by Knauss and Ballard need small terms in $v+\frac{1}{2}$ of higher order than the second to represent them exactly, but a quadratic expression has been fitted to these levels by the method of least squares and the errors are quite small.

Second Negative System O_2^+

Excited State (constants from Herzberg (1950)).

$\omega_e'=900$, $x'\omega_e'=13{\cdot}4$, $r_e'=1{\cdot}409\times10^{-8}$ cm.

Ground State (constants from Herzberg (1950)).

$\omega_e''=1876{\cdot}4$, $x''\omega_e''=16{\cdot}53$, $r_e''=1{\cdot}1227\times10^{-8}$ cm.

Calculated intensities at $T\rightarrow\infty$

v' \ v''	0	1	2	3	4	5	6	7	8	9	10	11
0					1	2 (8)	4·5 (7)	6·5 (8)	8 (8)	7·5 (6)	6 (5)	4 (3)
1			0·5	2 (3)	5·5 (5)	9 (6)	10 (7)	9 (8)	5	1·5 (1)		1
2		0·5 (1)	2 (2)	6 (7)	11 (8)	13 (8)	7 (4)	4 (2)		1	3	3
3		2 (1)	6 (2)	11 (8)	15 (7)	12 (6)	4 (a)		2 (a)	4 (a)	2	
4	1	4 (3)	11 (6)	17 (7)	15 (7)	6 (3)						
5	1·5	8 (2)	13 (8)	21 (7)	12	2						
6	3 (a)	13 (2)	23 (6)	19 (4)	6	(4)	5 (5)					
7	6 (a)	20 (3)	28 (6)	15 (1)	3	3 (3)	7 (2)					
8	11 (a)	28 (1)	29 (1)	8	(1)							

Numbers in brackets represent visual estimates made by Feast. (a)=band observed but not estimated.

Imperial College and
Northern Polytechnic,
Holloway, London.
18th July 1952.

M. E. Pillow.

Herzberg, G., 1950, *Molecular Spectra and Molecular Structure. I. Diatomic Molecules* (New York: van Nostrand), 2nd edn.
Feast, M. W., 1950, *Proc. Phys. Soc.* A, **63**, 557.
Knauss, H. P., and Ballard, S. S., 1935, *Phys. Rev.*, **48**, 796.
Pillow, M. E., 1951, *Proc. Phys. Soc.* A, **64**, 772.

Energy per Ion Pair for Argon with Small Admixture of other Gases

Measurements of the value of the average energy *w* required to form one ion pair in a range of gases may be made by observation of the ionization current produced in a gas by the complete absorption of, say, alpha-particles of known energy emitted at a measured rate from a source.

In the course of measurements of this kind on argon, air, N_2, O_2, CH_4 and CO_2 it has been observed that the ionization current in argon may be increased by about 1% (corresponding to a decrease in *w*) by the admixture of 2 to 5% of CO_2 or O_2 (other gases have yet to be tried). Since the value of *w* for O_2 and CO_2 is larger than that for argon (see table), and since the particle energy is completely absorbed in the gas, the effect must be due to a more efficient conversion of the particle energy into ionization, or to a more efficient collection of the current, such as might be caused by an increase in electron mobility offsetting recombination.

The latter hypothesis was rejected by observing that saturation was complete at the working value of the collecting field, and that the ratio $w(\mathrm{A})/w(\mathrm{A}+5\%\mathrm{CO_2})$ was constant at 1·01 over a range of collecting fields, and for alpha-particles from plutonium (thin source), uranium (thick source), and for beta-particles from ^{35}S slowed down by foils to a maximum energy of approximately 40 kev.

It would therefore appear that the contaminant increases the ionization current by the fruitful destruction of excited states, and that these account for about 1% of the energy abstracted from a charged particle in argon.

In the measurements of *w* for A–O_2 mixtures by Haerberli, Huber and Baldinger (1950) there are no experimental points in the effective region, and the effect is not shown. Their values were obtained from ion pulse measurements, and it would be of interest to determine whether the collection time in such apparatus is sufficiently long to allow for a high probability of energy transfer.

The absolute values of *w* obtained for Pu alpha-particles for the gases mentioned above are, to within 1%,

Gas	A	Air	O_2	N_2	CH_4	CO_2	$A+5\%CO_2$
w (ev)	26·3	35·6	32·9	36·4	29·1	34·2	26·1

This note is published by permission of the Director of this Establishment.

Ministry of Supply,
Atomic Energy Research Establishment,
Harwell, Didcot, Berks.
21st July 1952.

J. Sharpe.

Haerberli, W., Huber, P., and Baldinger, E., 1950, *Helv. Phys. Acta*, **23**, 481.

Paramagnetic Resonance in Potassium Chromicyanide

Resolution in the paramagnetic resonance spectra of most compounds is limited by the line width arising from the magnetic interaction of the paramagnetic ion with the nuclear magnetic moments of the neighbouring diamagnetic atoms. In hydrated compounds the protons give rise to a half width at half intensity of about 6 gauss, and using heavy water this can be reduced to 2 gauss (Bleaney, Bowers and Ingram 1951). In a cyanide such as $K_3Cr(CN)_6$, where the neighbouring nuclear magnets are small and further from the paramagnetic ion, the limit should be reduced to less than 1 gauss.

Single crystals were examined of potassium cobalticyanide, which is diamagnetic, containing between 1% and 0·1% of chromicyanide. Since no paramagnetic resonance spectrum could be observed of the undiluted manganicyanide in the temperature region 12°K to 290°K, manganicyanide was later also used as dilutant. In each case the spectrum corresponds to two ions in the unit cell, and can be fitted to the following spin Hamiltonian, with $S=3/2$:

$$\mathscr{H}=g\beta HS+D\{S_z^2-\tfrac{1}{3}S(S+1)\}+E(S_x^2-S_y^2)+ASI.$$

Using cobalticyanide as dilutant, the experimentally determined parameters are $g=1{\cdot}992$, $D=+0{\cdot}083\ \mathrm{cm}^{-1}$, $E=0{\cdot}011\ \mathrm{cm}^{-1}$, and with manganicyanide as dilutant the parameters are $g=1{\cdot}993$, $D=+0{\cdot}054\ \mathrm{cm}^{-1}$, $E=0{\cdot}012\ \mathrm{cm}^{-1}$. The experimental errors are $\pm 0{\cdot}002$ in g and $\pm 0{\cdot}001\ \mathrm{cm}^{-1}$ in D and E. The sign of D was found from the unequal intensities of the $(\tfrac{3}{2}\leftrightarrow\tfrac{1}{2})$ and $(-\tfrac{1}{2}\leftrightarrow -3/2)$ transitions at low temperatures. The minimum line width, observed for the $(\tfrac{1}{2}\leftrightarrow -\tfrac{1}{2})$ transition in a crystal of cobalticyanide containing probably rather less than 0·1% of chromicyanide, was $1{\cdot}0\pm 0{\cdot}3$ gauss.

In the determination of the nuclear spin of ^{53}Cr as 3/2 (Bleaney and Bowers 1951) an alum was used in which the spectrum was not fully resolved. In a cyanide crystal containing chromium enriched in ^{53}Cr a hyperfine structure of four lines of equal intensity (see figure) was clearly resolved at 90°K and 20°K, confirming the value of 3/2 for the nuclear spin. From the separation of these lines $|A|=0{\cdot}00147\pm 0{\cdot}00005\ \mathrm{cm}^{-1}$; A is isotropic.

To obtain an estimate of the nuclear magnetic moment of ^{53}Cr it was assumed previously, on empirical evidence (see Bleaney and Bowers 1951), that the magnetic field acting on the nucleus is the same as for the isoelectronic ion V^{2+}. Comparison of hydrated double sulphates of Cr^{3+} and V^{2+} then gave a value of 0·46 n.m. A second value can be obtained by comparison of the above value of A with that of diluted $K_4V(CN)_6.3H_2O$, for which J. M. Baker (unpublished) finds $|A|=0{\cdot}0056$ cm^{-1}. This gives $\mu=0{\cdot}58$ n.m., and suggests that $0{\cdot}5\pm0{\cdot}1$ n.m. is the probable value.

Single crystals of undiluted potassium chromicyanide gave a single broad isotropic line; the value of g is $1{\cdot}99\pm0{\cdot}01$. The line width was anisotropic, and its variation had roughly the same angular dependence as the separation of the outer two lines found in the diluted chromicyanide. The absence of resolved fine structure, the shape of the line, and the angular variation of the line width suggest that there are considerable exchange interactions between neighbouring ions in the concentrated salt.

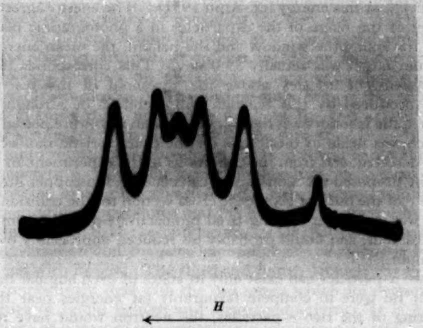

Hyperfine structure of ^{53}Cr in the electronic transition $(\frac{1}{2} \leftrightarrow -\frac{1}{2})$ of diluted potassium chromicyanide. The four lines are clearly resolved; the central line is due to even isotopes with zero nuclear spin. The small line on the right (low field) is due to an organic free radical, used as a field marker.

The author wishes to record his gratitude to Dr. B. Bleaney for generous help and discussion. His thanks are also due to the Director and the Electromagnetic Separator Group of the Atomic Energy Research Establishment, Harwell, who supplied the enhanced ^{53}Cr, and to Dr. P. F. D. Shaw for the preparation of various chemical compounds.

The Clarendon Laboratory,
Oxford.
K. D. Bowers.
14th August 1952.

Bleaney, B., and Bowers, K. D., 1951, *Proc. Phys. Soc.* A, **64**, 1135.
Bleaney, B., Bowers, K. D., and Ingram, D. J. E., 1951, *Proc. Phys. Soc.* A, **64**, 758.

A Search for the Nuclear Reaction ^{4}He$(\alpha, n)^7$Be

According to the atomic masses listed by Li *et al.* (1951), the nuclear reaction ^{4}He$(\alpha, n)^7$Be should be endothermic to the extent of $18{\cdot}98\pm0{\cdot}04$ Mev. This means that, if an α-particle beam is used to bombard a helium target, the threshold energy for the reaction in the laboratory system of coordinates is $38{\cdot}0\pm0{\cdot}1$ Mev. At the end of 1951, using the Birmingham 60-inch cyclotron, we made an effort to detect this reaction at an energy a little above the calculated threshold. This attempt was not successful, and we hope to repeat the experiment with some refinements at a slightly higher cyclotron energy when an opportunity occurs. However, as this may not be for some time, it seems worth while to report now the upper limit which we established for the cross section of the proposed reaction.

The layer of helium comprising the target was compressed to 3 atmospheres and was 9·2 cm thick. The external α-particle beam from the cyclotron was admitted to the target through a half-inch diameter hole covered by a mica window 3 mg/cm^2 thick. A measurement was made of the energy of the α-particle beam, before it entered the target chamber, by absorption in aluminium. This gave 39·9 Mev, with an estimated r.m.s. spread of beam energy (after allowing for straggling in the aluminium) of 0·2 Mev. This estimate of energy is based on the theoretical range–energy relation of Aron *et al.* (1949), which is believed to be accurate to within ½% at this energy (cf. Aron 1951). The energy agreed with an independent measurement of the range of the α-particles in a photographic plate. Owing to the loss of energy in traversing the window and the helium, the mean energy of the α-particle beam in the helium target was actually 39·0 Mev. This corresponds to an energy, in the centre-of-mass system, of 0·5 Mev above the threshold of the reaction $^4\mathrm{He}(\alpha, n)^7\mathrm{Be}$. Beryllium nuclei produced by this reaction will therefore be strongly collimated in the forward direction in the laboratory system. Aluminium foils were placed behind the helium target and a search was made in these foils for the characteristic radioactivity of ^{7}Be. No such activity was detected, and from the conditions of the experiment an upper limit for the cross section of the proposed reaction can be calculated. This upper limit is 7×10^{-28} cm^2, which is about 10^{-3} of the nuclear geometric cross section for the collision of two α-particles. (The upper limit was in part set by long-lived radioactivity produced directly in the foils by α-particle bombardment, and could probably be reduced appreciably by the use of foils of very pure aluminium.)

A system of two α-particles can exist only in states of even angular momentum. If the reaction $^4\mathrm{He}(\alpha, n)^7\mathrm{Be}$ were to compete favourably (at energies near the threshold) with the elastic scattering of the two α-particles, the neutron would have to be emitted with zero angular momentum, and this would require the ground state of ^{7}Be to have even parity. The present result indicates otherwise, and agrees with what one would expect from the nuclear shell model for the ground state of a nucleus of 4 protons and 3 neutrons, namely, odd parity (see for example Klinkenberg 1952).

The reaction $^4\mathrm{He}(\alpha, n)^7\mathrm{Be}$ is the mirror of $^4\mathrm{He}(\alpha, p)^7\mathrm{Li}$. The latter reaction is the inverse of the well-known reaction $^7\mathrm{Li}(p, \alpha)^4\mathrm{He}$, of which the excitation function (Rumbaugh *et al.* 1938*, Heydenberg *et al.* 1948) exhibits a maximum at a proton energy of 3 Mev. From general considerations based on this excitation function it seems possible that the reaction $^4\mathrm{He}(\alpha, n)^7\mathrm{Be}$ should be observable, in a more refined experiment with the present method, at an α-particle bombarding energy of about 41 Mev.

We should like to thank Professor W. E. Burcham and Professor R. E. Peierls for their interest in this work.

Physics Department,
University of Birmingham.
14th August 1952.

D. Walker.
W. T. Link.
W. I. B. Smith.

Aron, W. A., 1951, Dissertation (UCRL–1325), University of California, Berkeley.
Aron, W. A., Hoffman, B. G., and Williams, F. C., 1949, *Range–Energy Curves*, AECU–663, 2nd Revision, Radiation Laboratory, University of California.
Heydenberg, N. P., Hudson, C. M., Inglis, D. R., and Whitehead, W. D., 1948, *Phys. Rev.*, **74,** 407.
Klinkenberg, P. F. A., 1952, *Rev. Mod. Phys.*, **24,** 63.
Li, C. W., Whaling, W., Fowler, W. A., and Lauritsen, C. C., 1951, *Phys. Rev.*, **83,** 512.
Rumbaugh, L. H., Roberts, R. B., and Hafstad, L. R., 1938, *Phys. Rev.*, **54,** 657.

* The uncertainty in the absolute cross section for the reaction $^7\mathrm{Li}(p, \alpha)^4\mathrm{He}$ may amount to as much as a factor of 3.

REVIEWS OF BOOKS

Low Temperature Physics: Four Lectures, by F. E. Simon, N. Kurti, J. F. Allen, and K. Mendelssohn. Pp. vi + 132. (London: Pergamon Press, 1952.) 21*s*.

In recent years, and particularly since the war, there has been a considerable growth of interest in research at very low temperatures. On the one hand it is a relatively unexplored field where there are still many phenomena which are only imperfectly understood, so that comparatively simple experiments can yield results of fundamental interest, and on the other hand the development of the means of providing the very low temperature—particularly the development of the Collins helium liquefier as a commercial product—has made it possible to carry out such experiments at an ever increasing number of research centres. This little book collects together the texts of four lectures on low temperature physics delivered at the Royal Institution in 1950 by leading authorities in this country; the lectures have been revised to bring them up to date to about the end of 1951, and provide an interesting popular account of the present state of the subject.

In the first lecture Professor Simon surveys the whole field and emphasizes the special interest of low temperatures in making apparent quantum phenomena which at higher temperatures are masked by thermal agitation. His elegant account of the basic principles involved in the lowering of temperatures and the limitations imposed by Nernst's theorem serves also as an introduction to the second lecture by Dr. Kurti who deals with the method of adiabatic demagnetization and the new knowledge of the magnetic behaviour of paramagnetic salts gained with its aid. The third and fourth lectures, by Professor Allen and Dr. Mendelssohn respectively, deal with the two topics which are perhaps the most fascinating—the properties of liquid helium and superconductivity. It is probable that both involve manifestations of quantum phenomena on a macroscopic scale, but the basic theory is still very incomplete. It is this and the intrinsic beauty of many of the experimental phenomena, well brought out in both lectures, which make these topics so fascinating.

It is perhaps too much to ask for completeness in such a short account of a large and rapidly growing subject, but it should be noted that there is practically no mention of recent studies of the electrical and magnetic behaviour of non-superconducting metals at low temperatures—for instance of the high frequency behaviour of metals when the mean free path is very long, and of the peculiar field dependence of the magnetic susceptibility discovered by de Haas and van Alphen—studies which promise to throw new light on the fundamentals of the electron theory of metals. Otherwise the book may be confidently recommended as an attractive and lucid introduction which should be valuable not only to anyone embarking on research in the subject, but also to the general student of physics who is looking for a broad picture unburdened by too many technical details. D. SHOENBERG.

Verständliche Elemente der Wellenmechanik, Vol. I, by Karl Jellinek. Pp. xii + 304. (Basel: Wepf, 1950.) 34 S.fr.

This book, the first of two volumes, addresses itself primarily to experimental physicists and sets out to provide yet another introduction to wave mechanics. The usual topics are treated: a lengthy discussion of the wave and corpuscular aspects of light and of material particles leads to the introduction of Schrödinger's equation, which is then used to discuss the simpler one-electron problems, including the harmonic oscillator, the rigid rotator, the hydrogen atom and various types of potential barrier.

The author presupposes a minimum of mathematical knowledge on the part of his readers; his preoccupation with elementary mathematical details is a little wearisome at times, but no doubt many readers will regard this as a fault in the right direction. And it is good to find that the mathematical properties of the various types of wave function are fully and clearly discussed and illustrated by copious diagrams. Other welcome features of the book include the author's habit of illustrating his arguments by means of simple order-of-magnitude calculations, and his comparison on several occasions of the predictions of wave mechanics with those of classical theory and of the old quantum theory.

The value of the book is unfortunately greatly diminished by the author's eccentric ideas about the physical interpretation of wave mechanics. Not content with the accepted probability interpretation of Schrödinger's wave function, he attempts to picture the motion of a particle in a pseudo-classical way which is quite out of keeping with the philosophy of the subject. To this end he is at great pains to postulate and justify the existence of a ' world ether ', basing himself on quotations from writers on the theory of relativity ; wave functions are apparently to be regarded as describing the ' ability ' of the ' ether ' to transport particles or photons. One can imagine the bewilderment of the innocent reader, who on one page has learned for the first time that $e^{ix} = \cos x + i \sin x$, and who is asked a few pages later to consider (out of their context) some of Einstein's more abstruse remarks on the philosophical basis of general relativity. The author's attitude leads him to discuss whether or not particles ' cause ' wave functions and to ask ' how ' a particle can possibly move through points where its wave function is zero, or ' how ' a particle can ever be in a region where its kinetic energy is negative; to answer such questions he feels compelled to assume that the energy of a particle must be fluctuating rapidly owing to an exchange of energy between the particle and the ' ether '.

The reader must be warned to beware of the author's hobby-horse; if he can successfully avoid the evil eye of this strange animal, he will find much valuable information in the rest of the book. E. H. SONDHEIMER.

Philosophic Problems of Nuclear Science, by W. HEISENBERG (translated by F. C. HAYES). Pp. 126. (London: Faber, 1952.) 16*s*.

Under an inept title, this book is a somewhat halting English translation of a collection of Heisenberg's essays on general aspects of physics. These essays cover a wide range of subjects and stretch over a long period of time, the first dating from 1932 and the last from 1948, but they show a remarkable unity and continuity of thought. They deal mainly with historical and epistemological aspects of atomic physics, but they also include some consideration of the more directly human and social relations of science. One may take exception here and there to some interpretation of historical situations, as for instance to the overestimation, fashionable in German circles, of Goethe's scientific dilettantism. One may doubt the author's political wisdom when (p. 77) he describes Hitler's savage onslaught as a " reshaping " of the world, which (this was written in 1941) " absorbs all our powers ". But whether or not he agrees with the author's views, the reader is sure to derive inspiration from an intercourse with one of the most powerful minds in the realm of physics. L. ROSENFELD.

Introduction to the Transfer of Heat and Mass, by E. R. G. ECKERT. Pp. xiii+284. (New York, London: McGraw-Hill, 1950.) $4.00, 34*s*.

There are plenty of books on heat transfer, either theoretical or practical in outlook, but I know of none which presents the best of both in the way this does. The theory is quite straightforward in pure conduction and in pure radiation problems, and the numerical data are adequately known, but when convection plays a part the whole story is different. A few years ago the best one could do was to go to either of the two good books, one British and one American, in which experimental data were critically examined and collated in the light of similitude, and to take from them the nearest analogous case to the one in hand. One could also look at the mathematical attempts being made by men like Kármán and the theoretical workers in aerodynamics, but they seldom contributed to a complex practical problem. The third possibility, favoured by some chemical engineering teachers, was to pretend that everything could be reduced to an equivalent problem in pure conduction, taking the numerical constants from experiment.

The present book, designed primarily for chemical engineering students, treats the whole matter rationally on the basis of boundary-layer theory, thus providing logical reasons for the form of the basic equations. It has the additional merit that, when the form of the equation has been established, good values of the constants are given based on experiment. The student trained in this method will certainly see heat transfer as a field where a rational and not a rule-of-thumb approach is possible and desirable, and he will almost certainly design better apparatus for having studied in this way.

Naturally there are plenty of problems left where further study is needed, notably the problems of heat transfer between solid surfaces and fluids which are evaporating from or condensing on them. Here, the author gives a very good summary of the present position.

J. H. A.

X-ray Protection Design, by HAROLD O. WYCKOFF and LAURISTON S. TAYLOR, National Bureau of Standards Handbook 50. Pp. 36. (Washington, D.C.: U.S. Department of Commerce, 1952.) 15 c.

Actes du colloque internationale de mécanique (*Poitiers*, 1950), Tome IV. Pp. 338. (Paris : Publications Scientifiques et Techniques du Ministère de l'Air (No. 261), 1952.) 1800 fr.

Molecular Microwave Spectra Tables, by PAUL KISLUIK and CHARLES H. TOWNES, National Bureau of Standards Circular 518. Pp. vi+127. (Washington, D.C. : U.S. Department of Commerce, 1952.) 65 c.

CONTENTS FOR SECTION B

PAGE

Dr. J. BOR. A New Photographic Method of Measuring the Dispersion of the Optical Constants of Metals 753

Dr. J. F. ARCHARD, Dr. P. L. CLEGG and Prof. A. M. TAYLOR. Photoelectric Analysis of Elliptically Polarized Light 758

Dr. J. FRIEDEL. The Absorption of Light by Noble Metals and its Relation to the van der Waals Contribution to the Cohesive Energy 769

Dr. P. L. CLEGG. The Optical Constants of Thin Metallic Films Deposited by Evaporation 774

Dr. V. E. COSSLETT. Intensity Limitations in a Point Source of X-Rays . . 782

Dr. E. W. SAKER. The Optical Properties of Liquid Selenium 785

Dr. O. S. HEAVENS. The Contamination in Evaporated Films by the Material of the Source 788

Dr. H. EDELS. Self-Absorption in Arc Sources in Thermal Equilibrium . 794

Dr. E. R. ANDREW and Mr. F. A. RUSHWORTH. Ring Shims for Coned Magnet Polecaps 801

Dr. A. R. VERMA. Observations on Growth and Etch Phenomena on Haematite (Fe_2O_3) Crystals 806

Dr. F. C. FRANK and Mr. A. N. STROH. On the Theory of Kinking . . . 811

Letters to the Editor :

Mr. T. SMITH. Supplementary Note on Ray Tracing 822

Dr. S. R. KHASTGIR and Mr. P. S. V. SETTY. Positive and Negative Joshi Effect in a.c. ' Silent ' Discharges in Iodine Vapour 823

Mr. L. E. COLLINS and Dr. O. S. HEAVENS. The Epitaxial Growth of Germanium on Rocksalt 825

Reviews of Books 826

Contents for Section A 830

Abstracts for Section A 831

ABSTRACTS FOR SECTION B

A New Photographic Method of Measuring the Dispersion of the Optical Constants of Metals, by J. BOR.

ABSTRACT. The information from which the optical constants are determined is produced on a photographic plate as a vertical band of variable intensity for each wavelength. This is compared microphotometrically with an adjacent band of graded intensity produced by the same wavelength.

Photoelectric Analysis of Elliptically Polarized Light, by J. F. ARCHARD, P. L. CLEGG and A. M. TAYLOR.

ABSTRACT. Two photoelectric methods of analysis of elliptically polarized light have been devised. One is a development of that of Kent and Lawson in which a rotating analyser yields a zero signal only when the light is circularly polarized. We use a double image prism after a rotating analyser and the two resulting modulated beams are in anti-phase only when the axes of the double image prism coincide with the axes of the vibration ellipse. In our second method, the light is modulated by chopping, and a double image prism selects two components in phase. In principle these are equal only when the axes of the double image prism are at 45° to the axes of the vibration ellipse. Thus the directions of the major and minor axes are found, and if the outputs from the two photocells which receive the two components are balanced on an electrical bridge the axial ratio may be obtained. The double image prism plays here the part of the half shadow device in visual observations, but as its half shadow angle is 90° instead of only a few degrees, the photocells are used under optimum conditions, i.e. the signal-to-noise ratio is maintained as large as possible and the potential accuracy of the method greatly exceeds the limitations imposed by the rest of the apparatus. By slight modifications the method may be made partially self-recording.

Some examples are given of measurements made on metallic films undergoing surface changes.

The Absorption of Light by Noble Metals and its Relation to the van der Waals Contribution to the Cohesive Energy, by J. FRIEDEL.

ABSTRACT. Noble metals show absorption in the blue or ultra-violet; to this is due the colour of copper and gold. As was pointed out by Mott, the main absorption seems due to internal photoelectric effect, with excitation of a d electron. This absorption could be analysed—as for the alkalis—as a transition between two bands, described by Bloch orbitals, here d and s. But we must take into account the correlation between the hole created in the nd shell and the Fermi electrons. We can assume that the hole is screened by a $(n+1)$s electron bound to it, so that absorption should begin for the frequency of formation of the excited $n\mathrm{d}^9(n+1)\mathrm{s}$ configuration of the monovalent ion. Agreement with experiment obtained using this model is satisfactory both in the pure metals and their alloys. The same model may be used for x-rays, and optical absorption energy is related to the energy separation between the s and d parts of K and $\mathrm{L}_{\mathrm{II,\,III}}$ emission bands. An order of magnitude for the van der Waals interaction energy between d shells could perhaps be deduced from the structure on the short wavelength side of the absorption peak.

The Optical Constants of Thin Metallic Films Deposited by Evaporation, by P. L. CLEGG.

ABSTRACT. The optical properties of evaporated films of silver, gold, tin and indium have been determined by a photoelectric method. The influence of factors concerned with the evaporation procedure has been investigated in the case of the silver films. The experimental results are accounted for by the agglomerated state of the films, and the application of Maxwell Garnett's theory is shown to lead to qualitative agreement with the experimental values.

Intensity Limitations in a Point Source of X-Rays, by V. E. COSSLETT.

ABSTRACT. When the diameter of the focal spot of electrons on an X-ray target is reduced to the order of a micron, the conditions of heat dissipation become so favourable that a greatly increased specific loading is possible. The use of an electron lens to obtain such a small spot introduces a limitation on the rate of supply of energy, as its high spherical aberration requires insertion of a very small aperture, the size of which must be reduced *pari passu* with the size of spot desired. For magnetic lenses of usual design the rate of energy supply is then proportional to the radius of the spot. Comparison with the rate of heat dissipation shows that, for spots of the order of a micron, the limitation on X-ray intensity is not the thermal properties of the target, as in tubes with large focus, but the emission obtainable from the cathode. Specific loadings of the order of 10^7 watts cm^{-2} can be tolerated in a spot of 1 micron; the corresponding emission current density would be of the order of 100 amp cm^{-2}.

The Optical Properties of Liquid Selenium, by E. W. SAKER.

ABSTRACT. The optical properties of liquid selenium in the near infra-red have been measured for a temperature range up to about 400° C. The absorption edge moves out to longer wavelengths as the temperature increases by an amount corresponding to a change of energy gap of $1{\cdot}4\times10^{-3}$ ev/c°. Absorption is very small at low frequencies. For long wavelengths the refractive index decreases as the temperature increases by an amount corresponding to the thermal expansion.

The Contamination in Evaporated Films by the Material of the Source, by O. S. HEAVENS.

ABSTRACT. Two methods have been used to detect contamination in evaporated films of silver and germanium by the boats or filaments used as sources. It is shown that a limit of a few parts in ten thousand of tungsten or molybdenum is attainable by microchemical methods. The much lower limit of one or two parts in 10^7 is attained by the radioactive tracer method. The extent of contamination of films of silver and germanium by tungsten and tantalum boats has been studied using the tracer technique and the minimum contamination attainable found to be of the order of a few parts per million. The possibilities of transfer of the boat material by direct evaporation or by reaction with the residual gas in the system have been minimized; the results suggest that contamination arises by the solution of the boat materials by the molten silver or germanium.

.A
5
2

Self-Absorption in Arc Sources in Thermal Equilibrium, by H. EDELS.

ABSTRACT. An analytical determination of the self-absorption of a spectral line emitted by a source is not normally possible if account is taken of the spatial variations in the source of the excited atom concentrations and spectral line profiles. The problem is simpler for uniformly excited sources, for example sources in thermal equilibrium, but not for high-pressure arc sources normally assumed to be in thermal equilibrium, because of the existence of temperature gradients. In the paper an analysis is developed which shows that if such arcs are treated as uniformly excited, an error of less than 5% is introduced into the determination of the self-absorption of spectral lines, emitted by transitions between an upper state s and a lower absorbing state t, which satisfy the limits $h\nu_{sq}/kT_0 \geqslant 10$ and $\nu_{st}/\nu_{tq} \leqslant 0{\cdot}5$, where q is the ground state and T_0 the axial source temperature. The theory is then applied to the experimental data for a high-pressure mercury arc discharge and to new measurements of the line widths at 5461 and 4358 Å. It is shown that the calculated value of the self-absorption at 5461 Å agrees with the experimental value only when the line has a resonance profile. The existence of this form of profile is also indicated by considerations of the broadening processes in the discharge.

Ring Shims for Coned Magnet Polecaps, by E. R. ANDREW and F. A. RUSHWORTH.

ABSTRACT. The calculation of ring shims of the kind suggested by Rose has been extended to include polecaps in the form of truncated cones. Design data are presented in graphical form. Actual and predicted performances are compared for one magnet.

Observations on Growth and Etch Phenomena on Haematite (Fe_2O_3) *Crystals*, by A. R. VERMA.

ABSTRACT. New observations of growth and etch features on haematite (Fe_2O_3) crystals are reported. Of the many growth patterns observed, the simplest are the elementary 'molecular growth spirals' in accordance with the theory of Burton, Cabrera and Frank. The step height between the successive arms of an elementary spiral has been measured by the application of multiple beam interference fringes and is shown to be equal to the X-ray value of the repeat distance. More complex growth patterns are illustrated and discussed. The etch figures reported are also of molecular thicknesses and consist of a very large number ($\sim 10^7/\mathrm{cm}^2$ of the crystal surface) of similarly oriented small triangular figures, and some more complex shapes.

On the Theory of Kinking, by F. C. FRANK and A. N. STROH.

ABSTRACT. The concept of a kink-band is introduced. It is a thin plate of sheared material in a crystal, transverse to a slip direction, bounded by opposite 'tilt walls' of dislocations. It is shown that if the angle of kinking shear γ exceeds a critical value (estimated to be $3\frac{1}{2}°$) the stress concentration at the edges of the band is sufficient for the creation of new dislocation pairs or loops, and that if the applied stress exceeds a certain value, inversely proportional to the square root of the diameter of the kink-band, the kink-band will grow by this process. The stress field of a kink-band is similar to that of a slip-band, a plate of deformation twin, or a crack under tangential stress. In suitable circumstances these may act as sources for each other. The successive generation of kink-bands, inside each other, from the same source, will produce a kink of the kind experimentally observed.